symmetry

MDPI

Review

Review on Higgs Hidden–Dark Sector Physics at High-Energy Colliders

Theodota Lagouri

CERN-EP/UTA, Espl. des Particules 1, Meyrin, 1211 Geneva, Switzerland; theodota.lagouri@cern.ch

Abstract: The presence of a hidden or dark sector of phenomena that relates either weakly or in a particular way to Standard Model (SM) fields has theoretical as well as experimental support. Many extensions of SM use hidden or dark sector states to propose a specific candidate for dark matter (DM) in the universe or to explain astrophysical findings. If such a family of Beyond the Standard Model (BSM) particles and interactions exists, it is possible that they will be discovered experimentally at CERN's Large Hadron Collider (LHC, $\sqrt{s} \cong 14$ TeV) and future High Energy Colliders. The primary emphasis is on a few examples of searches undertaken at the LHC that are relevant to Higgs Hidden–Dark Sector Physics. These studies' existing constraints and prospects are also reported.

Keywords: BSM; Higgs; hidden–dark sector

Citation: Lagouri, T. Review on Higgs Hidden–Dark Sector Physics at High-Energy Colliders. *Symmetry* **2022**, *14*, 1299. https://doi.org/10.3390/sym14071299

Academic Editor: Andrea Lavagno

Received: 27 February 2022
Accepted: 26 May 2022
Published: 22 June 2022

1. Introduction

While the Standard Model (SM) is an excellent description of strong, electromagnetic, and weak interactions, it is not a suitable choice for explaining dark matter (DM). There is theoretical as well as practical support for the presence of a hidden or dark sector of events that couples to SM fields weakly or in a unique way. Naturalness, thermal DM, and electroweak baryogenesis drive hidden sectors toward the weak scale. The convincing potential of a spontaneously broken dark $U(1)_D$ gauge symmetry, mediated by a vector boson named the dark photon, can be considered a prototypical hidden sector. The physics program at the Large Hadron Collider (LHC) with a center-of-mass pp collision energy of $\sqrt{s} = 13$ TeV has included searches for this hidden region. The High Luminosity HL-LHC will also offer a unique future opportunity to investigate models in which these new states can be produced by using Exotic Higgs boson decays to light scalars or light vectors, as well as inclusive dark photon decays or associated productions, as a portal to this previously inaccessible hidden or dark sector.

The goal of this review study is to present an overview of the Higgs Hidden–Dark Sector Physics with emphasis provided at LHC and less on other High Energy Colliders. Ref. [1] has provided a broader overview of dark matter and Hidden–Dark Sector Physics in present and future High-Energy Colliders.

First, an outline of the motives behind the Beyond Standard Model (BSM) and new physics (NP) will be presented. In the major body of this study, some key components of Hidden–Dark Sector theory are discussed, as well as relationships between portals and particles, with a focus on the dark photon and dark Higgs boson. This paper focus on specific Hidden–Dark sector experimental searches at the LHC, including Exotic Higgs and Dark-Z boson searches, as well as their existing limits and prospects. Finally, results from other LHC searches for dark photons and Long-Lived Particles (LLPs) associated with Higgs and Hidden–Dark Sector particles will be presented.

The following is the major structure of this review paper: "Section 1 Introduction with subsections: Section 1.1 Physics of the Standard Model, Section 1.2 BSM-New Physics (NP) and Section 1.3 Energy and Intensity Frontiers, Section 2 Hidden–Dark Sector with subdivisions: Section 2.1 The Dark Photon Theory, Section 2.2 Overview of Dark Photon

Experiments (above 1 GeV), Section 2.3 Dark Photons at Low Energy (up to 10 GeV), Section 2.4 Dark Photon Search Strategies, and Section 2.5 Summary of Existing Constraints and Future Experiments, Section 3 The Hidden–Dark Sector at High-Energy Colliders, which is divided into three sections: Section 3.1 Dark Sector and Exotic Higgs Decays, Section 3.2 Higgs Hidden–Dark Sector and Theory Predictions for High-Energy Future Collider Searches, Section 4 Selected Dark Photon Studies at CERN's Large Hadron Collider (LHC), with primary subsections: Section 4.1 Higgs Decays Dark Massive Photon (ATLAS, CMS), Section 4.2 Higgs Decays Dark (massless) Photon (ATLAS, CMS), Section 4.3 Long-Lived Particles (LLPs) search with Leptons-jets (Prompt and Displaced) (ATLAS), Section 4.4 Displaced Leptons and Long-Lived Particles (LLPs) (ATLAS, CMS), and Section 4.5 Low Mass Di-muon Resonance Searches (ATLAS, CMS) (CMS, LHCb). Sections 5 and 6 contain Summary of the LHC's Dark Photon Studies, as well as Conclusions and Future Prospects."

1.1. Physics of the Standard Model (SM)

The Standard Model (SM) of particle physics has provided a consistent picture of Nature's fundamental elements and interactions. Numerous experiments have been conducted to test and confirm its predictions. The discovery of a Higgs boson-like particle with a mass of 125 GeV, the last crucial SM component, was made possible by the LHC at c.m.e. 7 and 8 TeV [2,3]. As a result, for the first time, we have discovered all of the particles required to explain the results of all previous accelerator studies. At the same time, neither direct nor indirect searches for novel physics uncovered any major deviations from the SM. For the Higgs mass at this precise value is feasible that the SM will remain mathematically consistent and valid as an effective field theory up to a very high energy scale, perhaps even up to the Planck scale, which is the size of quantum gravity. The SM, on the other hand, seems evident to be a partial theory. Several observable events in particle physics, astrophysics, and cosmology are unaccounted for by it.

1.2. BSM-New Physics (NP)

BSM problems are usually referred to as the following important unsolved challenges:

1. "Neutrino masses and oscillations": What causes neutrinos to vanish and then reappear in a new form? Why are neutrinos massless?
2. "Baryon asymmetry of the Universe": What mechanism generated the early Universe's minor matter-antimatter imbalance?
3. "Dark Matter": what is the most common type of matter in our Universe?
4. "Cosmological inflation": What caused the Universe to expand at an accelerated rate in the early stages of its evolution?
5. "Dark Energy (DE)": What is driving the Universe's current stage of evolution's accelerated expansion?

1.2.1. BSM-New Physics Motivations

As previously stated, the Higgs boson's discovery at the LHC provides the final missing component for experimental support of the SM. Another significant LHC result is that a wide new zone has been searched, although no unequivocal NP signal has yet been discovered. These findings, combined with several constraints from flavor phenomenology and the absence of any charged lepton flavor violation process, suggest that unless specific flavor structures–symmetries are postulated, there may be no NP with direct and sizeable coupling to SM particles up to energies of 10^5 TeV. It is now necessary to seriously investigate the likelihood that the SM extends considerably beyond the electroweak (EW) scale.

The SM theory is renormalizable and predictive, and the measured masses of the Higgs boson and top quark fall into a small range of parameters where SM consistency does not necessitate the creation of new particles up to a very high energy scale, maybe even up to the Planck scale. However, some observed phenomena in particle physics, astrophysics,

and cosmology, such as neutrino masses and oscillations, the universe's baryon asymmetry, the DM, and cosmological inflation, need some yet unknown particles or interactions [4].

Neutrino Oscillations

Different flavors of propagating neutrinos have been observed to oscillate. This suggests the presence of a neutrino mass matrix that distinguishes between the flavor and mass eigenstates. In the SM, this is not the case. Furthermore, explaining why the observed neutrino masses are so much less than the masses of other leptons is difficult. The so-called seesaw process, which introduces one or more heavy sterile neutrinos, is one frequent way of generating such a mass matrix. When this heavy mass scale is paired with the SM scales, very light mass eigenstates for electroweak neutrinos can be generated. The mass of these extra neutrinos has been estimated to be between 10^9 and 10^{15} GeV.

Abundance of Matter, Absence of Anti-Matter

All of the structure we see in the cosmos is formed of matter, and there is very little evidence that anti-matter exists in substantial quantities. Processes in the early cosmos that violated B-number conservation, as well as C and CP symmetry, and occurred outside of equilibrium can explain matter's supremacy over anti-matter. When assuming symmetric beginning conditions and CPT conservation, these Sakharov criteria required to induce baryon asymmetry. Without extending the SM in some fashion, neither the CP violation nor the out-of-equilibrium situation can be tolerated.

The improved knowledge of the Higgs process, in particular, means that we now know that the electroweak phase transition is not a strong first-order transition and hence cannot be the cause of the current universe's asymmetry between matter and antimatter.

A variety of galactic and cosmic observations provide DM evidence that the SM particles are not numerous enough to account for all of the matter in the universe. Galactic dynamics and the Cosmic Microwave Background are two important findings (CMB). Spiral galaxies' stability and observable rotation curves need the clustering of an extra (cold) matter component on a galactic scale. This additional component makes up a significant portion of the galaxy's overall mass and spans a larger area than observable galactic matter. The average features of the universe that these microwave photons have traveled through since the epoch of decoupling are revealed by observations of the CMB.

Again, this means that SM matter can only account for around 5% of the cosmos we observe on average and that the remaining 25% looks to be cold and dark non-relativistic matter. Many proposed DM models, ranging from ultra-light scalars with masses of 10^{-31} GeV to a dispersion of black holes with masses up to 10 M_{sun}, are compatible with these facts.

Cosmological Inflation and Dark Energy

Furthermore, studies of the CMB show that our universe began with exponential inflation and is now undergoing a second period of fast expansion. Within the SM, there is no explanation for either of these stages of the universe's history. There are a number of further indicators that physics outside the SM is necessary, in addition to the data outlined above. These are frequently extremely big parameter fine tunings that are difficult to explain within the SM framework. These should not be regarded as having the same status as the observational evidence described above in terms of driving NP but rather as possible indicators of portions of the model that are not yet fully understood.

Higgs Mass Fine Tuning

In the SM, the Higgs boson is the lone scalar field. Unlike the other particles we detect, no one knows how to safeguard the mass of the scalar Higgs field from quantum corrections that would drive it to a far larger scale without a lot of fine tuning. Low-scale supersymmetry, the existence of extra spatial dimensions, and dynamical relaxation mechanisms are all possible solutions to this dilemma.

Strong CP Problem

There's no reason to believe that the SM's strong sector will adhere to CP symmetry. This kind of CP violation would yield an electric dipole moment for the neutron at an observable level without a lot of fine tuning. It is not even possible to develop an anthropic argument for why the degree of CP violation in the strong sector should be unobservably small, unlike the other fine-tuning concerns described here. The introduction of a pseudoscalar field, the axion, which dynamically relaxes the degree of CP violation to minuscule values, is the most common explanation for this degree of fine tuning. The axion might likewise make up all or part of the DM in our universe if its mass is selected correctly.

Cosmological Constant and Dark Energy

As previously stated, the CMB, when paired with other cosmological data, such as Type 1a supernovae, implies that about 70% of the energy density in our current universe is attributable to a cosmological constant or something that works similarly. Quantum fluctuations in the vacuum naturally yield a cosmological constant term in the Einstein equations, but this is many orders of magnitude too high to be compatible with cosmological measurements. Explanation of why such a big cosmological constant is not observed usually necessitates a lot of fine tuning. There is a huge field of theoretical models available to meet some or all of the above-mentioned NP motivations.

Depending on the theory and the problems it solves, this often means introducing new particles, which can be bosons or fermions, heavy or light. There are theories that strive to make the SM as simple as possible while still addressing all of the motives for new physics that we have discussed, as well as model-independent approaches that try to parametrize all of the different ways specific types of new physics could extend the SM. We will go over the most common types of current theoretical concepts for BSM physics in this section.

New Physics at the TeV Scale and Beyond

If there is an intermediary size between the EW and the Planck scale, a way to safeguard the Higgs mass from massive quantum correlations must be introduced. The introduction of supersymmetry is by far the most researched option. There have been no convincing clues for supersymmetry at the LHC, implying that if this symmetry exists in nature, it can only be restored at a considerably higher energy scale than collider experiments can currently achieve. Precision measures, such as Kaon physics and B physics measurements, will show that precision measurements can indirectly seek NP at a much larger scale than the LHC or any future high-energy collider can directly probe.

Right-Handed Neutrinos

Right-handed neutrinos were introduced in response to explanations of neutrino masses, particularly their smallness via the seesaw mechanism. It can, however, be a useful component in producing baryon asymmetry via leptogenesis. If the new neutrino masses are on the GeV scale, baryogenesis might be used to induce this asymmetry. The introduction of such right-handed neutrinos can cause CP violation, but the scale at which this occurs is still unknown; if it is close to the electroweak scale, it could result in detectable EDMs. The neutrinos' masses can range from the GUT scale to less than ~100 MeV.

The Neutrino Minimal Standard Model (vMSM), which accounts for neutrino weights and oscillations, as well as the evidence of DM and the Universe's baryon asymmetry, is a plausible example that includes right-handed neutrinos. Only three right-handed singlet sterile neutrinos or Heavy Neutral Leptons (HNLs) are added to the SM in this model, one with a mass in the keV range that acts as a DM candidate and the other two with masses in the GeV range and Yukawa couplings in the range 10^{-11}–10^{-6} oscillations, for evidence of DM, and for the Universe's baryon asymmetry.

(WIMP) Dark Matter Models

Non-gravitational interactions between dark and ordinary matter are motivated by the assumption that the DM is a thermal relic from the hot early cosmos. A heavy particle with a mass of 100–1000 GeV interacting through the weak force (WIMPs) is the canonical example; however, no WIMP has been detected so far. Even if DM is not a WIMP, a thermal origin is equally compelling: DM with any mass from a MeV to tens of TeV can annihilate directly into SM matter to obtain the proper relic abundance. In the early Universe, thermal DM in the MeV–GeV range with SM interactions is overproduced; hence, plausible scenarios require extra SM neutral mediators to drain the overabundance. The DM mediator scan's sub-GeV range also provides an explanation for certain outstanding cosmological questions, such as why the mass distribution at the core of a galaxy is smoother than expected.

Axion Dark Matter Models

Axions are another highly driven DM option that may be able to solve both the CP and QCD challenges at the same time. Theoretical cosmology and theoretical particle physics are two large fields of theoretical inquiry. Ref. [5] provides an overview of the axion gravity. In addition, Ref. [6,7] provide a unified theoretical account of inflation and dark matter in contemporary theories of gravity, which may unite inflation with dark energy in the presence of axion fields.

Because axion DM particles are so light, they must be made non-thermally by a gravitational or misaligned mechanism. In the early cosmos, axions could have been heavy and created thermally. The mass and coupling constant of an axion are related in the minimum axion model. The theory can be generalized to one of the axion-like particles (ALPs) if this constraint is loosened, and such a generalization may be motivated by string theory. The hunt for axions and ALPs in the sub-eV mass range employs a variety of methodologies and experiments, including haloscopes, solar helioscopes, and pure laboratory studies, such as regeneration and light-shining-through-a-wall (LSW) tests. In accelerator-based experiments, ALPs with masses ranging from MeV to GeV can be created and perhaps detected.

Until now, the experimental focus has been on finding new particles with masses at or above the EW scale and significant couplings to SM particles. Another, mainly untested option is that particles responsible for the remaining unexplained phenomena outside the SM exist below the EW scale and have gone undetected because they interact very weakly with SM particles. The so-called hidden sector is hypothesized to be associated with such particles. Due to the extremely low couplings, a high-intensity source is required to produce them at a measurable rate: astrophysical sources, intense lasers, or high-intensity accelerator beams can all be used. What is currently known as the Intensity Frontier is the quest for NP in the low-mass and very low coupling region at accelerator beams.

1.2.2. Dark Matter and LHC

DM does not interact with electromagnetic force in the same way that conventional matter does. It does not absorb, reflect, or emit light, making it incredibly difficult to detect. Researchers have been able to deduce the existence of DM solely based on its gravitational effect on visible matter. DM appears to outnumber visible matter by a factor of six, accounting for nearly a quarter of the universe. Here's something to think about: The matter we know, which makes up all stars and galaxies, makes up only 5% of the universe's total mass. However, what exactly is DM? It could, for example, comprise "supersymmetric" (SUSY) particles, which are hypothetical particles that are counterparts to those found in the SM. Experiments at the LHC could yield more direct insights into DM.

According to many ideas, DM particles are light enough to be generated at the LHC [8,9]. They would slip via the detectors unnoticed if they were generated at the LHC. However, because they would take away energy and momentum following a collision, scientists could deduce their existence from the quantity of energy and momentum "missing." In theories that propose physics BSM, such as SUSY and additional dimensions, DM candidates appear

frequently. According to one theory, there is a "Hidden Valley," a parallel world comprised of DM that has little in common with the matter we know. If one of these hypotheses is shown to be correct, scientists will be able to learn more about the composition of our universe and how galaxies are held together.

Dark Matter Theoretical Hypotheses

There are relatively few experimental indicators of what DM might be. However, we may generate theoretical hypotheses about the nature of DM that will be valuable to experimentalists. Theorists and experimentalists frequently work together, as evidenced by the LHC DM Working Group [10]. Theoretical models of DM can provide further information about how DM interacts with conventional matter. We can then forecast what we should see in our detectors if that model were to be realized in nature. This is important to know when building detectors sensitive to DM, as well as for selecting how to analyze the collision products once they have been recorded.

Knowing what to search for is also helpful because we must determine which collisions to save data from in real time (this is performed using a complex trigger system). In order to put LHC findings into context and compare them to DM searches from other instruments, a good theoretical framework for DM is also required.

Theoretical models that allow us to explain the remnant density of DM with one or a few kinds of particles are widely used to direct searches for DM at the LHC. A "Weakly Interacting Massive Particle," a DM particle that only interacts weakly with regular particles and has a mass within the energy range that can be investigated at the LHC, is one example of a model that meets these characteristics (WIMP).

Using WIMP models as a starting point for LHC searches does not imply that we must confine ourselves to the concept that DM can be explained by a single particle and a single interaction. This is especially noteworthy when you realize that the content of DM in the universe is five times that of conventional matter, which is made up of a multitude of particles and interactions. We started our journey into various theoretical models of DM at the LHC in the hopes of detecting the few most conspicuous components and interactions of DM first, much as the electron, proton, and electromagnetic interaction were identified before all other SM particles.

In terms of particle content, the simplest models are those in which the DM particle is added to the SM. The interaction between visible and DM in these scenarios must be placed through existent particles such as the Z or Higgs boson. This suggests that, in addition to their usual decay mechanisms involving SM particles, the Z or Higgs boson might decay into two DM particles.

These DM models are characterized as "portal" models because known particles serve as a bridge between what we know (ordinary matter) and what we do not know (dark matter) (DM). While precision observations, such as those taken at CERN's LEP collider in the 1990s, constrain models with a Z boson gateway, this is the first time in particle history that we can investigate the properties of the Higgs boson in depth. We could see if one or more of those characteristics lead to a DM relationship.

In addition to DM, another particle not included in the SM that operates as a portal particle can be imagined. Because they mediate a new interaction between regular matter and DM, these particles are referred to as "mediator" particles. The mediator in the most basic forms of these models is an unstable heavy particle formed directly from the interaction with SM particles, such as quarks at the LHC. As a result, it must be capable of decaying into those identical particles or a pair of DM particles. If a model such as this exists in nature, we may be able to identify the mediator particle's SM decay products at the LHC, allowing us to discover it directly.

Other simple models do not feature a mediator that can decay to SM particles but instead predict the formation of DM particles in conjunction with SM particles, which can help detect the process over known backgrounds. While these models are frequently employed to understand the results of numerous LHC studies in terms of DM, they are

far too simplistic to accurately represent the whole complexity of a DM theory. They are, nevertheless, still helpful as building blocks for more comprehensive theories, including more elements.

Supersymmetry is the most well-known example of a more complete theory that contains a DM candidate (SUSY). SUSY was one of the first DM models to receive a lot of attention at the LHC. The comparatively modest mass of the Higgs boson and other electroweak particles in the Standard Model (about 100 GeV) compared to the Planck scale (1019 GeV), at which gravity is projected to become strong for the SM to break down, is an appealing aspect of SUSY. Such vast disparities in energy scale are inherently prevented by quantum field theories such as the SM; hence, a physical mechanism is necessary to generate them.

SUSY models provide such a mechanism and, in many circumstances, predict the formation of a new stable, invisible particle known as the "lightest supersymmetric particle" (LSP), which has all of the qualities necessary to be a WIMP DM particle. The LHC physics program focuses on the search for particles predicted by SUSY. These particles, if created in LHC collisions, could decay to produce a range of SM particles that can be seen in the detector, as well as two fleeing LSP DM particles that generate the E_T^{miss} signature mentioned earlier.

DM particle candidates can be found in many other theories of varying degrees of completeness and complexity. Others go beyond the WIMP paradigm and include mediators with extremely feeble interactions with known particles that only decay after traveling significant distances inside (or outside) the detector or more complicated sectors of particles mirroring the SM. It is critical for LHC searches to cover all of this terrain while also anticipating unexpected, unanticipated discoveries.

Particle physicists are becoming increasingly interested in figuring out what DM is, assuming it is made up of particles. Direct detection (DD) systems such as XENON [11] in Europe, LUX [12] in North America, and PANDA-X [13] in China are used by certain experimenters to seek for Galactic DM colliding with underground targets consisting of ordinary matter. Others use indirect detection (ID) experiments to look for the products of annihilating DM, which are typically high-energy photons (observed by telescopes such as Fermi-LAT [14], HESS [15], MAGIC [16], and VERITAS [17]), neutrinos (observed by neutrino telescopes such as IceCube [18]), or anti-particles (detected by space experiments such as AMS [19] on the International Space Station).

If DM's main interaction with conventional stuff is gravitational, these experiments may never be able to witness it directly. Both sorts of searches require DM to interact with ordinary matter in some way in order to succeed: In DD searches, DM-nucleon (or DM-electron) interactions or DM annihilation to SM particles.

Strategies of Dark Matter Searches

Experiments essentially "create it, break it, or shake it" to find DM. The LHC has been attempting to achieve it by colliding proton beams. Telescopes in orbit and on the ground are being used in some research to look for indirect indications of DM particles colliding and breaking apart in space. Others are pursuing these elusive particles directly in underground detectors, looking for the kicks, or "shakes," they deliver to atomic nuclei.

The "make-it" strategy to DM search at colliders complements the "break-it" and "shake-it" investigations, and if the LHC discovers a potential DM particle, confirmation from the other experiments will be required to verify that it is actually a DM particle. If direct and indirect experiments, particularly those using innovative analysis techniques discover a signal from a DM particle collision, experiments at the LHC might be developed to investigate the intricacies of the interaction.

Missing-Momentum Signal and Bump Hunting

So, how has the LHC searched for evidence of DM formation in proton collisions? The so-called missing transverse momentum is the major indicator of the presence of a

dark-matter particle in such encounters (E_T^{miss}). To find this signal, researchers tally up the momenta of the particles visible to the LHC detectors—more specifically, the momenta at right angles to the colliding protons—and check for any missing momentum needed to obtain the total momentum before the collision. Because the protons travel in the direction of the beams before colliding, the overall momentum should be zero. If the total momentum after the impact is not zero, the missing momentum could have been transported away by a dark-matter particle that went unnoticed.

Two types of searches at the LHC are based on missing momentum. One form is guided by SUSY models, which are so-called "complete" novel physics models. The known particles described by the SM of particle physics have a super-symmetric partner particle with a quantum characteristic called spin that is half a unit different from its counterpart in SUSY models. Furthermore, in many SUSY models, the lightest super-symmetric particle is a heavy particle with weak interactions (WIMP). Because they may generate the current quantity of dark matter in the universe, WIMPs are one of the most intriguing candidates for a dark-matter particle. Searches for missing momentum from a pair of dark-matter particles with a spray, or "jet," of particles and/or particles called leptons (mono-jet+MET search) are used to find SUSY WIMPs.

Simplified models that incorporate a WIMP-like DM particle and a mediator particle that interacts with the known ordinary particles steer another sort of search employing the missing-momentum signature. A known particle, such as the Z boson or the Higgs boson, or an unknown particle can act as a mediator. Because they are very simple yet generic in nature (full models are particular and thus restricted in scope), these models have acquired a lot of popularity in recent years, and they may be used as benchmarks for comparing data from the LHC and non-collider DM studies. This second form of search looks for at least one extremely energetic item, such as a jet of particles or a photon, in addition to missing momentum from a pair of DM particles.

In simplified models, an alternative to missing-momentum searches is to look for "the mediator particle" through its transformation, or "decay," into ordinary particles rather than the DM particle. This method looks for a bump in the mass distribution of events with two jets or two leptons in the collision data, such as a bump in the mass distribution of events with two leptons.

Narrowing down the WIMP Territory

What findings have these WIMP searches yielded in the LHC experiments? The short answer is that no indications of WIMP DM have yet been discovered. The lengthier explanation is that they have ruled out wide swaths of theoretical WIMP territory and imposed strict constraints on the permitted values of DM and mediator particle attributes such as masses and interaction strengths with other particles. LHC experiments carried out a huge number of dedicated searches for invisible particles and visible particles that would arise in DM processes and interpreted the results in terms of a variety of WIMP DM scenarios, ranging from basic models to SUSY models.

Collaboration between experimentalists and theorists aided this work, as seen through discussion platforms such as the LHC DM Working Group (LHC DM WG), which includes theorists and members from the ATLAS, CMS, and LHCb Collaborations. Placing the LHC results in the context of the global WIMP search, which includes direct- and indirect-detection experiments, has also been a topic of debate in the DM community, and the debate continues to this day on how to best exploit synergies between different experiments with the same scientific goal of discovering DM.

For example, mono-X (MET+X) searches of DM pair creation, seeking for MET recoiling against visible SM "X" (mono-jet), and di-jet searches of a DM mediator decaying into two jets are highly powerful ATLAS and CMS experiments [20–23].

Finally, although nothing has been discovered yet for quite large LHC center-of-mass energies, the prospect of finding supersymmetric dark matter particle candidates remains a possibility in nature. Gravitational Waves (GW) Laser Interferometers are one of the future

options since they will look for primordial inflationary gravity waves in order to discover a signal that indicates a supersymmetry breaking during the re-heating period. Future GW experiments, such as the BBO [24,25], which work in tandem with the LHC, may provide light on this supersymmetry potential.

1.3. Energy and Intensity Frontiers

In order to explain these mysteries and solve these questions, some yet unknown particles or interactions would be required. However, if that is the case, why have they not been noticed yet?

The so-called "Energy Frontier" research suggests that the hypothetical particles are heavy and require much more collision energy to be observed. This path has been followed by major particle physics experiments in the previous few decades, including CERN's LEP and LHC, as well as Tevatron in the United States. Another theory is that our inability to observe new particles is due to their highly "weak" interactions rather than their large mass. If this is correct, it means that detecting them requires a different approach: an experiment must cross the "Intensity Frontier" rather than the "Energy Frontier" (see Figure 1).

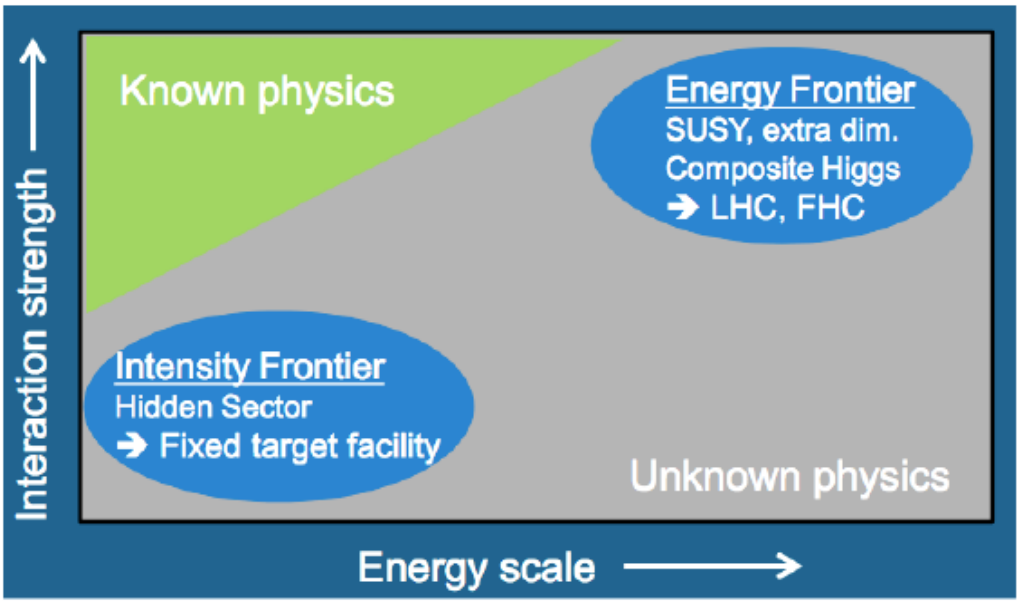

Figure 1. Energy Frontier investigations can unveil new physics when combined with Intensity Frontier experiments.

2. Hidden–Dark Sector

The goal of elementary particle physics is to find and comprehend Nature's most fundamental constituents. The SM of particle physics contains all of our existing knowledge. The SM is recognized to be incomplete, despite its extraordinary accomplishment in accurately explaining the physics of familiar matter in a wide range of situations and across a vast energy range. New physics must be accountable for the DM, neutrino masses, and matter-antimatter asymmetry in Nature, in particular. The search for physics beyond the SM takes various different paths.

The quest for a dark sector in Refs. [26,27], described as a cluster of particles that are not charged directly under the SM strong, weak, or electromagnetic forces, is one of these directions. These particles are thought to have gravitational interactions and may interact with familiar matter via a series of "portal" interactions controlled by the SM's symmetries.

The intriguing prospect of a dark sector is fueled in part by the simplicity with which dark sectors can explain the SM's acknowledged gaps (DM, neutrino masses, and a baryon asymmetry). The only well-known characteristics of DM are its abundance and lack of strong or electro-magnetic interactions. A dark sector is a natural explanation for the lack

of interactions and can easily yield the DM abundance observed. Similarly, the classic idea for the origination of neutrino masses is sterile neutrinos, which are a very simple dark sector. The components needed to establish a matter-antimatter asymmetry and transmit it to the baryon sector can easily be introduced by the interactions of sterile neutrinos or a more complicated dark sector.

Self-interactions of DM may affect the dynamics of galactic structure formation, and "portal" interactions can affect precision measurements such as the anomalous magnetic moment of the muon and the proton charge radius; indeed, discrepancies between simulation/theory and experiment in all of these measurements have been suggested, as probable signs of a dark sector.

One or more "mediator" particles connected to the SM via a "portal" are common in dark sectors. The "mediator" spin and parity determine the "portal" crucial for dark sector-SM interactions: it might be a scalar, a pseudo-scalar a, a fermion N, or a vector A'. The SM's gauge and Lorentz symmetries severely limit the mediator's ability to couple to the SM. The following SM gauge singlet operators, as shown in Figure 2, are the most important interactions between the SM and these mediators.

$$\mathcal{L} \supset \begin{cases} -\dfrac{\epsilon}{2\cos\theta_W} B_{\mu\nu} F'^{\mu\nu}\,, & \text{vector portal} \\ (\mu\phi + \lambda\phi^2) H^\dagger H\,, & \text{Higgs portal} \\ y_n L H N\,, & \text{neutrino portal} \\ \frac{a}{f_a} F_{\mu\nu}\widetilde{F}^{\mu\nu}\,, & \text{axion portal.} \end{cases}$$

Figure 2. Portals to the Dark Sector. Reprinted/adapted with permission from Ref. [1]. 2022, Physica Scripta, Th. Lagouri.

Under the SM gauge group "$SU(3)_c \times SU(2)_L \times U(1)_Y$", H is the SM Higgs doublet with charge assignment (1, 2, +1/2), L is a lepton doublet of any generation transforming as (1, 2, −1/2), "$B_{\mu\nu} \equiv \partial_\mu B_\nu - \partial_\nu B_\mu$" is the "hypercharge field strength tensor", "$F_{\mu\nu}(\widetilde{F}_{\mu\nu})$" is the "SM photon field's (dual) field-strength tensor", "θ_W" is the "weak mixing angle", and "$F'_{\mu\nu} \equiv \partial_\mu A'_\nu - \partial_\nu A'_\mu$" is the "field strength" of a dark $U(1)_D$ vector boson.

The "vector portal" will be the focus, and if the "mediator" is a scalar, it will be able to interact through the Higgs "portal." This is investigated in a variety of ways, including exotic Higgs decays at high-energy colliders like the LHC [28,29], as well as other methods that will be discussed later. If the "mediator" is a vector boson from an additional $U(1)_D$ gauge group under which DM is charged, the "kinetic mixing" interaction "$\varepsilon/\cos\theta_W B_{\mu\nu} F'^{\mu\nu}/2$" is invariant under gauge transformations of both $U(1)_D$ and $U(1)_Y$ [30]. Where ε is a priori a free parameter that is commonly assumed to be $\varepsilon \leq 10^{-3}$ [30].

2.1. The Dark Photon Theory

Beyond the SM, new particles have always been assumed to be charged by at least some of the same gauge interactions as conventional particles. Although this assumption has guided both theoretical and experimental investigations over the last 50 years, it has been progressively challenged by the negative outcomes of all of these searches and the failure to find any of these potential new particles. As hope for a solution along these lines fades, interest in a dark sector—defined as not being charged under the SM gauge groups—increases: perhaps no new particles have been discovered since they do not interact via the SM gauge, as explained in Refs. [27,28].

The dark sector is supposed to exist in a parallel universe to ours. Depending on the model, it may include a few or many states, which can be fermions, scalars, or both. DM is one of these states, and its presence is assumed to be required to explain astrophysical data. The relic density can be calculated and restricted using observational data. Furthermore,

the dark states can interact; depending on the model, these interactions can be Yukawa-like, mediated by dark gauge bosons, or both.

There would be minimal chance of observing dark sector particles in the laboratory if the dark and visible sectors merely interacted gravitationally, which they cannot avoid. For DM, there is a similar issue: Although gravitational physics motivates its existence, it is mostly sought through its hypothesized weak interactions, as in searches for a weakly interacting massive particle using direct and indirect detection methods. For the same reason, we must stake our hopes on the assumption that dark and ordinary sectors interact through a "portal"—as the present terminology has it—in a feeble but (at least in theory) experimentally accessible fashion.

The "portal" can assume many different forms, which can be categorized based on the type and dimension of its operators. Relevant operators take different forms depending on the spin of the mediator in the best-motivated and most investigated cases: vector (spin 1), neutrino (spin 1/2), Higgs (scalar), and axion (scalar) (pseudo-scalar). The vector portal is one of these hypothetical "portals" where contact occurs due to kinetic mixing between one dark and one visible Abelian gauge boson (non-Abelian gauge bosons do not mix). The "visible" photon is assumed to be the boson of electromagnetism's *U(1)* gauge group—or, above the electroweak symmetry-breaking scale, the hypercharge—while the dark photon is assumed to be the boson of an extra *U(1)* symmetry. "Para-", "hidden-sector", "secluded photon", and "*U*-boson"are all terms that have been used to refer to the same particle. The notion of adding a new gauge boson to the SM that is similar to the photon was first proposed in supersymmetric theories.

Because of its dynamic mixing with the ordinary, visible photon, the dark photon can be identified. Because the field strengths of two Abelian gauge fields can be multiplied together to generate a dimension four operator, kinetic mixing is always conceivable. Because of the existence of such an operator, the two gauge bosons can collide as they propagate. The "portal" connecting the "dark" and "visible" sectors is provided by this kinetic mixing. It is through this portal that the dark photon can be detected in the experiments.

The concept of a portal is a significant departure from the gauge principle and the assumption that all interactions must be explained by a gauge theory, which is the major conceptual conclusion of our study of particle physics. The portal, along with the unique interactions it introduces, offers a substantial exception to this rule. The vector example deviates the least from the gauge principle of all the conceivable portals because it just creates a mixing for the gauge bosons while the interaction with matter remains gauge type (albeit with an un-quantized charge). Instead, the other kinds of portals necessitate a clear new violation of the gauge principle, one of which is the Yukawa and self-interactions of the Higgs boson, which are the least known aspect of the SM precisely because they are not gauge interactions.

Another compelling reason to investigate the dark sector in general, and the dark photon, is this: The primary motivation for developing new-physics situations is to utilize them as a foil for the SM when mapping any experimental differences. The various characteristics of supersymmetric extensions to the SM, or even the effective field theory approach to physics beyond the SM, are working against its usefulness in the absence of clearly identifiable additional states. Instead, each dark sector can be reduced to a few parameters—in the case of the dark photon, just two—so that potential disparities with respect to the SM can be more clearly mapped in experimental searches, and the prospective discovery can be discerned.

The physics of this novel gauge boson is explored from both a theoretical and experimental standpoint in Ref. [31]. The dark photon's role in laboratory, astrophysical, and cosmological observations, as well as DM physics, is discussed. There are two types of dark photons: massless and massive, which have quite different theoretical frameworks and experimental characteristics. They provide birth to dark sectors with various characteristics; their physics and experimental searches should be examined independently.

Because it connects directly to the SM currents and is more easily accessible in experimental investigations, the massive dark photon has received the most attention so far.

In comparison to the massive scenario, the massless dark photon originates from a good theoretical foundation and presents a comparably rich, though maybe more complex, experimental target. The ultraviolet (UV) completion of dark photon models, for example, aids in understanding the origin of their interactions with SM particles. The interaction between the dark photon and DM is described, as well as several of the definitions utilized in the experimental searches. The properties of massless and large dark photons are described in terms of existing and future experimental limits. All of these constraints are described for both the massless and massive cases.

Ref. [31] provides an in-depth look at the physics of the dark photon. Several papers on the dark sector (and the massive dark photon) have been published in recent years [26–31]. There, the interested reader will find a variety of perspectives to complement the current review, as well as extra information on the other portals.

2.2. Overview of Dark Photon Experiments (above 1 GeV)

For numerous reasons, searching for dark photons with masses more than 1 GeV is more difficult. These dark photons have smaller production cross-sections and (in the case of "visible" decays) shorter decay lengths. As a result, while dedicated fixed-target experiments are important for low-mass dark sector searches, searches at multi-purpose colliders, such as high-luminosity B-factories (Belle-II) and high-energy pp collider experiments (ATLAS, CMS, and LHCb) are best for searches above 1 GeV (see Figure 3). Provided these experiments' unusual mass reach, it is critical to create approaches and improvements that can increase their sensitivity to dark regions and fully exploit them with customized triggers.

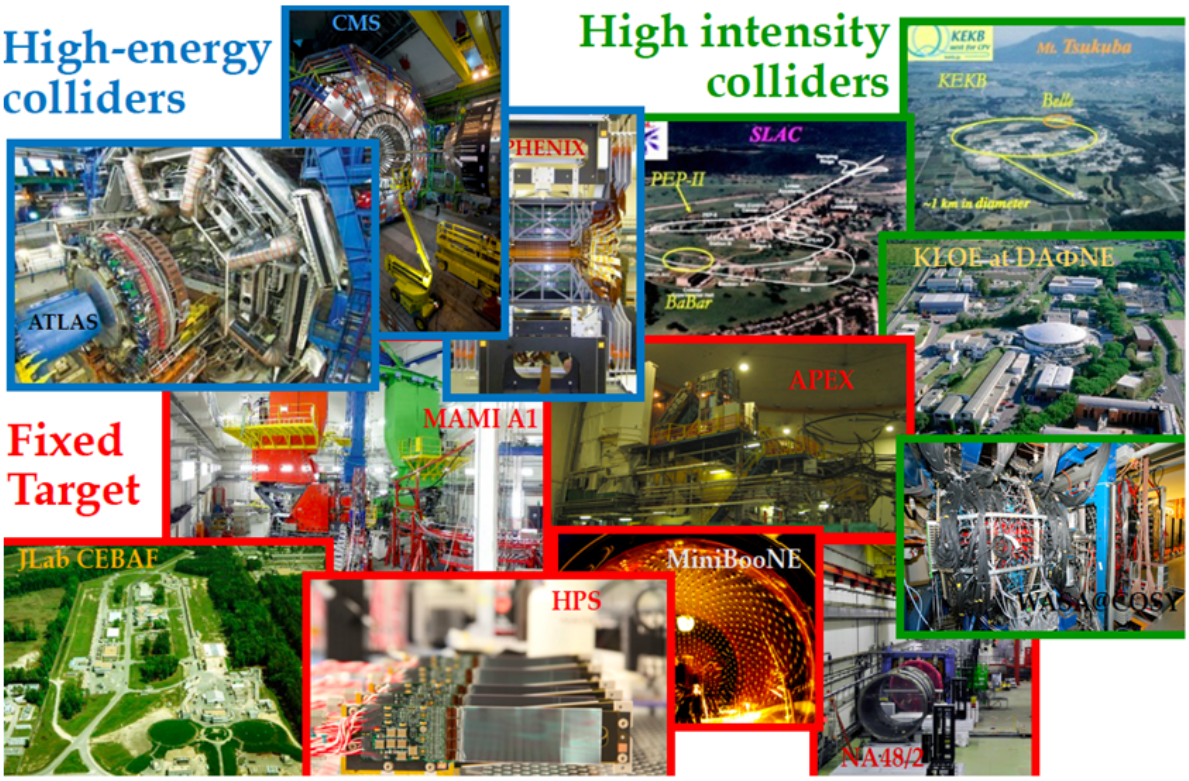

Figure 3. Experiments using dark photons at High-Energy Colliders, High-Intensity Colliders, and Fixed Target Experiments.

2.3. Dark Photons at Low Energy (up to 10 GeV)

The SM of particle physics describes strong, weak, and electromagnetic interactions in terms of a gauge theory based on the "$SU(3) \times SU(2) \times U(1)_Y$" symmetry that describes strong, weak, and electromagnetic interactions The model is phenomenologically successful, but it does not explain the origin of the symmetry. Additional gauge interactions may be included in a more comprehensive theory of Nature. Many theoretical extensions of the SM, such as supersymmetric models or string theory, have additional gauge groups. Furthermore, the existence of DM encourages the expansion of the SM to include a "dark sector", which consists of fields that do not have any SM gauge charges. Additional gauge symmetries may exist in the dark sector. Indeed, as previously established, an Abelian gauge boson of the dark sector can operate as a natural "portal" coupling between the dark sector and the SM. Experimental investigations for non-SM gauge bosons associated with such extended symmetry structures are motivated by this, and such studies will be explored in this section.

This section will concentrate on accelerator experiments searching for gauge bosons with masses ranging from 1 to 10 GeV. The known bounds from accelerator experiments, cosmology, and astrophysics define the lower bound of this range. The kinematic reach of the high-intensity accelerator facilities under consideration dictates the upper bound. Of course, investigations at energy-frontier facilities such as the LHC, which are sensitive to extra gauge bosons with greater masses, up to a few TeV, but with lower sensitivity to portal couplings, supplement these studies.

In collider experiments, the production of non-SM gauge bosons is based on the couplings of new vector bosons to SM particles, principally electrons, and quarks. Such couplings result from the "kinetic mixing" interaction, which combines the gauge boson of a non-SM "dark" gauge group $U(1)_D$ with the SM photon in the simplest situation. This coupling occurs in theories including new fields charged under both $U(1)_D$ and $U(1)_{em}$. If kinetic mixing is observed at the one-loop level, it is predicted to be in the range of 10^{-4} to 10^{-2}. The one-loop contribution to kinetic mixing may disappear in some instances; for example, if the heavy states that cause it appear in multiplets of an $SU(5)$ or a larger "Grand Unified Theory" (*GUT*) group.

The one-loop contribution to kinetic mixing may disappear in some instances, for example, if the heavy states that cause it appear in multiplets of an $SU(5)$ or a larger Grand Unified Theory (*GUT*) group. If both $U(1)$'s are in unified groups, the leading contribution is at two loops and 10^{-6}–10^{-3}, with values as low as 10^{-7} conceivable. Because kinetic mixing is a marginal operator, the masses of the heavy particles that cause it have no impact on these calculations. The physical consequences of kinetic mixing are best understood in the context of canonical kinetic terms. The theory incorporates two gauge bosons, the ordinary photon A and the dark photon A'. The predicted branching ratios of $A^{'}$ decays are shown in Figure 4.

In addition, the dark photon may couple to other non-SM particles in the dark sector: new matter states charged under $U(1)_D$, for example, could comprise particles that make up DM. If kinematically forbidden dark photon decays to dark-sector states, such couplings are irrelevant to the phenomenology of the experiments reported here, and the branching ratios of Figure 4 hold. This is the case of the "visible" dark photon model, which is the subject of this section. If the dark photon can decay into dark-sector states, on the other hand, the branching ratios into the SM will be decreased.

In the most basic instance, the dark sector decays of the A' are "invisible" to standard particle detectors (it is likely that dedicated downstream detectors will be sensitive to long-lived dark sector states created in A' decays). Missing-mass or missing-momentum approaches can be used to detect such undetectable decays. A' can also decay into mixed final states, including both SM and dark sector particles, depending on the dark sector model.

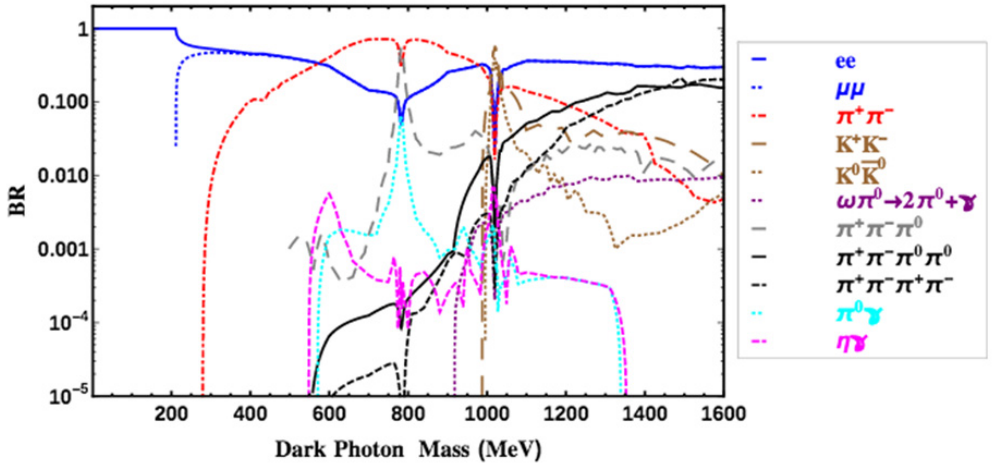

Figure 4. "Visible" dark photon decay branching ratios. Reprinted/adapted with permission from Ref. [1]. 2022, Physica Scripta, Th. Lagouri.

2.4. Dark Photon Search Strategies

The methodologies for producing and detecting dark photons can be used to categorize current and planned dark photon searches. The following are the primary production channels:

Bremsstrahlung: $e^- Z \rightarrow e^- ZA'$, for electrons colliding with a charge Z nuclear target. The A' is produced very forward in a fixed-target setup, carrying the majority of the beam energy (for $E_{beam} >> mA'$), whereas the electron exits at a greater angle. Acceptance for the forward-moving $A^{'}$ can be nearly complete; high-resolution spectrometers with higher acceptance require higher-current beams. Mass reach extends theoretically up to beam energy, but it rapidly decreases as mass increases. Bremsstrahlung production, $pZ \rightarrow pZA'$, is also used in proton-beam fixed-target experiments.

Annihilation: $e^+e^- \rightarrow \gamma A'$. This method of production is preferred for searches that emphasize invisible A' decay modes, in which the unseen A' is reconstructed as a missing mass; visible modes can also play a role. Fixed-target experiments using e^+ beams and e^+e^- collider experiments are both pursuing annihilation pathways. In all circumstances, the available A' mass is constrained by $\sqrt{s}$.

Meson decay: Dalitz decays, $\pi^0/\eta/\eta' \rightarrow \gamma\ A'$, and rare meson decays such as $K \rightarrow \pi\ A'$, $\varphi \rightarrow \eta\ A'$, and $D^* \rightarrow D^0\ A'$, can all create low-mass dark photons if their coupling to quarks is not zero. Hadronic environments, either in colliders or fixed-target setups, offer copious meson production and make this a favored production channel. In e^+e^- colliders, such as $e^+e^- \rightarrow \varphi$ (KLOE, KLOE-2). The parent meson mass limits the A' mass's reach.

Drell–Yan: $q\bar{q} \rightarrow A' \rightarrow (l^+l^-$ or $h^+h^-)$ Hadron colliders and proton fixed-target experiments also benefit from this approach.

The A' detection approaches can be stated as follows: (1) "Bump hunt" in visible final-state invariant mass. (2) "Missing-mass bump hunt". (3) "Vertex detection".

The three detection procedures stated above correspond to (ε^2; mA') parameter plane areas. The sensitivity zones for the three generic experimental procedures are depicted in Figure 5, which illustrates the sensitivity regions for the three generic experimental approaches. The horizontal axis represents available kinematic reach, the vertical axis represents integrated luminosity (increasing downwards), and the diagonal axis represents rising decay length. The gap between areas A and B emphasizes the difficulty of bridging the gap between bump hunts and displaced vertex searches by increasing luminosity (for bump hunts) or improving vertex resolution for short decay lengths, or both.

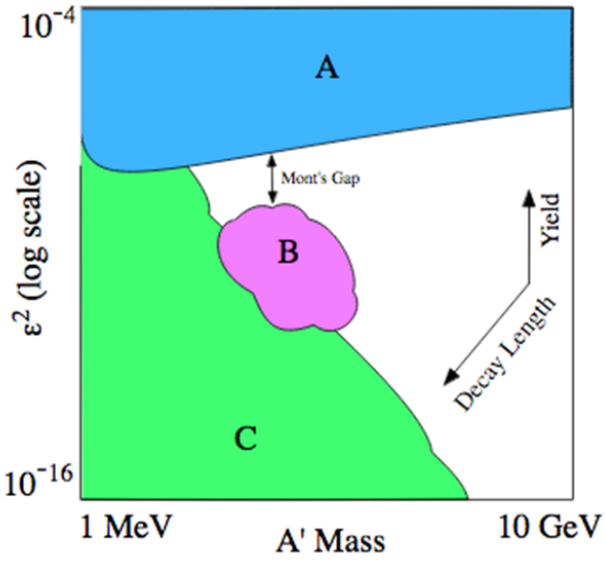

Figure 5. Parameter plane ε^2 vs. A' mass (1 MeV–10 GeV). Region A: bump hunts, visible or invisible modes. Region B: displaced vertex searches, short decay lengths; Region C: displaced vertex searches, long decay lengths. Reprinted/adapted with permission from Ref. [1]. 2022, Physica Scripta, Th. Lagouri.

2.5. Summary of Existing Constraints and Future Experiments

The current experimental situation for the "visible" dark photon hypothesis is summarized in Figure 6. It shows the dark-photon parameter plane, ε^2 against mA', with existing exclusion zones shown in gray and expected exclusion reaches of planned investigations shown in colorful curves.

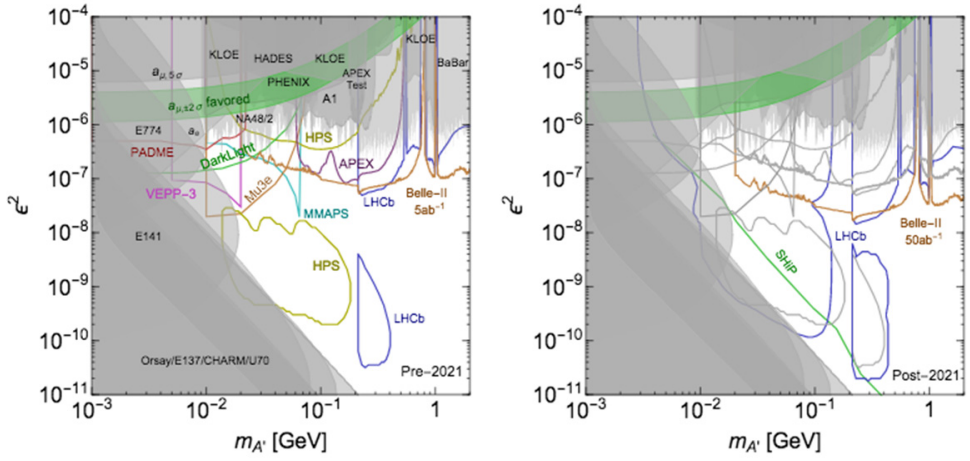

Figure 6. Exclusive experiments targeting "visible" decay modes entail sensitivity to $A' \to l^+l^-$. Experiments that can yield results until 2021 are shown on the left. Existing boundaries are indicated by shaded areas. The green band depicts the 2σ region in which an A' can explain the difference between the calculated and measured muon g-2 value. Right: Longer-term possibilities for experimental sensitivity (beyond 2021). All projections on the left plot are grayed out. It is worth noting that LHCb and Belle-II can probe to masses greater than 2 GeV, while SHIP can probe to lower values. Reprinted/adapted with permission from Ref. [1]. 2022, Physica Scripta, Th. Lagouri.

Experiments looking for a bump in the l^+l^- invariant mass distribution rule out values of above 10^{-3} in the 10 MeV–10 GeV mass range, with the NA-48/2, A1, and BaBar experiments providing the strongest constraints. Meson decays (NA-48/2), bremsstrahlung (A1), and annihilation are among the dark photon production mechanisms used in these

investigations (BaBar). They are supplemented by beam dump experiments such as E141 and E137 at SLAC, E774 at Fermilab, and others, which place upper bounds on as previously mentioned. The measurement of the electron's anomalous magnetic moment a_e also imposes a limitation.

The existing limitations already rule out the "visible" dark photon scenario as a possible explanation for the observed departure of the anomalous magnetic moment of the muon from the SM prediction. Dark photon masses of less than 10 MeV are generally ruled out as well. However, a significant portion of the parameter space has yet to be investigated. In the case of dark photons with a substantial decay branching percentage to dark-sector ("invisible") final states, the situation is far less limited.

3. Hidden–Dark Sector at High-Energy Colliders

3.1. Dark Sector and Exotic Higgs Decays

Exotic Higgs decays represent a relatively unexplored discovery opportunity for the LHC collaborations, as they are frequently ignored by other searches, as discussed in Ref. [28].

The discovery of a Higgs-like particle near 125 GeV at the LHC [2,3] (referred to simply as "the Higgs," H) is a triumph for theoretical and experimental particle physics, and it marks the end of decades of experiments. The experimental exploration of this new state, on the other hand, has only just begun. The Higgs plays a crucial role in particle physics' Standard Model (SM) and has far-reaching implications for novel physics outside the SM (BSM). The finding of this new state opens up a wide range of experiments, including accurate measurements of its couplings to SM particles, the hunt for more Higgs-like states, and the search for "exotic" decays, i.e., decays involving new light states not found in the SM.

The Higgs provides a coherent explanation of a broad class of both simplified and complete models that give rise to typical patterns of exotic Higgs decays [28].

As evidenced by a large and developing literature, non-standard Higgs decays have always been a well-motivated possibility. Even with the discovery of a Higgs particle that is compatible with the simplest SM assumptions, they remain a well-motivated possibility. Indeed, they may be the only way to see BSM physics at the LHC, and they must be explicitly sought out because they are frequently unconstrained by other analyses. The search for non-standard Higgs decays is an essential part of the LHC's and future colliders' experimental programs.

3.1.1. General Motivation to Search for Exotic Higgs Decays

Non-standard Higgs decays exhibit a wide range of properties. The reasons why searches for exotic Higgs decays are such a rich and fruitful technique to hunt for new physics are discussed in Ref. [28]. The data from the LHC7 ($\sqrt{s}$ = 7 TeV) and LHC8 ($\sqrt{s}$ = 8 TeV) experiments may potentially contain O (50,000) exotic Higgs decays per experiment, presenting us with a substantial discovery potential for new physics that is mostly uncontrolled by existing analyses. Indeed, based on present data, the branching ratio (Br) of the 125 GeV Higgs boson into BSM states can be as high as O (20–50%), despite limits imposed by seeing the Higgs boson in several SM channels.

By fitting the couplings of Higgs-to-SM states, some theoretical and experimental studies have constrained the possible Br into an invisible or (as yet) undiscovered final state. If the Higgs is produced with SM strength, these "coupling fits" constrain Br($H\rightarrow$BSM) $\leq$ 20% at 95% CL; a larger BSM branching fraction, Br($h\rightarrow$BSM) $\leq$ 30%, is attainable if new physics is allowed to affect the loop-induced Higgs couplings to both gg and $\gamma\gamma$. Larger (60%) BSM branching fractions can be achieved with more conservative approaches to the theoretical uncertainty on the SM Higgs production cross-sections. This finding is identical to that of the ATLAS and CMS Collaborations.

For models with Higgs couplings to gauge bosons larger than in the SM, certain bounds can be relaxed further. Future LHC forecasts suggest an ultimate precision of

O (5–10%) on this indirect measurement of Br($h \rightarrow$BSM). As a result, branching fractions of O (10%) into exotic decay modes are not only still possible but will also be feasible targets for the lifetime of the LHC's physics program. If the decay signal is both observable and clear, branching fractions as small as O (10^{-6}) could be identified, owing to the high rates for creating these exotic states.

A full experimental characterization of the Higgs is required, as it is for every newly found particle. An extensive examination of its decay modes is required as part of such an experimental characterization. These algorithms have been developed for additional particles, such as the top quark, Z-boson, and B-hadrons, because rare decay modes of SM particles are good locations for new physics to emerge. It is worth noting, though, that the Higgs boson is an exception. Exotic Higgs decays are a natural and predicted characteristic of a very broad class of theories outside the SM due to the small natural width of the SM Higgs boson and the ease with which the Higgs can mediate interactions with other phenomena.

An SM-like Higgs boson with a mass of "m_H = 125 GeV" has an extremely narrow width, "$\Gamma_H \cong 4.07$ MeV", so that "$\Gamma h / m_H \cong 3.3 \times 10^{-5}$" even a modest coupling to another light state can easily open up additional large decay modes.

Indeed, there are compelling grounds to believe that novel physics will preferentially couple to the Higgs boson. A quick review of simplified models and theories that create exotic Higgs decays will provide plenty of evidence to back up this claim. More broadly, the Higgs is one of only a few "portals" that allow SM matter to interact with non-charged hidden-sector matter, and where the leading interaction is renormalizable. Small couplings of the Higgs boson to novel states outside of the SM can lead to potential signals at the LHC. The Higgs portal allows for a wide range of interactions.

Searches for exotic Higgs decays can easily be sensitive to novel physics scales > 1 TeV, which is a notable and generic property of these interactions. Exotic Higgs decays can thus indirectly test new physics scales outside the LHC's kinematic reach, and they may be the only evidence of a new sector accessible to the LHC.

The following "simplifying" assumptions can be made:

(1) "The observed Higgs at 125 GeV" is principally responsible for breaking the electroweak symmetry.
(2) "The observed Higgs at 125 GeV" decays to new particles beyond the SM.

3.1.2. SM + Vector

An additional "$U(1)_D$ gauge symmetry" to the SM is "theoretically" well-motivated and can be found in a variety of top-down and bottom-up extensions of the SM. The "$U(1)_D$ vector boson" (also known as the "dark photon" or "dark-Z") is commonly referred to as A', Z', γ_{D}, or Zd, and there are several ways to relate the additional $U(1)_D$ to the SM. The focus in Ref. [28] is on Higgs decays involving an A', with the A' mass ranging from MeV to 63 GeV. Due to anomalies associated with DM and as an explanation for the mismatch between the estimated and measured muon anomalous magnetic moment, a sub-GeV A' has sparked a lot of attention in recent years.

With measurements of the "muon anomalous magnetic moment", "supernova cooling", and "rare meson decays" an A' with a sub-GeV mass can be investigated at beam dumps and colliders (see Figure 7). Exotic Higgs decays can also result from a broken $U(1)_D$, especially if the two Higgs sectors are mixed. The equivalent vector field is referred to as Zd in this context.

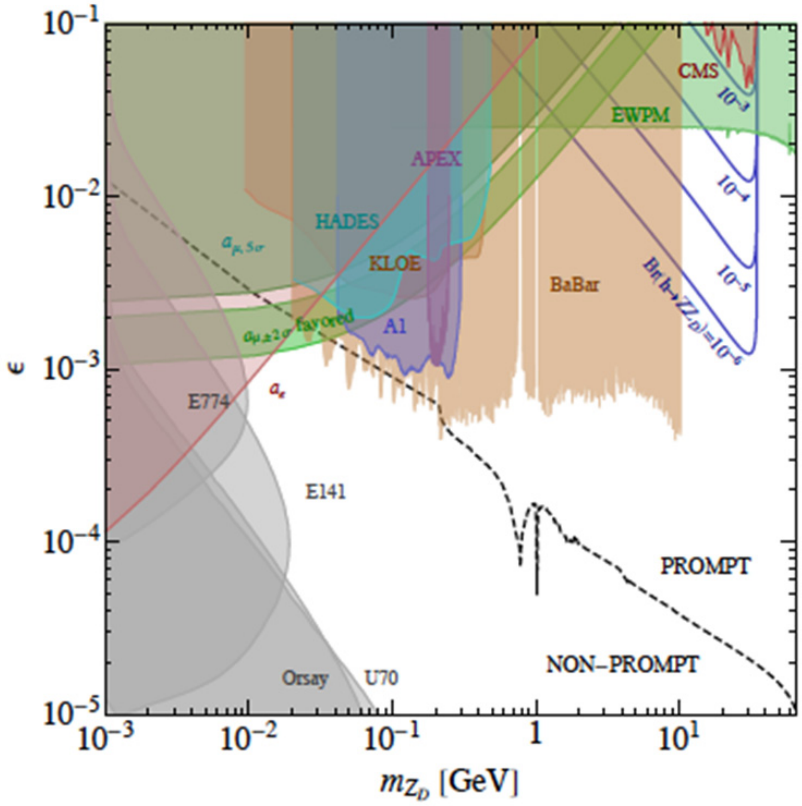

Figure 7. For m_{Zd} ~MeV–10 GeV, constraints on ε, m_{ZD} for pure kinetic mixing (no additional source of *Z*-*Zd* mass mixing). Prompt ($c\tau$ < 1 μm) and non-prompt *Zd* decays are distinguished by the black dashed line. The three blue lines represent $Br(H \rightarrow ZZd)$ contours of 10^{-4}, 10^{-5}, and 10^{-6}, respectively. Existing experimental restrictions are shaded regions. The CMS 20 + 5 fb^{-1} $H \rightarrow ZZ^*$ analysis [32] yielded the red-colored region "CMS." The related ATLAS analysis [33] yielded a similar bound. For some masses, this new constraint can be improved with a specific LHC measurement, potentially outperforming the Electroweak Precision Measurement Bounds (green region designated "EWPM"). Reprinted/adapted with permission from Ref. [1]. 2022, Physica Scripta, Th. Lagouri.

Given the existing constraints illustrated in Figure 7, prompt *Zd* decays are assumed, which necessitates m_{Zd} > 10 MeV. Precision electroweak measurements provide the most rigorous limitations for m_{Zd} >10 GeV. The tree-level shift to the *Z* mass is largely responsible for these limitations, which set a limit of $\varepsilon \leq 0.02$ for $m_{Zd} < m_H/2$. A constraint derived by recasting the LHC7+8 Run1 CMS 20 + 5 fb^{-1} $H \rightarrow ZZ^*$ analysis [32] is also displayed in Figure 7. The related ATLAS analysis [33] yielded a similar bound. For some masses, this bound is almost as good as the "Electroweak Precision Measurement" Bounds (green region labeled "EWPM"), and it can be improved further with a dedicated search. LHC14 with 300 fb^{-1} is projected to be as sensitive to "Br($H \rightarrow ZZd$)" as low as ~10^{-4} or 10^{-5}. This would make the LHC the best probe of dark vector "kinetic mixing" for 10 GeV < m_{Zd} < $m_H/2$ in the future.

The most significant qualitative difference from scalar decays is that branching ratios are ordered by "gauge coupling" rather than "Yukawa coupling", which means that decays to e^+e^- and $\mu^+\mu^-$ are largely beyond the τ thresholds. As shown in Figure 7, which highlights the limits on *Zd* "kinetic mixing" for our regime of interest for m_{ZD} ~ 1 MeV–10 GeV, prompt *Zd* decay necessitates $\varepsilon > 10^{-5}$–10^{-3}.

When gauge mixing is dominant, when $\varepsilon >> \zeta$, the dominating exotic Higgs decay is $h \rightarrow ZZd$. When $\zeta >> \varepsilon$, Higgs mixing dominates, but depending on the spectrum of the dark sector, $h \rightarrow ZdZd$ and *ss* are both feasible. The value of ε is considered to be large enough for *Zd* to decay promptly.

Theoretical Motivation $H \to ZZd \to 4l$

In several theories, the SM photon and Z-boson are mixed in a hidden $U(1)$ sector with small kinetic or mass mixing. This option is frequently associated with DM, but similar phenomenology can also be found in more broad hidden valley models. A kinetic mixing term between the hypercharge gauge boson and the dark $U(1)$ gauge boson is required to cause $H \to ZZd$ decay. This connection will cause Zd to decay to SM fermions if it is the lightest state in the dark sector. The greatest Br($H \to ZZd$) permissible from indirect constraints is $\sim 10^{-3}$, and prompt decay requires $\varepsilon > 10^{-5}$–10^{-3} (depending on m_{ZD}), see Figure 7.

There are several limitations to the existence of a Zd (most of them not from high-energy colliders), yet there remain substantial regions of parameter space crucial for exotic Higgs decays that are not precluded (see Figure 7). $H \to ZZ^* \to 4l$ by ATLAS [33] and CMS [32], where $4l$ stands for electrons and muons, is the most relevant existing search sensitive to $H \to ZZd$. These existing searches are quite sensitive to ZZd decaying into leptons due to the clean $4l$ decay. $H \to ZZ^*$ LHC7+8 already provides large direct constraints to $H \to ZZd \to 4l$ for $m_{Zd} > 12$ GeV. In particular, for very light Zd, a Z+lepton jet search might be able to impose tight constraints.

For 12 GeV $< m_X <$ 34 GeV and $l = e, \mu$, the bound on $Br(H \to ZX) \times Br(X \to ll)$ is $<10^{-4}$–10^{-3} which corresponds to $Br(H \to ZZd) < 2 \times 10^{-3}$, (using Figure 8), representing a new direct constraint on dark photons imposed by the LHC, (see Figure 7). With a specific analysis, this limit can be optimized, making LHC measurements the most sensitive probe of dark vector kinetic mixing in the mass range of 10 GeV $< m_{Zd} < m_H/2$.

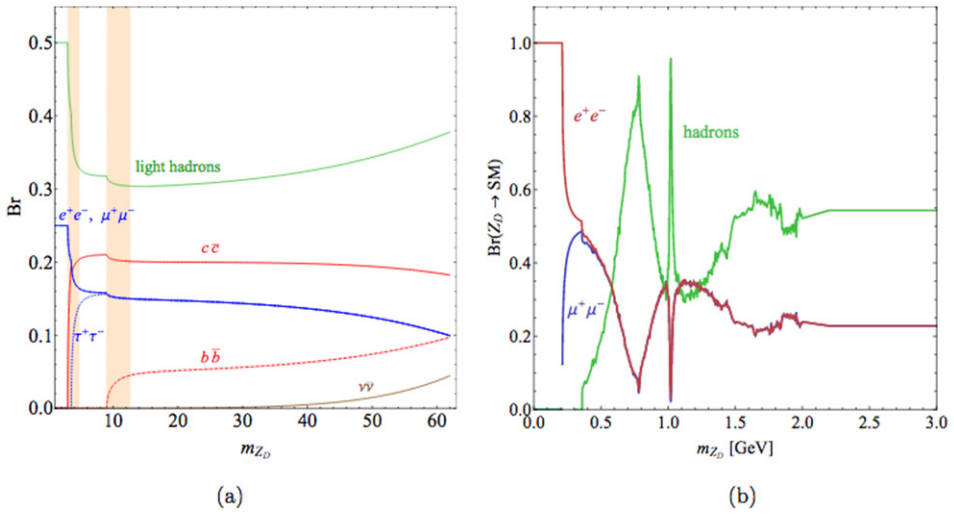

Figure 8. (**a**) Branching ratios for Zd decay to lowest order and without QCD corrections, assuming kinematically forbidden decays to the dark sector. (**b**) For $m_{ZD} < 3$ GeV, branching ratios for Zd decay, including non-perturbative QCD effects. Reprinted/adapted with permission from Ref. [1]. 2022, Physica Scripta, Th. Lagouri.

Theoretical Motivation, $H \to ZdZd \to 4l$

Two types of models can yield a Higgs to four-lepton signature, with two pairs of electrons and/or muons reconstructing the same resonance, as discussed in the previous section: The $H \to ZdZd$ decay, followed by $Zd \to l^+l^-$, may occur in models with an additional $U(1)_D$ gauge group. The dark $U(1)_D$ is broken in the minimum model by a dark scalar that does not mix with the SM Higgs. Because the fourth power of the kinetic mixing parameter ε suppresses the branching ratio of the Higgs to two Zd gauge bosons, the kinetic mixing operator involves the hypercharge gauge field B^μ and the $Z^\mu{}_D$ field leads to only a tiny branching ratio of the Higgs to two Zd gauge bosons.

By introducing a mixing term between the scalar that breaks the $U(1)_D$ symmetry and the Higgs of the SM: "$\zeta \mid S \mid^2 \mid H \mid^2$", far greater branching ratios can be obtained. In these models, even $\zeta \sim 10^{=2}$ can result in branching rates for $H \rightarrow ZdZd$ as high as 10% in certain parameter space regions. Furthermore, a longer Higgs sector scan results in higher branching ratios. For example, "Br($H \rightarrow ZdZd$)" ~10% is conceivable in "2HDM+S" models where the "SM singlet" and one of the "two Higgs doublets" is charged under $U(1)_D$, as shown in Ref. [28].

As reported in Ref. [1], "two classes of models can give a Higgs to four-lepton signature, with two pairs of electrons and/or muons reconstructing the same resonance: models with an additional $U(1)_D$ gauge group may lead to the $H \rightarrow ZdZd$ decay, followed by $Zd \rightarrow l^+l^-$. In the minimal model, the dark $U(1)_D$ is broken by a dark scalar that does not mix with the SM Higgs. Then the kinetic mixing operator involving the hypercharge gauge field B^μ and the ${Z^\mu}_D$ field leads to only a small branching ratio of the Higgs to two Zd gauge bosons since it is suppressed by the fourth power of the kinetic mixing parameter ε. Much larger branching ratios can be obtained by introducing a mixing term between the scalar that breaks the $U(1)_D$ symmetry and the Higgs of the SM: $\zeta \mid S \mid^2 \mid H \mid^2$. In these models, even $\zeta \sim 10^{-2}$ can lead to branching ratios for $H \rightarrow ZdZd$ as large as ~10% in certain regions of parameter space. Furthermore, a more extended Higgs sector scan also leads to sizable branching ratios. In particular, a "$Br(H \rightarrow ZdZd)$" ~10% is possible in "2HDM+S" models where the SM "singlet" and one of the "two Higgs doublets" is charged under $U(1)_D$".

Decays $H \rightarrow ZdZd$, ZZd

The potential of the Higgs decaying to two dark vector bosons Zd or one Zd and one SM Z is taken into account. This can happen in dark vector settings and hidden valleys in general. Because Zd branching ratios are ordered by SM gauge charge rather than mass, high leptonic branching fractions result. The $H \rightarrow ZZd$ search can also be used to constrain the $H \rightarrow Za$ scenario, in which an α is a pseudoscalar that decays into fermions in proportion to their masses.

Not unexpectedly, the search for $H \rightarrow (l^+l^-)\ (l^+l^-)$ comes first for the $H \rightarrow ZdZd$ decay since it allows full reconstruction at "high-resolution" and is the most powerful. The published data on four-lepton events utilized in the Higgs hunt and $Z^{(*)}Z^{(*)}$ research place great constraints on this decay, which has already reached "Br($H \rightarrow ZdZd$)" $< 4 \times 10^{-4}$ according to a reinterpretation of the published data. The constraints discovered in this well-motivated model must be improved.

The $H \rightarrow Z^*Z$ search imposes a lot of restrictions. They are still one order of magnitude weaker than indirect electroweak precision measurements for m_{Zd} >10 GeV in the case of ZZd. The limitations are even tighter with $m_{Zd} < 10$ GeV. A more optimized search at the 14 TeV LHC with appropriate luminosity will produce competitive or even superior bounds for $m_{Zd} > 10$ GeV. In the case of ZZd (but also $ZdZd$ in general), the study should ideally extend to very low Zd mass ranges, where isolation cuts and "quarkonium" backgrounds are a concern.

3.2. Higgs Hidden–Dark Sector and Theory Predictions for High-Energy Future Collider Searches

Dark photons, the mediators of a broken dark $U(1)$ gauge theory that kinetically mixes with the SM hypercharge, have a special sensitivity at high-energy colliders explained in Ref. [28].

Dark photons can be found in the exotic decay of the 125 GeV Higgs boson, $H \rightarrow ZZd \rightarrow 4l$, and in Drell–Yan events, $pp \rightarrow Zd \rightarrow ll$, as previously described. If a hidden-sector Higgs mechanism breaks the dark $U(1)$, mixing between the dark and SM Higgs bosons also causes the exotic decay $H \rightarrow ZdZd \rightarrow 4l$. Both the 14 TeV LHC and the 100 TeV proton–proton collider can explore both exotic Higgs decay channels. Direct Drell–Yan production provides the best sensitivity to Zd in the case of kinetic mixing alone and can probe $\varepsilon > 9 \times 10^{-4}$ (4×10^{-4}) at the HL-LHC (100 TeV pp collider).

Although the exotic Higgs decay $H \rightarrow ZZd$ has a little lower sensitivity, both measurements are required to separate the "kinetically" mixed dark photon from other possibilities. If "Higgs mixing" is present, the decay $H \rightarrow ZdZd$ can be used to detect the Zd for $\varepsilon > 10^{-9}$–10^{-6} (10^{-10}–10^{-7}) in the mass range $2m_{\mu} < m_{Zd} < m_H/2$ by looking for displaced dark photon decays. The indirect but model-independent sensitivity of global fits to electroweak precision observables is compared to the Zd sensitivity at pp colliders. The dark photon model is also suited with a global electroweak fit. At LEP, Tevatron, and the LHC, electroweak precision measurements rule out values as low as 3×10^{-2}. With HL-LHC data, sensitivity can be improved by up to a factor of two, and with ILC/GigaZ data, it can be improved by a factor of four.

The LHC is revolutionizing our understanding of physics at the electroweak scale and beyond. This significant progress is attributable not just to the LHC's exceptional center-of-mass energy but also to the large luminosity it can achieve. This opens the door to the finding of light, weakly coupled states, as well as heavy states with SM quantum numbers. The physics program at the LHC and future colliders, such as the envisioned 100 TeV proton–proton collider, includes searches for such hidden-sector degrees of freedom. Naturalness, thermal DM, and electroweak baryogenesis all motivate hidden sectors around the weak scale, but they also constitute a generic expectation for physics beyond the SM.

The intriguing potential of a spontaneously broken "dark $U(1)_D$ gauge symmetry", mediated by a vector boson called the "dark photon," Zd, was proposed as a prototype hidden sector, as previously reported. The only renormalizable interaction between the dark photon and the SM is kinetic mixing with the hypercharge gauge boson. Furthermore, if the spontaneous breakdown of the $U(1)_D$ gauge symmetry is caused by a dark Higgs process, the dark Higgs boson will have a renormalizable coupling to the 125 GeV SM-like Higgs, resulting in a mixing of the two physical scalar states.

The dominant interactions of the hidden sector with the SM might thus be via the "hypercharge portal", via the "kinetic mixing coupling", which is designated as ε, or the "Higgs portal", via the "Higgs mixing", which is denoted as κ. The LHC and future hadron colliders' impressive integrated luminosities make them powerful probes of the hidden sector through these two portals, while current and future electron–positron colliders can place interesting limits on kinetic mixing from precision electroweak tests (EWPTs), independent of the hidden sector's detailed spectrum.

Through the hypercharge portal, the dark photon mixes with the SM photon and the Z boson. This mixing causes the dark photon to decay entirely to SM particles, with a large branching ratio to leptons, if there are no hidden-sector states below the Zd mass. The dark photon mass range $m_{ZD} > 2m_e$ ~1 MeV, where the Zd can decay to SM fermions, is the emphasis. Precision QED measurements, rare meson decays, supernova cooling, collider experiments, and beam dumps are among the many experimental probes of dark photons with masses above 1 MeV that decay directly to SM particles.

Although recent ideas for studying heavier Zd exist much of the current effort in the hunt for dark photons above the MeV scale is directed to $m_{ZD} < 10$ GeV. Since m_{Zd} is a free parameter, in theory, there is no compelling reason not to explore the complete mass range that is experimentally accessible. The ~3.6σ discrepancy between the measured and SM value of the "muon anomalous magnetic moment" and numerous dark-matter-related anomalies could be explained by dark photons with sub-GeV masses via new DM-Zd interactions28,29 Several concrete scenarios have been proposed in which a sub-GeV mass is created naturally, albeit in many cases, this is not the case.

Several concrete scenarios have been proposed in which a sub-GeV mass is naturally created, while masses beyond 10 GeV are likewise natural in many circumstances. However, one of the reasons for the focus on sub-GeV masses is practicality: the high-intensity experiments required to directly probe dark photons, such as the B- and Φ-factories, as well as various fixed-target and beam dump experiments, lack particle beams with sufficient energy to probe masses above 10 GeV.

We will have the wonderful possibility to study dark photons much above 10 GeV with the 14 TeV run at the LHC, including the "high-luminosity" run (HL-LHC), a possible future 100 TeV proton–proton collider, and other options for future electron–positron colliders. These experiments are the only known probes of dark photons above 10 GeV that look at levels that are not favored by existing EWPT.

In Drell–Yan (DY) events, $pp \to Zd \to l^+l^-$, the hypercharge portal allows for direct production of the dark photon. It also produces the rare Higgs decay $H \to ZZd$. Higgs mixing opens up the possibility of a new exotic Higgs decay, $H \to ZdZd$. Importantly, the Higgs portal can provide experimental sensitivity to values ε far below those reached by searches that simply use the hypercharge portal, allowing us to gaze deeper into the hidden sector.

As previously stated, existing data from LHC Run I (7 and 8 TeV) can already set new limits on dark photons. Ref. [28] used data from the LHC Run I to determine constraints on the exotic Higgs decays $H \to ZZd \to 4l$ and $H \to ZdZd \to 4l$. While the former decay investigates an area of the ε-m_{Zd} plane that was previously ignored by EWPTs, the latter yields the first constraints on Higgs portal couplings for dark photon masses greater than a few GeV. Both studies show that future exotic Higgs decay investigations will be sensitive to dark photons. Figure 9 depicts the Zd leptonic branching fraction and the total width of the dark photon.

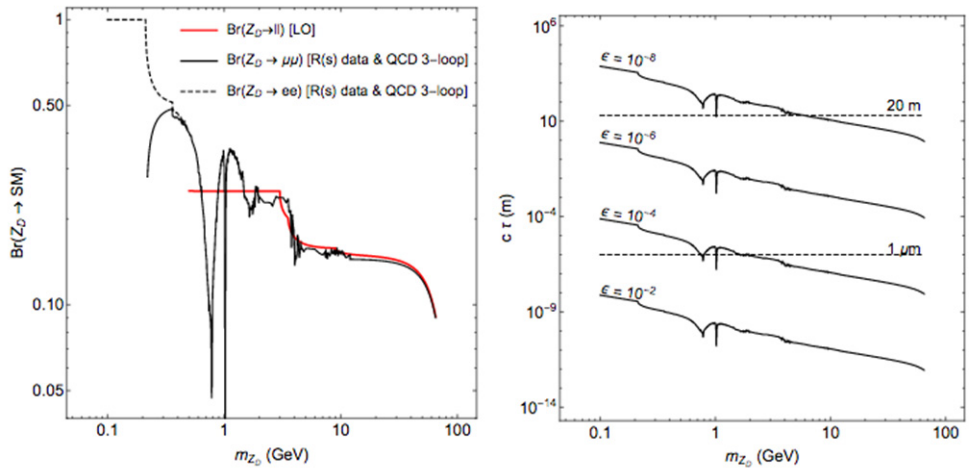

Figure 9. Zd's leptonic branching fraction on the left. Right: Zd decay lengths for various ε. The "dashed" lines designate the transition between two qualitatively distinct experimental regimes: "prompt" decay for $c\tau > 1$ μm and likely escape from an ATLAS-sized detector for $c\tau > 20$ m. Reprinted/adapted with permission from Ref. [1]. 2022, Physica Scripta, Th. Lagouri.

The forthcoming HL-LHC collider, as well as a future 100 TeV collider, will greatly improve the sensitivity of these direct searches. In addition, the LHC and a future ILC/GigaZ collider will improve the measurement of some key electroweak precision observables (EWPOs).

The decay $H \to ZdZd$ is also caused by the kinetic mixing interaction. Because both Z's in $H \to ZZ^{(*)}$ must mix with the Zd, this decay is severely suppressed, and it occurs first at $O(\varepsilon^4)$. If the SM Higgs interacts with the hidden-sector Higgs, however, this decay can take place via Higgs portal mixing, allowing it to be potentially large.

Summary of Dark Photon Future Collider Prospects

Dark sectors with a broken $U(1)_D$ gauge group that "kinetically" mixes with the SM "hypercharge" are well-motivated and show up in a wide range of new physics scenarios. The LHC14, a 100 TeV collider, and an ILC/GigaZ are high-energy proton–proton and electron–positron colliders with remarkable sensitivity to dark photons. In fact, they may be the only way to detect dark photons with masses more than 10 GeV, as high-intensity beam-

dump experiments and B-factories lack the energy to explore this mass range. Furthermore, the 125 GeV Higgs boson plays a key role in these searches, offering even more incentive to look for exotic (non-standard) decays.

The "dark photon" can be produced in "Drell–Yan" events and the exotic Higgs decay $H \to ZdZ^{(*)}$ if the only connection between the dark and SM sectors is kinetic mixing (i.e., the hypercharge portal). Furthermore, the SM expectation for electroweak precision observables would be altered. If the dark photon mass is generated by a Higgs mechanism, renormalizable mixing between the 125 GeV Higgs and the hidden-sector Higgs (i.e., a Higgs portal) is expected. The exotic Higgs decay $H \to ZdZd$ would be possible as a result of this. For the pure hypercharge portal example [28], these diverse options are described in Figure 10.

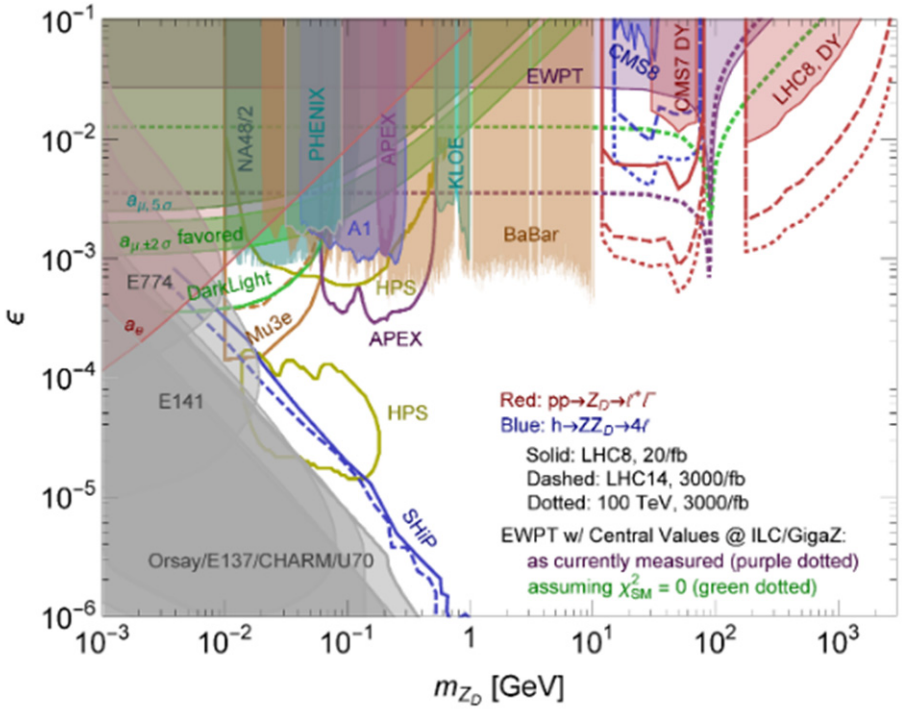

Figure 10. Constraints and prospects for dark photons in a nutshell. Precision QED observables and searches at B- and Φ-factories, beam dump experiments, and fixed target-experiments explore lower masses, while high-energy colliders (LHC14, 100 TeV, ILC/GigaZ) are uniquely sensitive to dark photons with $m_{Zd} > 10$ GeV. In the exotic decay of the 125 GeV Higgs boson, $H \to ZZd \to 4l$ (blue curves), in Drell–Yan events, $pp \to Zd \to ll$ (red curves), and through improved measurements of electroweak precision observables (green/purple dashed curves), dark photons can be detected in a significant part of open parameter space at high-energy colliders. Except for the precision measurements of the electron/muon anomalous magnetic moment and the electro-weak observables, all constraints and prospects assume that the dark photon decays directly to SM particles. If the 125 GeV Higgs mixes with the dark Higgs that breaks the dark $U(1)$ in addition to kinetic mixing, then the decay $H \to ZdZd$ would provide constraints on ε that are orders of magnitude stronger than other searches down to dark photon masses of 100 MeV. Reprinted/adapted with permission from Ref. [1]. 2022, Physica Scripta, Th. Lagouri.

If the dark Higgs does not mix with the SM-like Higgs boson, the Drell–Yan production is the most promising dark photon detection channel. Recasts of current LHC Run 1 data have already established some of the best bounds for several dark photon masses above 10 GeV, particularly at about 180 GeV. Data from the planned HL-LHC run, as well as a future 100 TeV collider, can probe $\varepsilon > 9 \times 10^{-4}$ and 4×10^{-4}, achieving the same sensitivity to dark photon masses above 10 GeV as BaBar data did below 10 GeV. More experimental

studies of the DY dilepton mass spectrum at the Z-peak are needed to close the gap between the high- and low-mass DY constraints.

Exotic Higgs decays $H \to ZdZ^{(*)} \to 4l$ serve as a complementary discovery channel to DY production, providing an additional powerful probe of dark photons with masses below the Z-boson. The large branching ratio anticipated for $H \to ZdZ^{(*)}$ in the event of a "kinetically-mixed" Zd makes this exotic Higgs decay a vital diagnostic in proving the features of any newly discovered vector boson.

The advantage of "electroweak precision constraints" is that they are independent of the dark photon decay mode (see Figure 11). For masses less than 80 GeV, existing constraints demand $\varepsilon < 3 \times 10^{-2}$. In the same mass range, the forthcoming HL-LHC can probe down to 10^{-2}, while an ILC/GigaZ can probe down to almost 3×10^{-3}. The limitation and prospects decline above the Z-pole, although they are still stronger than any other extant constraint up to around 180 GeV. If the dark photon decays directly to SM particles, the above-mentioned searches in DY events and exotic Higgs decays will be much more potent than measurements of electroweak observables in the full mass range above 10 GeV.

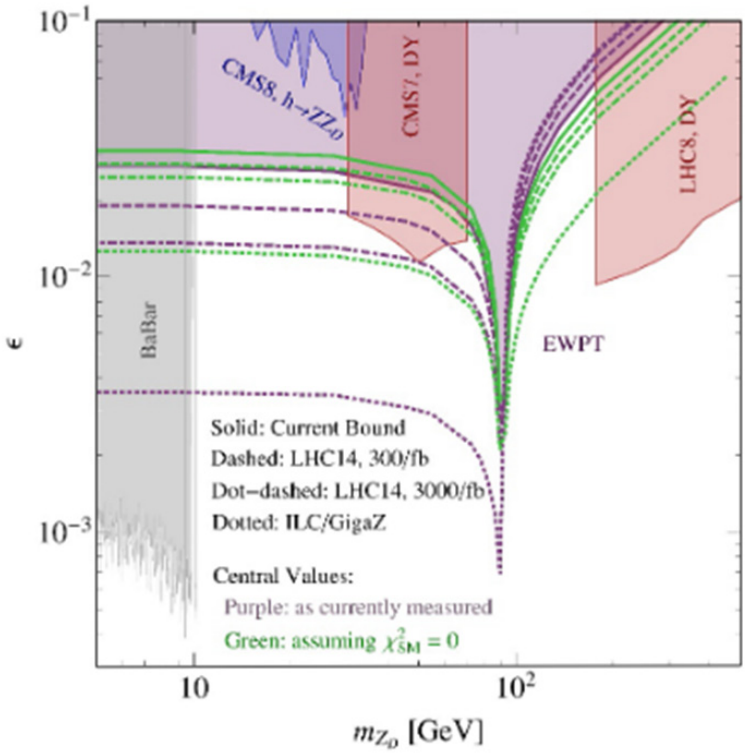

Figure 11. The kinetic mixing coefficient is currently constrained (purple shaded region) by the fit to electroweak precision observables. The dashed, dot-dashed, and dotted lines represent future expected reach at the "14 TeV LHC" with 300 fb^{-1} and 3000 fb^{-1} of data, and at the "ILC/GigaZ", respectively. The boundaries reached by retaining the central values of the measurements as they are now, or by adjusting the central values to the values predicted by the SM best fit, are represented by purple and green lines, respectively. The "14 TeV LHC" (3000 fb^{-1} data) precision observations of m_H and m_t are assumed for the "ILC/GigaZ" bound. Expected improvements in the measurement of $\Delta\alpha^{(5)}_{\text{had}}$ using "VEPP-2000/BaBar" data are also included in the "HL-LHC" and "ILC/GigaZ" projections. Reprinted/adapted with permission from Ref. [1]. 2022, Physica Scripta, Th. Lagouri.

Direct production of the dark photon through the hypercharge portal in the present or proposed colliders is extremely unlikely for $\varepsilon < 10^{-3}$. The remarkable exotic decay $H \to ZdZd \to 4l$ delivers an additional probe into the hidden sector through the Higgs portal if the dark Higgs mixes with the 125 GeV Higgs. The HL-LHC (100 TeV collider) can constrain the effective Higgs-mixing parameter to be $\kappa' <$ few 10^{-5} (few 10^{-6}) [28]. Because

the detection of the $H \rightarrow ZdZd \rightarrow 4l$ decay relies on dark photons decaying straight to leptons, any such discovery would also offer hypercharge portal sensitivity at the $\varepsilon < 10^{-7}$–10^{-6} level, which is the smallest kinetic mixing for which practically all dark photons decay inside the detector.

Furthermore, because future lepton colliders are expected to constrain the invisible Higgs decay branching fraction at the 0.5% level], f $Br(H \rightarrow ZdZd)$ is of this size, values as low as 10^{-9}–10^{-6} (10^{-10}–10^{-7}) can be probed at the HL-LHC (100 TeV collider) by looking for highly displaced dark photon decays.

Ref. [28] focuses mostly on one example of future colliders' exceptional sensitivity to light hidden sectors. For relatively light particles, such as the SM Higgs boson, discovery necessitates both massive center-of-mass energies and enormous production rates. If sensitivity to low-p_T particles is maintained, future hadron colliders will afford unique discovery pathways on both frontiers.

4. Selected Dark Photon Studies at LHC at CERN's Large Hadron Collider (LHC)

Selected dark photon analyses from the ATLAS, CMS, and LHCb experiments at CERN's LHC (Figure 12) are presented in this section.

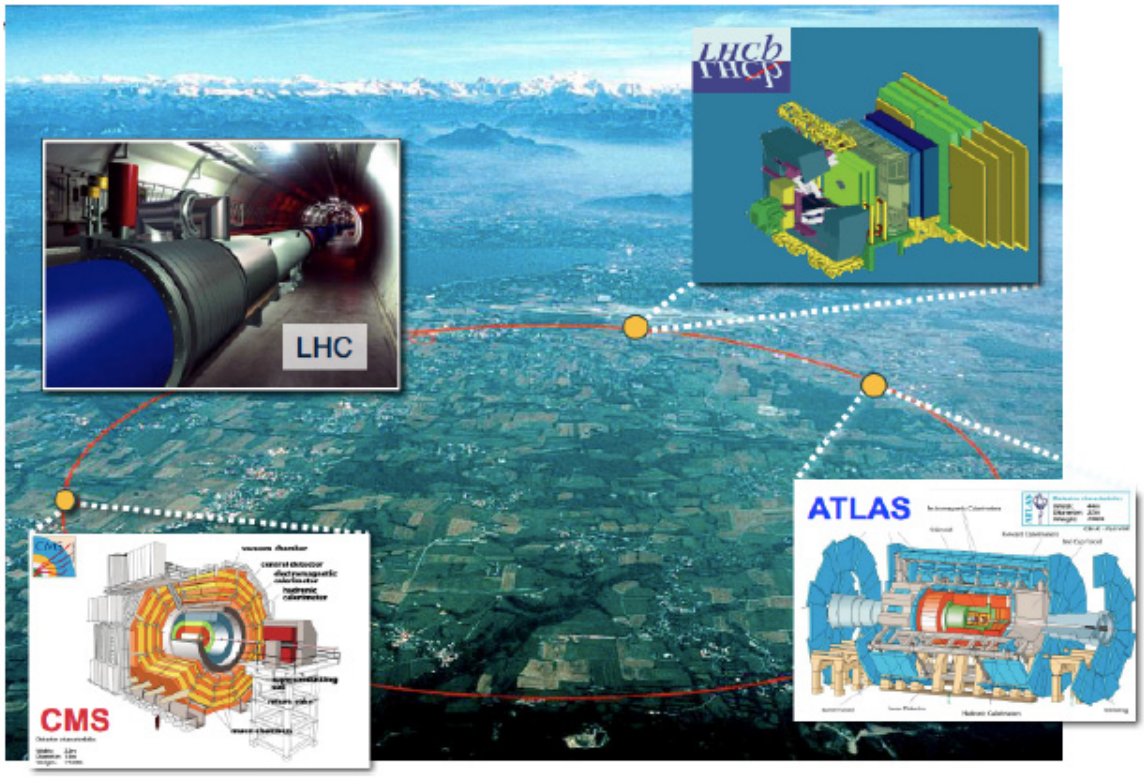

Figure 12. ATLAS, CMS and LHCb experiments at the LHC at CERN. Reprinted/adapted with permission from Ref. [1]. 2022, Physica Scripta, Th. Lagouri.

4.1. Higgs Decays Dark Massive Photon (ATLAS, CMS)

Despite the discovery of the Higgs boson at the LHC in 2012 [2,3], there is reason to assume that the Higgs sector of the SM is still incomplete. Extensions to the Higgs sector of the SM could account for some of the astrophysically motivated dark components of the universe's matter, in addition to the well-known difficulties of naturalness and baryon asymmetry.

Non-standard ('exotic') Higgs boson decays are an appealing technique to look for new physics in the Higgs sector. Non-standard decays can still have up to a 30% branching fraction based on current accuracy measurements of the Higgs boson's properties. Furthermore, because the Higgs boson's decay width is predicted to be relatively narrow by

the SM, even a tiny coupling to a new light state could result in a substantial branching percentage to that state. Novel hidden-sector particles may also preferentially couple to the Higgs boson, giving it a 'portal' into this new physics.

Many suggested extensions to the SM, including the "Next-to-Minimal Supersymmetric SM" (NMSSM), models with a first-order "electroweak phase transition", and models with neutral naturalness], anticipate exotic Higgs boson decays. They are also anticipated by theories with a hidden ('dark') sector and numerous DM models, including several proposed to explain observed positron excesses.

Many DM theories foresee a 'dark' or 'hidden' sector, which interacts with the known SM only through 'mediator' or 'portal' interactions (or via gravity). The addition of a $U(1)_d$ dark gauge symmetry, which "kinetically" mixes with the "hypercharge" gauge field with some strength ε, is a concrete implementation of such a mediator. The Zd vector boson, commonly known as a 'dark photon,' is the gauge boson of this symmetry. Such models have been proposed to explain astrophysical positron excesses and to provide a candidate for the DM in the universe.

The mixing parameter ε determines the Zd boson's coupling strength to SM particles and thus its lifetime. The gauge couplings, on the other hand, influence the decays of the Zd boson, which are substantially independent of ε for $\varepsilon << 1$. The branching ratio for decays to electron or muon pairs can be 10–15% for the Zd mass range $1 < m_{Zd} < 60$ GeV. The decay would be prompt for $\varepsilon > 10^{-5}$ across the same mass range. The decay would be greatly displaced for lower values of ε, whereas the decay products would be strongly collimated for small ε and Zd boson mass less than a few GeV. The Zd boson would most likely escape the detector at $\varepsilon < 10^{-8}$.

There could be mixing with strength, κ, between the SM Higgs and the dark Higgs if the $U(1)_d$ symmetry is broken by an extra dark Higgs boson. The observed Higgs would be the lighter (or heavier) of the pair, with the possibility of decaying into dark-sector particles. A mass mixing between the Zd and the SM Z boson is another option, with the Zd coupling to the Z proportional to the mass mixing parameter, δ.

Figure 13 depicts the mechanisms in which an SM Higgs boson decays to Z_d bosons, which are included in the benchmark "Hidden Abelian Higgs Model" (HAHM) [28]. The process $H \to ZdZd$ has a low SM background and is thus susceptible to tiny kinetic mixing values ε, where the sole need is that the mixing is large enough for the Z_d boson to decay quickly. This mechanism, however, necessitates the mixing of the SM and dark-sector Higgs bosons and hence is dependent on κ.

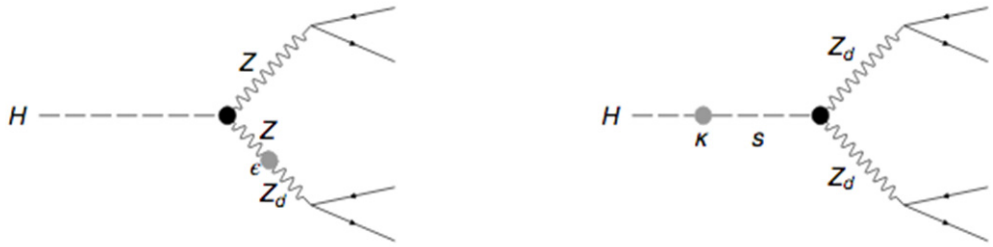

Figure 13. Exotic Higgs decays to four leptons induced by intermediate "dark vector bosons": $H \to ZZd \to 4l$ (**left**) via "hypercharge portal", and $H \to ZdZd \to 4l$ (**right**) via "Higgs portal". Reprinted/adapted with permission from Ref. [1]. 2022, Physica Scripta, Th. Lagouri.

Precision electroweak measurements spanning the range 1 GeV $< m_{Zd} <$ 200 GeV have placed limits on the kinetic mixing of $\varepsilon < 0.03$. $\varepsilon < 0.005$–0.020 for $20 < m_{Zd} < 80$ GeV based on searches for dilepton resonances, $pp \to Zd \to ll$, at the LHC for $m_{Zd} < m_Z$. Other searches rule out $\varepsilon > 10^{-3}$ for 10 MeV$< m_{Zd} <$ 10 GeV. The Higgs mixing parameter κ is constrained by the $H \to ZdZd \to 4l$ search.

4.1.1. Search for Higgs Decays to BSM Light Bosons in Four Leptons with ATLAS at $\sqrt{s}$ = 13 TeV

ATLAS has undertaken a search [34] for new spin 0 or spin 1 bosons utilizing events in which a 125 GeV Higgs boson decays to four leptons ($l = e, \mu$). This decay is αssumed to take place through an intermediate state containing two on-shell, rapidly decaying bosons: $H \to XX/ZX \to 4l$, where the new boson X has a mass of 1 to 60 GeV. The data were collected with the ATLAS detector at the LHC, which has an integrated luminosity of 139 fb^{-1} at a center-of-mass energy of $\sqrt{s}$ = 13 TeV. The data are examined to see if it matches the SM expectations. Fiducial cross-section limits and the branching ratio limits of the Higgs boson to decay to XX/ZX are both set. "Mixing parameters" limits relevant in extensions of the SM comprising a dark sector where X is considered as a dark boson are also set.

This ATLAS study [34] describes three searches for an SM Higgs boson H decaying via a new boson to a final state comprised of four charged leptons ($l \equiv e, \mu$). The new boson might be a dark sector vector boson or a scalar boson, labeled X, according to the models that underpin these analyses. The following are the three searches that have been considered:

- High-mass (*HM*): $H \to XX \to 4l$ (15 GeV < m_X < 60 GeV).
- Low-mass (*LM*): $H \to XX \to 4\mu$ (1 GeV< m_X < 15 GeV).
- Single Z boson (ZX): $H \to ZX \to 4l$ (15 GeV< m_X < 55 GeV).

Because the efficiency of selecting isolated muons is substantially higher than that of selecting electrons in this mass range, the LM analysis only employs the 4μ final state. These searches should be sensitive to any intermediate bosons that are narrow, on-shell, and decay quickly within the mass ranges investigated. This ATLAS publication [34] provides model-independent fiducial cross section limits as well as model-specific limits.

This research builds on prior work [35], in which an ATLAS analysis of Run-1 LHC data of 20 fb^{-1} collected at $\sqrt{s}$ = 8 TeV were reported. Early ATLAS results with partial Run-2 LHC data of 36.1 fb^{-1} at $\sqrt{s}$ = 13 TeV were also published [36]. The signal region selection of the HM analysis has been re-optimized, in addition to increased statistics and improved lepton identification.

Benchmark Models

Two well-motivated "benchmark models" for exotic decays to "light BSM" bosons are summarized below and utilized to understand the results in the publication [34]. The SM is extended with a dark-sector *U(1)* group, abbreviated $U(1)_d$, in the first BSM benchmark model, resulting in the development of a BSM vector boson, Zd. Two Higgs doublets and an extra singlet scalar field (2HDM+S) are present in the second BSM benchmark model. A BSM pseudoscalar boson, α, appears as a result of this. In the decays $H \to ZX \to 4l$ and $H \to XX \to 4l$, the Zd boson and the pseudoscalar, α, might both represent the intermediate state, with the first benchmark model chosen for a higher mass range and the second for a lower mass range.

An extra $U(1)_d$ dark gauge symmetry, related to the SM through "kinetic mixing" ε with the "hypercharge" gauge field, introduces a dark sector [26]. The Zd vector boson is the symmetry's gauge boson. The gauge coupling determines the branching ratios of the Zd, which are independent of the kinetic mixing strength. Because of this coupling, a large percentage of decays (15%) result in pairs of electrons or muons. For Zd masses of 1 to 60 GeV, the decay would be prompt (compared to the ATLAS detector's vertex resolution) for $\varepsilon > 10^{-5}$ [28].

The misplaced decays produce a distinctive signal for smaller values of ε, which has previously been searched for with the ATLAS detector in 8 TeV collisions [37]. The decay products would be extremely collimated for Zd masses below a few GeV and tiny values of ε and would require a specific study. Another theory is that the Z boson and Zd mass combine, allowing the Zd to decay to SM particles more easily. The strength of the mixing in this process is governed by the "mass mixing" parameter δ. There could be mixing

between the SM Higgs boson and the dark Higgs boson if the $U(1)_d$ symmetry is broken by the introduction of a dark Higgs boson. The Higgs portal coupling governs the strength of the Higgs coupling to dark vector bosons in this scenario. The observed Higgs boson is the lightest in an extended Higgs sector, and it could decay into dark-sector particles.

The decay $H \to ZZd$ probes the parameter space of ε and m_{Zd} for the processes outlined in this study [34] and is independent of the occurrence of mixing between the SM Higgs boson and the dark-sector Higgs boson, κ. On an event-by-event basis, however, this BSM signal is indistinguishable from SM $H \to ZZ$ and hence must originate as a resonance in the dilepton mass above this background process. The SM background to the $H \to ZdZd$ process, on the other hand, is easier to distinguish from the signal. This property makes the latter channel susceptible to significantly lower kinetic mixing values, with the sole need being that the kinetic mixing is large enough for the Zd to decay quickly. However, because mixing between the SM Higgs boson and the dark-sector Higgs boson is required for this process, it explores the parameter space of κ and m_{Zd}. These processes (Figure 13 are part of the "Hidden Abelian Higgs Model" (HAHM), which is utilized as the benchmark vector-boson model in the paper [34].

The presence of the dark sector could be deduced from Higgs boson decays through novel intermediate states or deviations from the SM-predicted rates of Drell–Yan (DY) events. Because the LHC experiments are the only ones sensitive to the production of Higgs bosons, the search for the presence of a Higgs portal proposed here is possible. The $H \to ZdZd \to 4l$ search can be used to probe constraints on the Higgs mixing parameter κ, as well as the $H \to ZZd \to 4l$ search on the kinetic mixing parameter ε and the mass-mixing parameter δ.

Extended Higgs Sector models (2HDM+S) [28] with "two Higgs doublets" and an extra scalar field are also interesting for the search $H \to XX \to 4\mu$. Two-Higgs-doublet models (2HDMs) have two neutral scalars $H_{1,2}$, two charged scalars $H\pm$, and one neutral pseudoscalar A in general. The observable Higgs boson H is identified as the lighter of the neutral scalars H_1, whereas the other states are restricted to be heavy by available data. A scalar s and a pseudoscalar α are created by adding a complex scalar singlet that mixes weakly with $H_{1,2}$. If these are less than $m_H/2$, $H \to aa$ and $H \to ss$ decays are permitted (Figure 14). This work investigates the process $H \to aa \to 4\mu$, however the same constraints that apply to $H \to aa \to 4\mu$ also apply to $H \to ss \to 4\mu$.

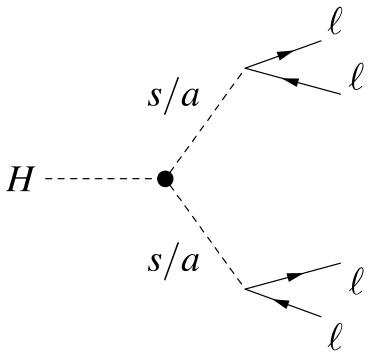

Figure 14. In models with an extended Higgs sector, the decay of a Higgs boson produces dark Higgs scalars s or pseudoscalars a that couple to SM particles via kinetic mixing with the SM Higgs field. Reprinted/adapted with permission from Ref. [1]. 2022, Physica Scripta, Th. Lagouri.

- Analysis Event Selections

All of the analyses in this study are based on the search for mass resonances in final states containing a quadruplet of two same-flavor opposite-sign (SFOS) lepton pairs: $(e^+e^- + e^+e^-)$, $(e^+e^- + \mu^+\mu^-)$, or $(\mu^+\mu^- + \mu^+\mu^-)$. The two pairs' invariant masses are denoted m_{12} and m_{34}, with m_{12} being the one closest to the mass of the Z boson, $|m_{12} - m_Z| < |m_{34} - m_Z|$. Alternative SFOS pairings can be defined for a provided

m_{12} and m_{34} labeling if all four leptons have the same flavor. The positively charged lepton of the m_{12} pair is combined with the negatively charged lepton of the m_{34} pair to form m_{14}. The other possible pairing, m_{23}, is built similarly.

In all three studies, a Higgs boson decays to a pair of new bosons X or to a pair of new bosons X and a Z boson, which decay to pairs of leptons. Assuming that the X bosons are on-shell, the technique is to look for resonances in the relevant dilepton mass distributions. Each analysis creates a signal region (SR) by making a set of choices on measured parameters that enhance the signal's sensitivity.

All analyses have the same preselection, but they differ in the stages of picking candidate final-state leptons, turning them into quadruplets, selecting one of those quadruplets, and applying additional conditions to that quadruplet. The event selections for the various analyses are shown in Table 1.

Table 1. For the *ZX*, *HM*, and *LM* analyses, a summary of event selection requirements from Ref. [34]. $m_{J/\Psi}$ = 3.096 GeV, $m_{\Psi(2S)}$ = 3.686 GeV, $m_{\Upsilon(1S)}$ = 9.461 GeV, and $m_{\Upsilon(3S)}$ = 10.355 GeV are the quarkonia masses. Other definitions can be found throughout the text. Reprinted/adapted with permission from Ref. [1], 2022, Physica Scripta, Th. Lagouri.

	$H \to ZX \to 4l$ (15 GeV < m_X < 55 GeV)	$H \to XX \to 4l$ (15 GeV < m_X < 60 GeV)	$H \to ZX \to 4\mu$ (1 GeV < m_X < 15 GeV)
Quadruplet Selection	- Require at least one quadruplet of leptons consisting of two pairs of same-flavour opposite-sign leptons - Three leading-p_T leptons satisfying p_T > 20 GeV, 15 GeV, 10 GeV - At least three muons are required to be reconstructed by combining ID and MS tracks in the 4μ channel		
	- Select best quadruplet (per channel) to be the one who the (sub)leading dilepton mass (second) closest to the Z mass - 50 GeV < m_{12} < 106 GeV - 12 GeV < m_{34} < 115 GeV - $m_{12,34,14,32}$ > 5 GeV	Leptons in the quadrupled tare responsible for firing at least one trigger. In the case of multi-lepton triggers, all leptons of the trigger must match to leptons in the quadruplet	
	$\Delta R(l, l')$ > 0.10 (0.20) for same-flavour (different-flavour) leptons in the quadruplet		-
Quadruplet Ranking	Select first surviving quadruplet from channels, in the order: 4μ, $2e2\mu$, $2\mu2e$, $4e$	Select quadruplet with smallest $\Delta m_{ll} = \lvert m_{12} - m_{34} \rvert$	
Isolation & IP	Track & Calorimeter Isolation $d_0/\sigma(d_0) < 5$ for e, $d_0/\sigma(d_0) < 3$ for μ		
m_{4l}	115 GeV < m_{4l} < 130 GeV		120 GeV < m_{4l} < 130 GeV
Z-Veto	-	10 GeV < $m_{12,34}$ < 64 GeV $4e$ and 4μ channels: 5 GeV < $m_{14,32}$ < 75 GeV	-
Heavy Flavor Veto	-	Reject event if: $(m_{J/\Psi} - 0.25$ GeV) < $m_{12,34,14,32}$ < $(m_{J/\Psi} - 0.30$ GeV) or $(m_{\Upsilon(1S)} - 0.70$ GeV) < $m_{12,34,14,32}$ < $(m_{\Upsilon(1S)} - 0.75$ GeV)	
Signal Region	-	$m_{34}/m_{12} > 0.85 - 0.1125$ $f(m_{12})$	1.2 GeV < $m_{12,34}$ < 20 GeV m_{34}/m_{12} > 0.85 Reject event if m_{12},m_{34} in: 2 GeV–4.4 GeV or 8–12 GeV

- ZX Analysis: $H \rightarrow XX \rightarrow 4l$ (15 GeV < m_X < 55 GeV)

The ZX analysis looks for decays of an SM Higgs boson into a Z boson and a new boson X, where both bosons decay in turn to pairs of electrons or muons. It entails finding two same-flavor opposite-sign lepton pairs with an overall invariant mass consistent with SM Higgs boson decay. The analysis then looks for a peak in the invariant mass distribution of the other pair, which must be roughly consistent with the decay of a Z boson.

The $H \rightarrow ZZ^* \rightarrow 4l$ (about 65% of the total) and non-resonant $ZZ^* \rightarrow 4l$ are the most common backgrounds in this study (about 33% of the total). The triboson processes ZZZ, WZZ, and WWZ are included as additional prompt backgrounds. These are calculated through simulation, although the $ZZ^* \rightarrow 4l$ background estimate is verified through background-enriched validation samples. Other reducible backgrounds, such as Z + jets, $t\bar{t}$, and WZ processes, comprise only a few percent of the background and contain either extra non-isolated leptons from heavy-flavor decay or objects misinterpreted as leptons. The ATLAS SM $H \rightarrow ZZ^* \rightarrow 4l$ analysis [38,39] employed the same data-driven technique to estimate the total yield of these backgrounds. Finally, simulation is used to determine the shape of the m_{34} distribution for the reducible background. Due to variations in the lepton isolation requirements between this study and the ATLAS SM $H \rightarrow ZZ^* \rightarrow 4l$ analysis, the reducible background estimate is provided with a 10% systematic uncertainty.

Figure 15 depicts the final m_{34} distribution for this study, while Table 2 describes the final yields and uncertainties. The modeling of the electron identification efficiency is the source of the majority of systematic uncertainty in final states, including electrons. The modeling of muon isolation is the source of the most systematic uncertainty in the 4μ channel. With an expected background of 319.7 $\pm$ 17.0, a total of 356 events are seen. As a test statistic, the profile-likelihood ratio is utilized. The $H \rightarrow ZZ^*$ background's normalization is allowed to float (as an unconstrained nuisance parameter), resulting in a normalization of 1.2 $\pm$ 0.16. At roughly m_X = 39 GeV, the highest excess, with a local significance of around 2σ, is found.

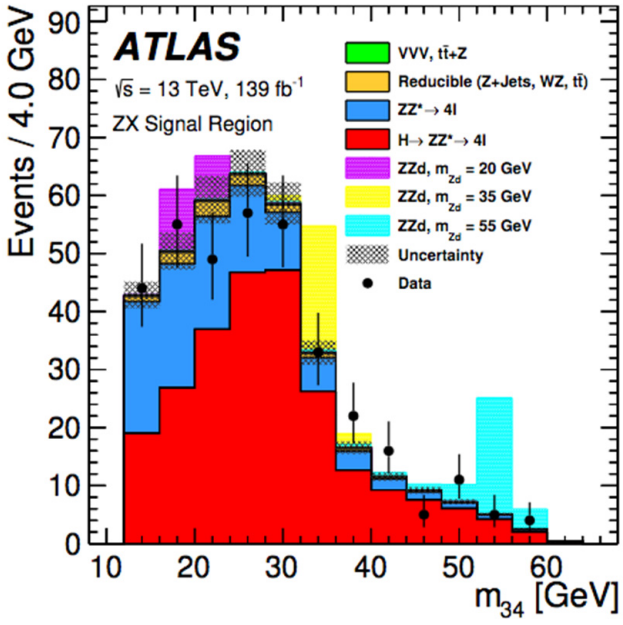

Figure 15. After the $H \rightarrow ZX \rightarrow 4l$ selection, the distribution of m_{34} for data and background events in the mass range 115 GeV < m_{4l} < 130 GeV. The fit provides the background normalization. The shaded band represents the background prediction's overall uncertainty. For certain masses, the signal's expectations are also shown. The signal histograms are layered on top of the background histograms, and the predicted yields are normalized using σ ($pp \rightarrow H \rightarrow ZZd \rightarrow 4l$) = $^{1/10}$ σ_{SM} ($pp \rightarrow H \rightarrow ZZ^* \rightarrow 4l$). For the $H \rightarrow ZZd \rightarrow 4l$ model, three signal points are shown. Reprinted/adapted with permission from Ref. [1]. 2022, Physica Scripta, Th. Lagouri.

Table 2. After the $H \rightarrow ZX \rightarrow 4l$ event selection defined by the mass range 115 GeV < m_{4l} < 130 GeV, the expected and observed numbers of events in each channel. Prior to the fit, the background normalization is performed. The systematic uncertainty in background estimates is highly correlated across different background sources. Reprinted/adapted with permission from Ref. [1], 2022, Physica Scripta, Th. Lagouri.

Process	**Yield (±Stat. ±Syst.)**		
	2l2μ	***2l2e***	***Total***
$H \rightarrow ZZ^* \rightarrow 4l$	$127.9 \pm 0.1 \pm 3.6$	$76 \pm 0.1 \pm 10$	$204 \pm 0.2 \pm 12$
$ZZ^* \rightarrow 4l$	$70.2 \pm 0.2 \pm 1.9$	$33.0 \pm 0.2 \pm 3.6$	$103 \pm 0.3 \pm 4.6$
Reducible	$4.9 \pm 0.1 \pm 0.3$	$5.8 \pm 0.3 \pm .0.6$	$10.7 \pm 0.3 \pm 1.0$
VVV, $t\bar{t} + Z$	$1.1 \pm 0.1 \pm 0.04$	$0.7 \pm 0.1 \pm 0.1$	$1.8 \pm 0.1 \pm 0.1$
Total	$204.1 \pm 0.3 \pm 5.5$	$116 \pm 0.5 \pm 14$	$320 \pm 0.5 \pm 17$
Data	237	119	356

- *HM* Analysis: $H \rightarrow XX \rightarrow 4l$ (15 GeV< m_X < 60 GeV)

The high-mass analysis looks for SM Higgs boson decays to a pair of new bosons X, where X can be Zd, a, or s, which decay to pairs of electrons or muons. Finding two same-flavor opposite-sign pairs of leptons of equal invariant mass that are consistent with the decay of an SM Higgs boson but not with the decay of Z bosons is required for event selection.

Simulations are used to estimate four prompt lepton backgrounds, which are then validated using data from background-dominated control samples. $H \rightarrow ZZ^* \rightarrow 4l$ (about 72% of the total background) and $ZZ^* \rightarrow 4l$ (approximately 72% of the total backdrop) are the most common backgrounds (about 24% of the total background). $t\bar{t}Z \rightarrow 4l$ and processes with three-gauge bosons are examples of similar processes. These are discovered to be insignificant.

Processes containing leptons originating from the decay of heavy-flavor jets, or jets misidentified as leptons, are examples of reducible backgrounds. Data are used to estimate the background from the Z + jets procedure. This provides a background estimate for the Z + jets process in the signal region that is compatible with zero. Simulation is used to estimate other reducible backgrounds. With around 3% of the entire background, $t\bar{t}$ is the most important contributor. Other similar backgrounds are shown to be insignificant, such as diboson synthesis and heavy flavor processing. Four dedicated background-enriched validation zones, chosen so that they do not overlap with the HM signal region, are used to verify the background estimations.

Table 3 summarizes the final yields and uncertainties in the signal region indicated in Table 1, while Figure 16a shows the resulting $\langle m_{ll} \rangle$ distribution for this analysis. There are a total of 20 events, with an expected background of 15.6 ± 1.3 events. The test statistic is the profile-likelihood ratio. Around m_{Zd} = 28 GeV, the largest deviation from SM expectations occurs, corresponding to an event with $\langle m_{ll} \rangle \approx 28$ GeV and a local significance of 2.5σ. Figure 16 depicts the distribution of m_{34} versus m_{12} for the selected occurrences (b).

Table 3. SM background processes expected event yields and data for the *HM* $H \to XX \to 4l$ (15 GeV < m_X < 60 GeV) selection. Three of the 20 observed events are beyond the range 15 GeV < $\langle m_{ll} \rangle$ < 60 GeV and hence are not considered when setting limits. The systematic uncertainty in background estimates is highly correlated across different background sources. Reprinted/adapted with permission from Ref. [1], 2022, Physica Scripta, Th. Lagouri.

Process	Yield (±Stat. ±Syst.)
$H \to ZZ^* \to 4l$	$11.1 \pm 0.1 \pm 1.0$
$ZZ^* \to 4l$	$3.38 \pm 0.05 \pm 0.25$
$t\bar{t}$	$0.47 \pm 0.13 \pm 0.09$
Z + jets	$0.43 \pm 0.39^{+0.17}_{-0.01}$
$Z + t\bar{t} \to 4l$	$0.09 \pm 0.02 \pm 0.02$
WZ	$0.05 \pm 0.03^{+0.05}_{-0.00}$
VVV/VBS	Negligible
Heavy Flavor	Negligible
Total	$15.6 \pm 0.4 \pm 1.2$
Data	20

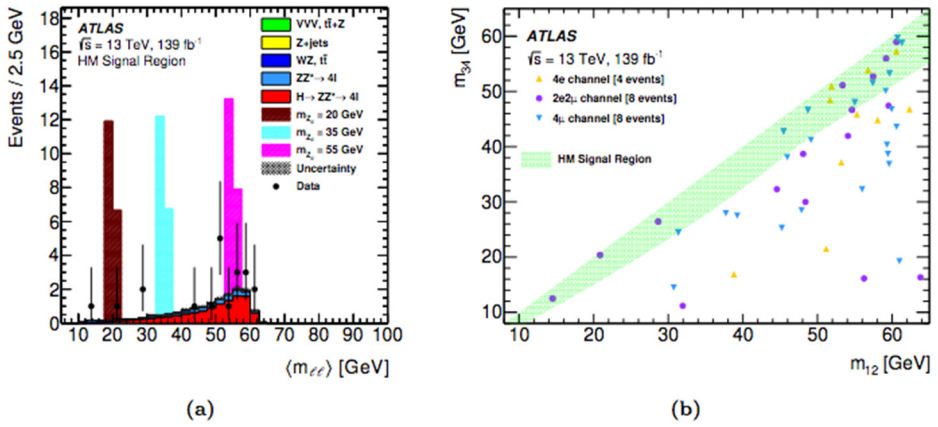

Figure 16. For events selected in the *HM* $H \to XX \to 4l$ (15 GeV < m_X < 60 GeV) study, distribution of (**a**) $\langle m_{ll} \rangle$ and (**b**) m_{34} vs. m_{12}. The (pre-fit) background expectations are also represented in the $\langle m_{ll} \rangle$ distribution (**a**); the hatching band encompasses the statistical and systematic uncertainty. For certain masses, the signal's expectations are also shown. The predicted yields are normalized using σ ($pp \to H \to ZdZd \to 4l$) = $^{1}/_{10}$ σ_{SM}($pp \to H \to ZZ^* \to 4l$) = 0.60 fb (ggF process only), and the signal histograms are stacked on top of the background histograms. Each marker corresponds to an event that passes the Higgs boson window requirement and Z boson veto in the m_{34} vs. m_{12} distribution (**b**). The events of the signal region are represented by the markers (differentiated by channel) that fall within the green shaded area. Reprinted/adapted with permission from Ref. [1]. 2022, Physica Scripta, Th. Lagouri.

- *LM* Analysis: $H \to XX \to 4\mu$ (1 GeV< m_X < 15 GeV)

The LM analysis extends the HM analysis to the 1 GeV < mX < 15 GeV area, where $X = Zd$, a, or s. For this analysis, only the fourth final state is taken into account. With certain adaptations for the different kinematic regions, the event selection is comparable to that of the HM analysis.

MC simulations are used to estimate backgrounds involving four prompt leptons. The $H \to ZZ^* \to 4\mu$ and $ZZ^* \to 4\mu$ processes account for almost two-thirds of the total background estimate. Higher-order electroweak processes, such as triboson production and vector-boson scattering, are discovered to be insignificant. Non-prompt leptons are present in the

remaining backgrounds, mostly from decays of heavy-flavor hadrons in events involving multiple b-quarks, such as $b\bar{b}$. Double semi-leptonic decays, in which a b-hadron decays into a muon and a c-hadron, which then decays into another muon and light hadrons, account for a large portion of this contribution. The heavy-flavor vetoes on dilepton masses necessary as part of the LM event selection virtually fully suppress resonances produced in the b-hadron decay chain (i.e., ω, ρ, φ, J/ψ).

There is also a minor contribution from $b\bar{b}\ b\bar{b}$, where each muon comes from its own b-quark. B-jet tagging is not beneficial for minimizing these backgrounds because the muons chosen are all isolated. Using a data-driven manner, the backgrounds from various processes are combined. On the heavy-flavor background yield, the overall systematic error is calculated to be 50%.

Figure 17 depicts the $\langle m_{ll} \rangle$ distribution in the LM signal region (a). Figure 17b depicts the m_{12} vs. m_{34} distribution, whereas Table 4 summarizes the final yields and uncertainties. With a total background prediction of 0.89 ± 0.15 events, no events are detected.

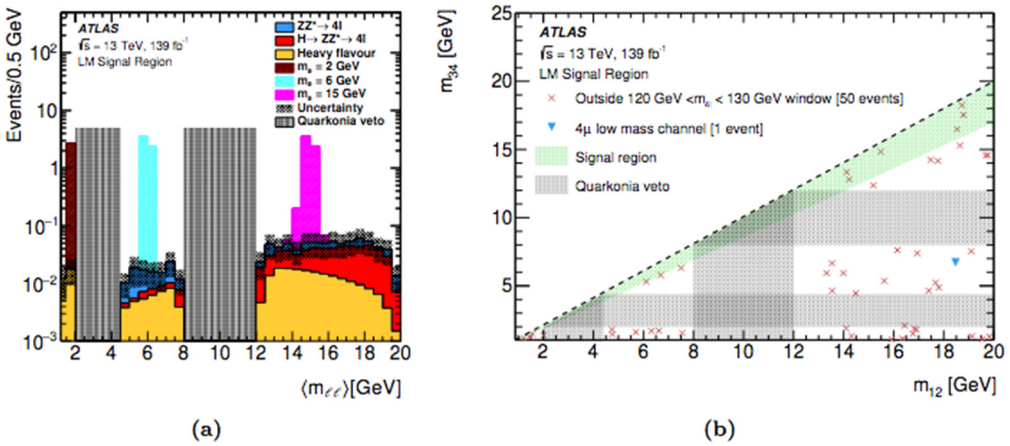

Figure 17. For events selected in the *LM* $H \to XX \to 4\mu$ (1 GeV < m_X < 15 GeV) study, distribution of (**a**) $\langle m_{ll} \rangle$ and (**b**) m_{34} vs. m_{12}. There are no data events that pass the criteria. For certain masses, the expectation for $H \to aa \to 4\mu$ signal is also shown. The predicted yields are normalized using $\sigma\ (pp \to H \to aa \to 4\mu) = {}^{1}/_{10}\ \sigma\text{SM}\ (pp \to H \to ZZ \to 4\mu) = 0.15$ fb (ggF process only), and the signal histograms are layered on top of the (pre-fit) background histograms. The shaded band shows the prediction's total uncertainty. The crossed-through points in (**b**) correspond to the 50 events that are beyond the m_{4l} mass window of 120 GeV < m_{4l} < 130 GeV. The events outside the green signal zone are those that do not meet the $m_{34}/m_{12} > 0.85$ criteria and include one event that falls within the m_{4l} mass window. Reprinted/adapted with permission from Ref. [1], 2022. Physica Scripta, Th. Lagouri.

Table 4. Expected SM background process event yields and data for the *LM* $H \to XX \to 4\mu$ (1 GeV < m_X < 15 GeV) selection. The systematic uncertainty in background estimates is highly correlated across different background sources. Reprinted/adapted with permission from Ref. [1]. 2022, Physica Scripta, Th. Lagouri.

Process	**Yield (±Stat. ±Syst.)**
$H \to ZZ^* \to 4\mu$	$0.41 \pm 0.01 \pm 0.03$
$ZZ^* \to 4\mu$	$0.22 \pm 0.04 \pm 0.04$
VVV/VBS	Negligible
Heavy Flavor	$0.26 \pm 0.09 \pm 0.10$
Total	$0.89 \pm 0.10 \pm 0.11$
Data	0

Limits and Interpretations

For any of the analyses considered, no significant excess is seen above SM background predictions. Consequently, the results are interpreted in terms of exclusion limits. Fiducial cross-section model-independent limits are first set. The benchmark models are then used to determine model-dependent exclusion limits.

Limits on Fiducial and Total Cross-Sections

For the *HM*, *LM*, and ZX studies, model-independent cross-section limits are calculated using fiducial areas defined on generator-level parameters. These fiducial selections are meant to resemble the signal region selection criteria.

Figure 18a shows the efficiency inside the fiducial regions for the *HM* and *LM* analyses using the benchmark $H \to Z_d Z_d$ model, while the efficiencies for $H \to aa \to 4\mu$ over the range 1 GeV < m_a < 15 GeV are identical to $H \to Z_d Z_d \to 4\mu$ to within a relative difference of 3%. Using the CLs frequentist formalism [40] and the profile likelihood ratio test statistic [41], these efficiencies are used to compute 95% CL upper bounds on the cross section within the fiducial region. Figure 19 depicts the resulting bounds. These constraints should hold for any model of the SM Higgs boson decaying to four leptons via two narrow, on-shell intermediate bosons that decay promptly.

The model-dependent acceptances for the *HM* and *LM* analyses for the $H \to Z_d Z_d$ and $H \to aa \to 4\mu$ models are displayed in Figure 18b. For the *HM* analysis, the upper limit on the product of the total cross section and decay branching ratio for the benchmark model σ(gg H$\to Z_d Z_d \to 4l$) is presented in Figure 20, while the upper limits on $\sigma(gg \to H \to Z_d Z_d \to 4\mu)$ and $\sigma(gg \to H \to aa \to 4\mu)$ for both the *HM* and *LM* studies are shown in Figure 21. These results are unaffected by assumptions about the Z_d and a bosons' decay branching ratios. Specifically, Figure 21b also applies to the scalar case $\sigma(gg \to \mathrm{H} \to ss \to 4\mu)$.

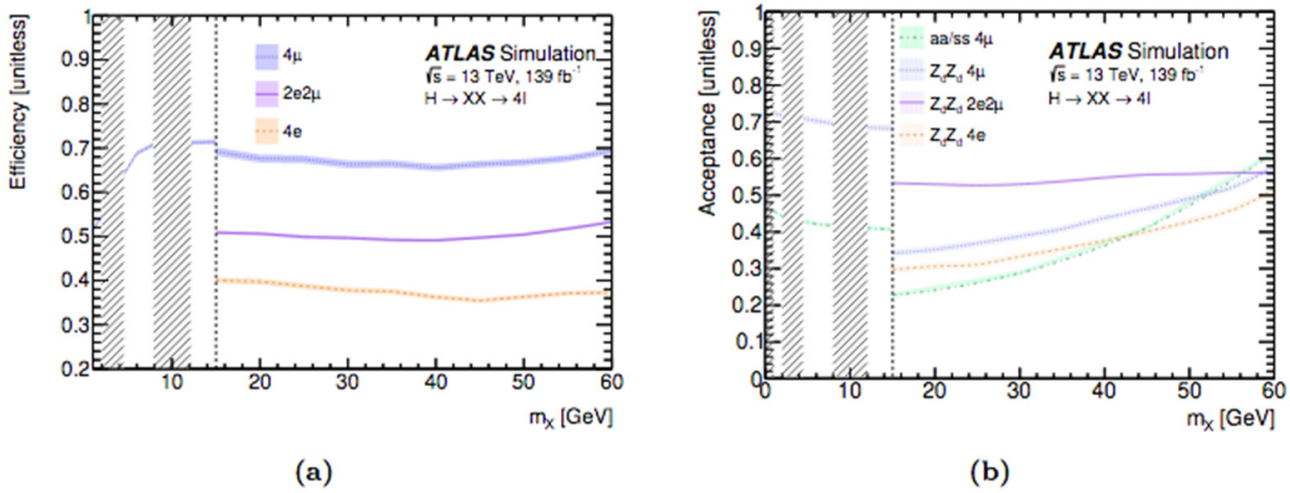

Figure 18. (**a**) Model-independent per-channel efficiencies ϵc estimated in fiducial volumes in the 1 GeV < m_X < 15 GeV and 15 GeV < m_X < 60 GeV (phase spaces above and below 15 GeV are defined separately). (**b**) For the $H \to Zd\ Zd \to 4l$ and $H \to aa \to 4\mu$ processes, model-dependent per-channel fiducial area acceptances. The quarkonia veto regions are shaded areas. Reprinted/adapted with permission from Ref. [1]. 2022, Physica Scripta, Th. Lagouri.

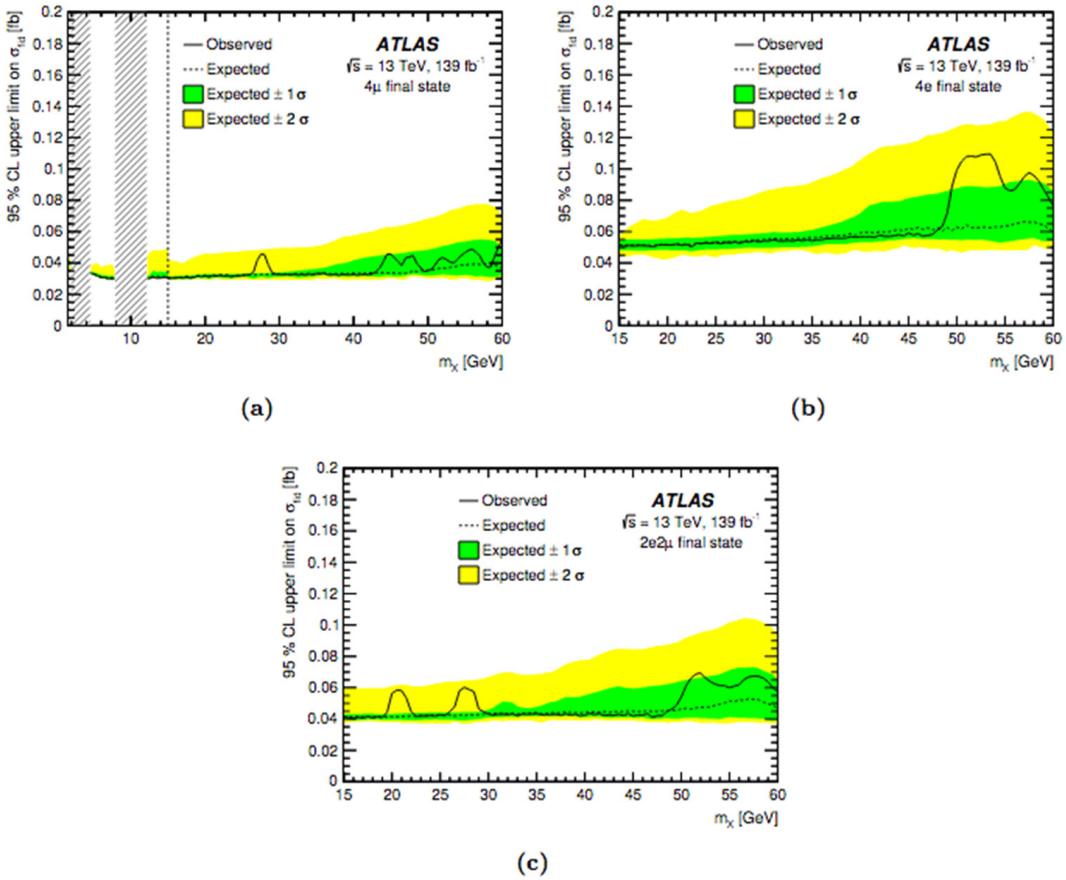

Figure 19. Per-channel upper limits on fiducial cross sections for the $H \to XX \to 4l$ process at 95% CL for the (**a**) 4μ, (**b**) $4e$, and (**c**) $2e2\mu$ final states. The change in efficiency produced by the change in fiducial phase-space definition causes the step change in the 4μ channel at m_X = 15 GeV. The quarkonia veto regions are shaded areas. Reprinted/adapted with permission from Ref. [1]. 2022, Physica Scripta, Th. Lagouri.

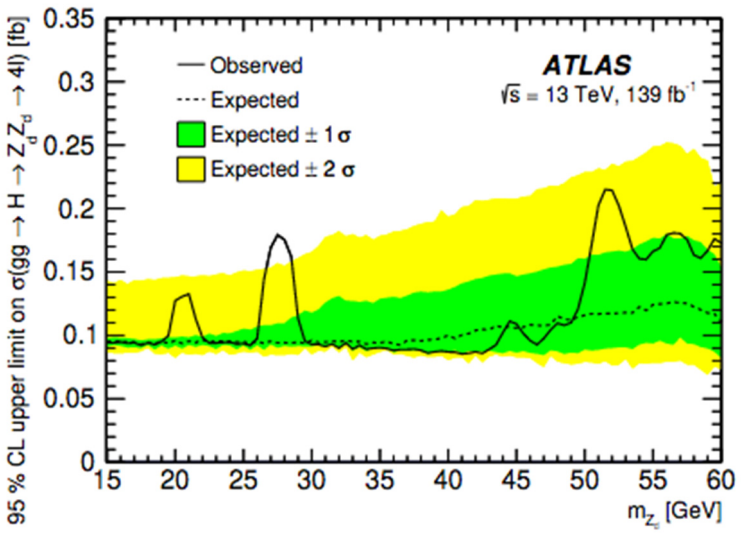

Figure 20. Upper limits observed and expected for the cross section of the $H \to ZdZd \to 4l$ process at 95% CL, assuming SM Higgs boson production via the gluon-gluon fusion process. All final states are combined. HAHM parameters were set to $\kappa = \varepsilon = 10^{-4}$. Reprinted/adapted with permission from Ref. [1]. 2022, Physica Scripta, Th. Lagouri.

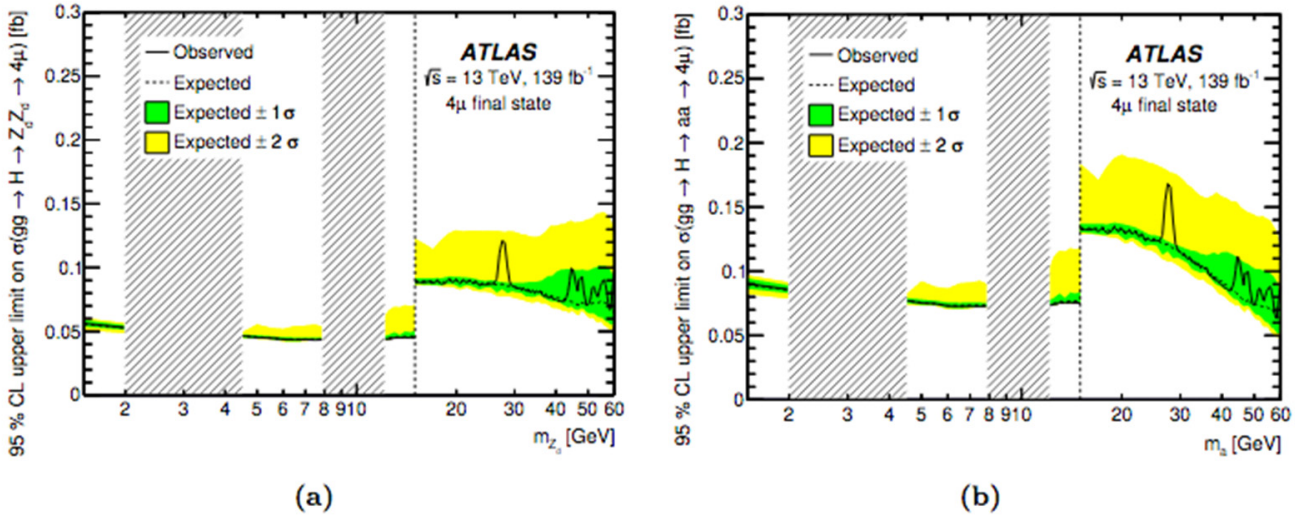

Figure 21. Upper limits observed and expected for the cross sections of the (**a**) $H \to Z_d Z_d \to 4\mu$ and (**b**) $H \to aa \to 4\mu$ processes at 95% CL, assuming SM Higgs boson generation via the gluon-gluon fusion process. The quarkonia veto regions are the shaded zones. HAHM parameters were set to $\kappa = \varepsilon = 10^{-4}$. At $m_{Z_d} = 15$ GeV, the step shifts are attributable to a transition from the LM to the HM analysis. Reprinted/adapted with permission from Ref. [1]. 2022, Physica Scripta, Th. Lagouri.

The normalization of the non-resonant $ZZ^* \to 4l$ background is checked using control samples for limits involving ZX processes, but the normalization of the remaining significant background, $H \to ZZ^* \to 4l$, is left to float as an unconstrained nuisance parameter in the limit determination. Figure 22a depicts the model-independent efficiency within the fiducial region, whereas Figure 23 depicts the 95% CL upper limit on the fiducial region cross section. Figure 22b shows the fiducial region acceptance for the $H \to ZZd \to 4l$ process, while Figure 24 shows the upper limits on the product of the total cross section and decay branching ratio for the benchmark models $\sigma(gg \to H \to ZZd \to 4l)$ and $\sigma(gg \to H \to Za \to 2l2\mu)$.

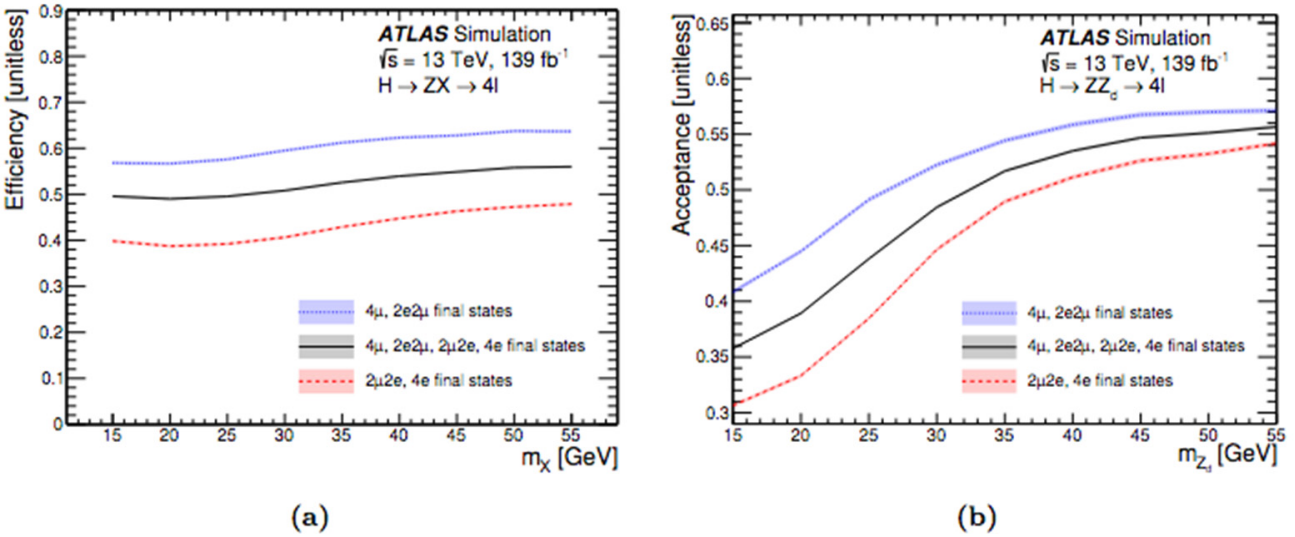

Figure 22. (**a**) Model-independent efficiencies ϵc for the $H \to ZX$ process calculated in the fiducial volumes for various combinations of the final state. (**b**) For different combinations of the final state, model-dependent per-channel fiducial region acceptances for the $H \to ZZd$ $4l$ process. Reprinted/adapted with permission from Ref. [1]. 2022, Physica Scripta, Th. Lagouri.

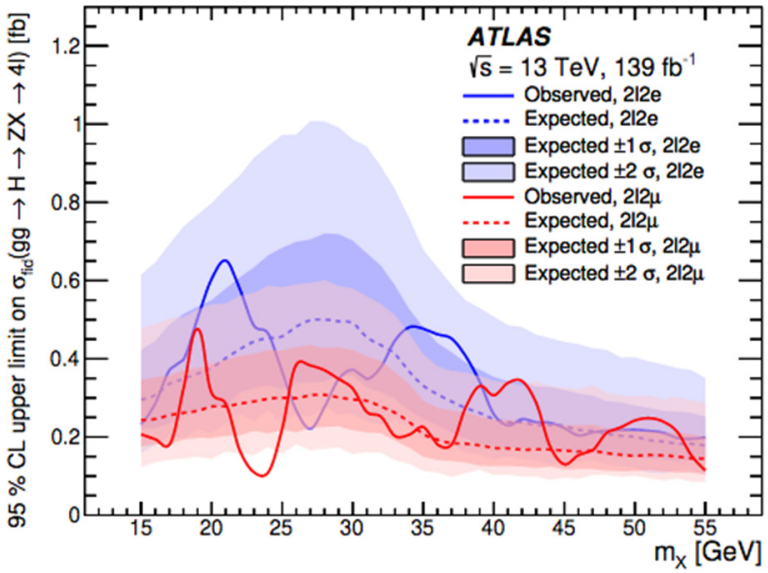

Figure 23. Per-channel upper limit on the fiducial cross section for the $H \to ZX \to 4l$ process at 95% CL. Reprinted/adapted with permission from Ref. [1]. 2022, Physica Scripta, Th. Lagouri.

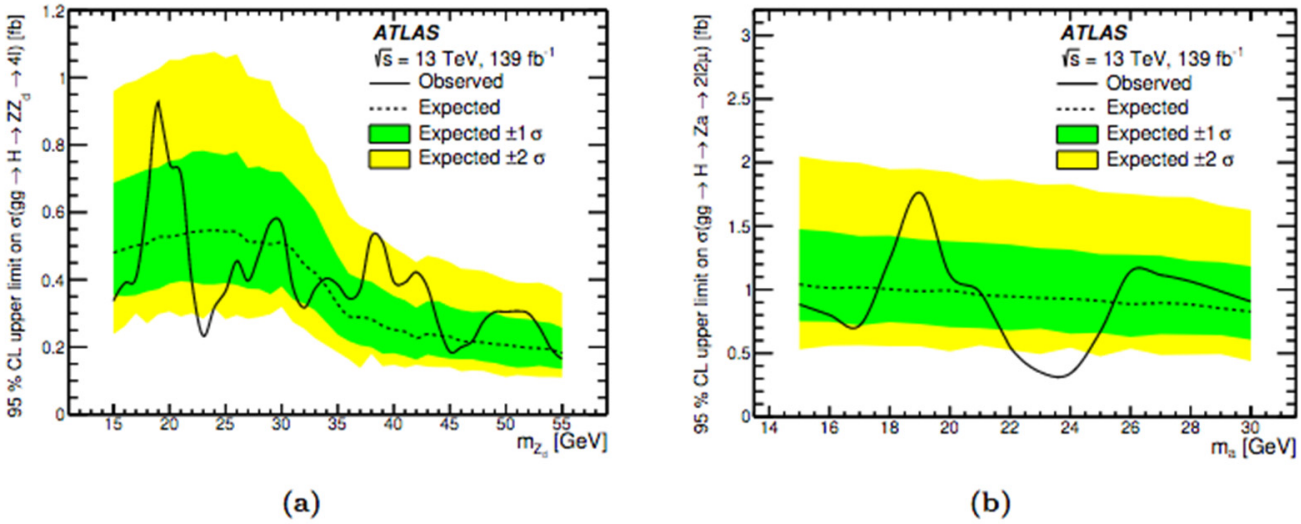

Figure 24. Upper limits observed and expected for the cross sections of the (**a**) $H \to ZZd \to 4l$ and (**b**) $H \to Za \to 2l2\mu$ processes at 95% CL, assuming SM Higgs boson production via the gluon-gluon fusion process. HAHM parameters were set to $\varepsilon = 10^{-4}$ and $\kappa = 10^{-10}$. All final states are combined. Reprinted/adapted with permission from Ref. [1]. 2022, Physica Scripta, Th. Lagouri.

Limits on Branching Ratios

The following relations can be used to convert a (model-dependent) cross-section limit to a branching ratio limit:

$$\mathrm{BR}(H \to XX \to 4l) = \sigma(H \to XX \to 4l)/\sigma(H) \quad (1)$$

$$\mathrm{BR}(H \to XX) = \mathrm{BR}(H \to XX \to 4l)/[\Sigma l_{1=e,\mu}\, \Sigma l_{2=e,\mu}\, \mathrm{BR}(H \to X \to 2l_1)\, \mathrm{BR}(H \to X \to 2l_2)] \quad (2)$$

where $\sigma(H \to XX \to 4l)$ represents the model-dependent total cross section, $\sigma(H)$ is the SM Higgs boson production cross section for the ggF process (48.58 pb for $m_H = 125$ GeV), and $\mathrm{BR}(X \to 2l)$ is the model-dependent branching ratio for each decay to one lepton flavor. The branching ratios for $Zd \to ll$ and $a\mu\mu$ are taken from benchmark models [28,29], where the

branching ratios for the two lepton flavors are assumed to be equal in the $Zd \to ll$ case. Over the range of m_a studied here, the branching ratio for the $a \to \mu\mu$ case varies significantly in a model-dependent manner. The branching ratio limits that arise are provided in Figure 25.

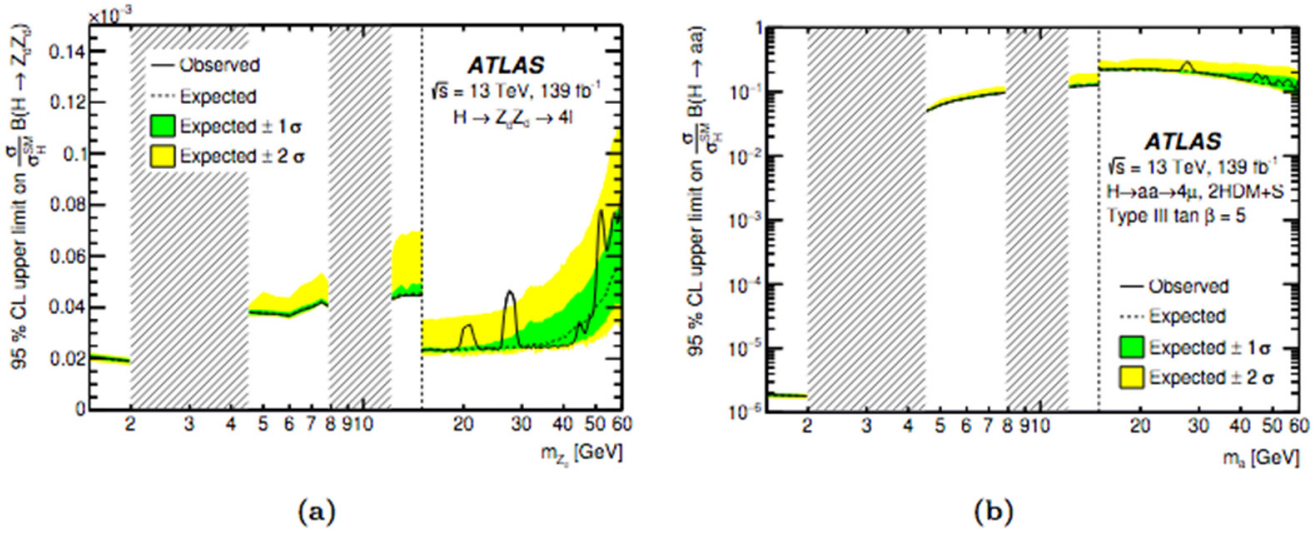

Figure 25. For (**a**) the $H \to ZdZd$ process for the benchmark HAHM with $\kappa = \varepsilon = 10^{-4}$ and (**b**) the $H \to aa$ process for the benchmark 2HDM+S model, 95% CL upper bounds on the cross section times the model-dependent branching ratio divided by the SM Higgs boson production cross section. The quarkonia veto regions are the shaded zones. At $m_{Z_d} = 15$ GeV, the step shifts are attributable to a change from the LM to the HM analysis. Reprinted/adapted with permission from Ref. [1]. 2022, Physica Scripta, Th. Lagouri.

Limits on Mixing Parameters

The branching ratio limit can also be interpreted as a limit on the effective Higgs mixing parameter κ', which is defined as

$$\kappa' = \kappa \frac{m_H^2}{|m_H^2 - m_S^2|}$$

where κ is the Higgs portal coupling and m_S is the mass of the dark Higgs boson. The dependencies on κ and m_s are combined into a single parameter when you use κ' instead of κ. Then, using Equation (2.33) of Ref. [25] and assuming $m_S > m_H/2$:

$$\kappa'^2 = \frac{\Gamma_{SM}}{f(m_{Z_d})} \frac{BR(H \to Z_d Z_d)}{1 - BR(H \to Z_d Z_d)}$$

where Γ_{SM} is the *SM* width of the 125 GeV Higgs boson,

$$f(m_{Z_d}) = \frac{v^2}{32\pi m_H} \sqrt{1 - \frac{4m_{z_d}^2}{m_H^2}} \frac{(m_H^2 + 2m_{Z_d}^2)^2 - 8\left(m_H^2 + m_{Z_d}^2\right) m_{Z_d}^2}{m_H^4}$$

and $v \approx 246$ GeV is the vacuum expectation value of the Higgs field. Figure 26 shows the resulting limit.

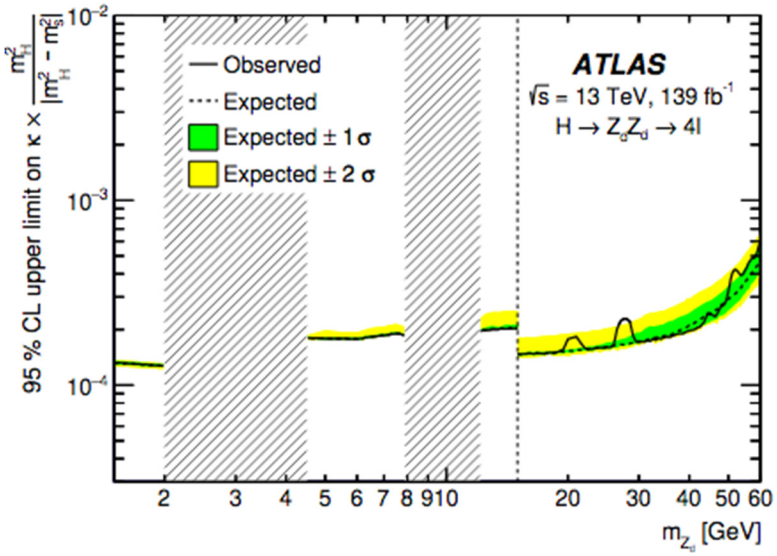

Figure 26. The upper limit at 95% CL on the effective Higgs mixing parameter $\kappa' = \kappa m_H^2 / |m_H^2 - m_S^2|$, with ε set to 10^{-4}. The change in selection from the *LM* to the *HM* analysis causes the step change at m_{Z_d} = 15 GeV. The quarkonia veto regions are shaded areas. Reprinted/adapted with permission from Ref. [1]. 2022, Physica Scripta, Th. Lagouri.

As mentioned in Ref. [28], the $H \to ZZd$ analysis can also be utilized to determine limits on the Zd mixing parameter, ϵ, and the Z-Zd mass mixing parameter, δ. Assuming the SM Higgs boson production cross section, they are displayed in Figure 27.

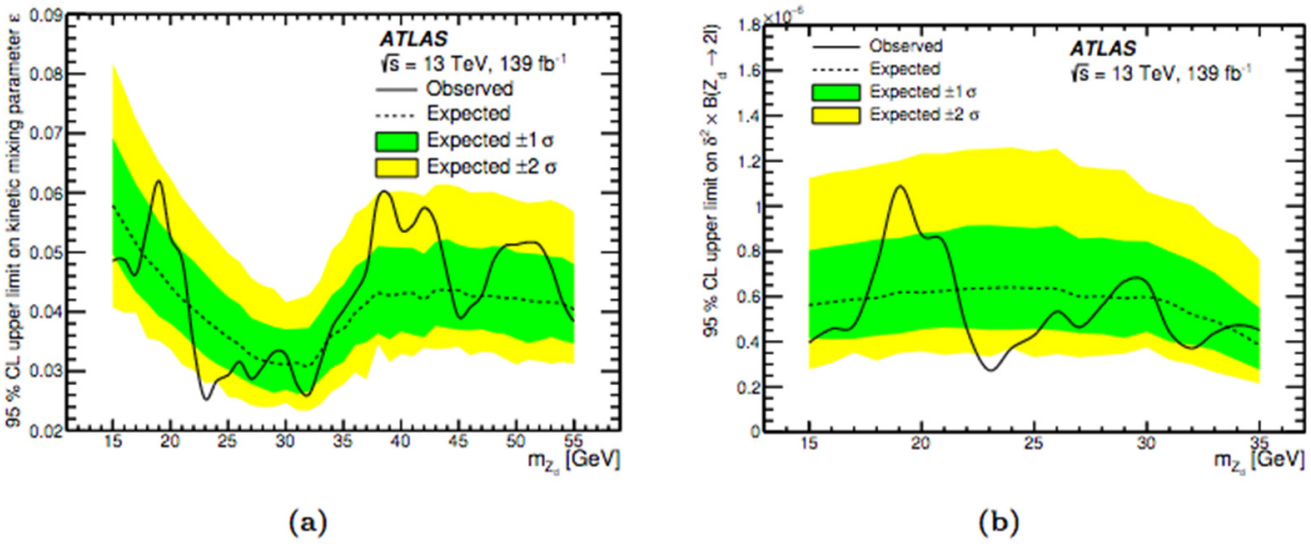

Figure 27. Using the SM Higgs boson production cross section, the upper limit at 95% CL on (**a**) the Zd mixing parameter ε, κ set to 10^{-10} and (**b**) the Z-Zd mass mixing parameter $\delta^2 \times BR(Zd \to ll)$. Reprinted/adapted with permission from Ref. [1]. 2022, Physica Scripta, Th. Lagouri.

4.1.2. Search for a Low-Mass Di-Lepton Resonance in Higgs Decays to Four Leptons with CMS at $\sqrt{s}$ = 13 TeV

The CMS Collaboration [42] is conducting a generic search for a low mass dilepton resonance in Higgs boson decays in the four-lepton final state. Two new particles (BSM) or one new particle in combination with a Z boson are assumed to be involved in the decay.

Using a sample of pp collision data at a center-of-mass energy of 13 TeV at LHC acquired by the CMS experiment in 2016, 2017, and 2018, this analysis searches for generic exotic Higgs boson decay signatures $H \to ZX$ or $H \to XX$ in the four-lepton final state. The

integrated luminosity of the examined data sample is 137 fb^{-1}. X is a hypothetical BSM particle that could decay into two "opposite-sign same-flavor" (OSSF) leptons. Many physics models outside of the SM propose such decays. Two unique BSM models were investigated in this search. Leptonic decays of X and Z to "di-electrons" or "di-muons" produce the $4e$, 4μ, and $2e2\mu$ end states in both models.

Only the mass range $m_X < 35$ GeV ($m_X < m_H/2 \approx 62.50$ GeV) is kinematically viable for $H \to ZX$ ($H \to XX$) assuming on-shell decays. The signal-to-background ratio of the decay channel $pp \to H \to 4l$ is quite high. The kinematics of the Higgs boson can be completely reconstructed using final-state decay particles thanks to this clean channel. BSM can also offer hints to unusual Higgs boson decays through this pathway. The mass range considered in this study is $4 < m_X < 35$ GeV ($4 < m_X < 62.5$ GeV).

The first model, called the "dark photon model," is concerned with theories that include a hidden "dark" sector [28], with X serving as the dark photon in the model (Zd). A dark Higgs process spontaneously breaks a dark $U(1)_D$ gauge symmetry, which is mediated by the dark photon Zd. The dark sector can interact with SM particles via a "hypercharge portal" (by the "kinematic mixing coupling", ε) or a "Higgs portal" (via the "Higgs mixing coupling", κ) [28] contains further information on this theory and its phenomenological implications. Several collider experiment collaborations have already searched for Zd, including ATLAS [35,36] and LHCb [43]. Other experiments, such as beam dumps, fixed target experiments, helioscopes, and cold dark matter searches, provide further dark photon sensitivities.

ALPs (axion-like particles) are used in the second model, with X being a "gauge singlet pseudoscalar" (a). ALPs were first proposed to solve the "strong CP problem", but they were recently offered to explain the observed anomaly in the muon's magnetic moment. The model is expressed as an ALP-coupled effective field theory with numerous SM particles. The theory, in particular, permits coupling between the Higgs boson, Z boson, and the ALP field, or the Higgs boson and the ALP field, as represented by the "Wilson coefficient" $C^{eff}{}_{ZH}/$and $C^{eff}{}_{aH}/\Lambda^{2}$, respectively, where Λ is the effective field theory's decoupling energy scale. The exotic decay of $H \to Za$ ($H \to aa$) is caused by the former (later) coupling. Several experimental searches for $H \to aa$ have been carried out, but no similar search for $H \to Za$ has yet been carried out. This search adds to the coverage of the ALP model's phase spaces, notably for high ALP masses.

There is no significant deviation from the SM expectation. Model-independent cross sections and Higgs boson decay branching fractions have upper limits set at a 95% confidence level. Limits on dark photon and axion-like particle models are also discussed.

Analysis Event Selection

In the ZX and XX event topologies, a set of constraints is implemented to maximize the sensitivity of searches for a potential signal. At least four well-identified and separated leptons from the primary vertex, potentially accompanied by an FSR photon, are required in both searches. $\Delta R(l_i, l_j) > 0.02$ must be used to isolate all four leptons from one another. To satisfy $p_T > 20$ GeV ($p_T > 10$ GeV), the (sub-)leading lepton p_T is required. The mass of the four-lepton invariant m_{4l} must be between 118 GeV and 130 GeV. All opposite-charge lepton pairs, regardless of lepton flavor, must meet $m_{ll} > 4$ GeV to further decrease background contributions from hadron decays in jet fragmentation or from the decay of low-mass resonances.

ZX dilepton pair candidates are produced by pairing all leptons with the same flavor, and opposite charge for each event evaluated in the ZX and XX searches. Each ZX candidate must have a dilepton invariant mass m_{ll} within $4 < m_{ll} < 120$ GeV. The narrow mass window ($8.5 < m_\Upsilon < 11.0$ GeV) around the Υ states is ruled out. The ZX or XX event candidate is formed by pairing two dilepton candidates. Z_1 is the opposite charge dilepton pair with the invariant mass closest to the Z boson mass (representing Z in ZX) for the ZX search, and Z_2 is the other pair (X). Z_1 is the same flavor, opposite charge dilepton pair with the largest invariant mass in the XX search, while Z_2 is the lower mass pair. The XX candidate with the least $(m_{Z1} - m_{Z2})/(m_{Z1} + m_{Z2})$ is chosen for situations where alternate pairings of

XX candidates are possible. The ZX search requires m_{Z1} to be greater than 40 GeV, and m_{Z1} and m_{Z2} must be between 4 and 62.5 GeV for the XX search.

Four final-state lepton categories can be defined, 4μ, $2\mu 2e$, $4e$, and $2e2\mu$, with the dilepton labels in the order of the lepton flavor for Z_1 and Z_2, respectively. Alternative pairings of the four leptons marked Z_a and Z_b are available for the 4μ and $4e$ final states. To suppress background contributions from on-shell Z and a low-mass dilepton resonance, events with $m_{Zb} < 12$ GeV and m_{Za} closer to the Z boson mass than Z_1 are eliminated for the ZX search. The invariant masses from alternate pairings in the 4μ and $4e$ channels are not required for the XX search.

- Background Estimation

"Irreducible background estimation": Irreducible backgrounds for this search arise from SM Higgs boson processes, including gluon fusion, vector boson fusion, associated production with top pair and vector boson, production of ZZ via quark-antiquark annihilation or gluon fusion, and rare backgrounds such as $t\bar{t}$+Z and triboson production. Simulation is used to estimate these backgrounds.

"Reducible Background estimation": In the $4l$ final state, reducible backgrounds can emerge from leptonic decays of heavy-flavor hadrons, in-flight decays of light mesons within jets, and charged hadrons misidentified as electrons when near a π^0. The Z+jets method is principally responsible for these backgrounds. $t\bar{t}$, $Z\gamma$, and WZ are some of the other physical processes that create these backgrounds.

Results

Figures 28 and 29 illustrate the distributions for the ZX and XX selections, respectively. Within the allocated uncertainty, the observed distributions agree well with expectations in all cases. There is no evidence of a major deviation from the SM background prediction.

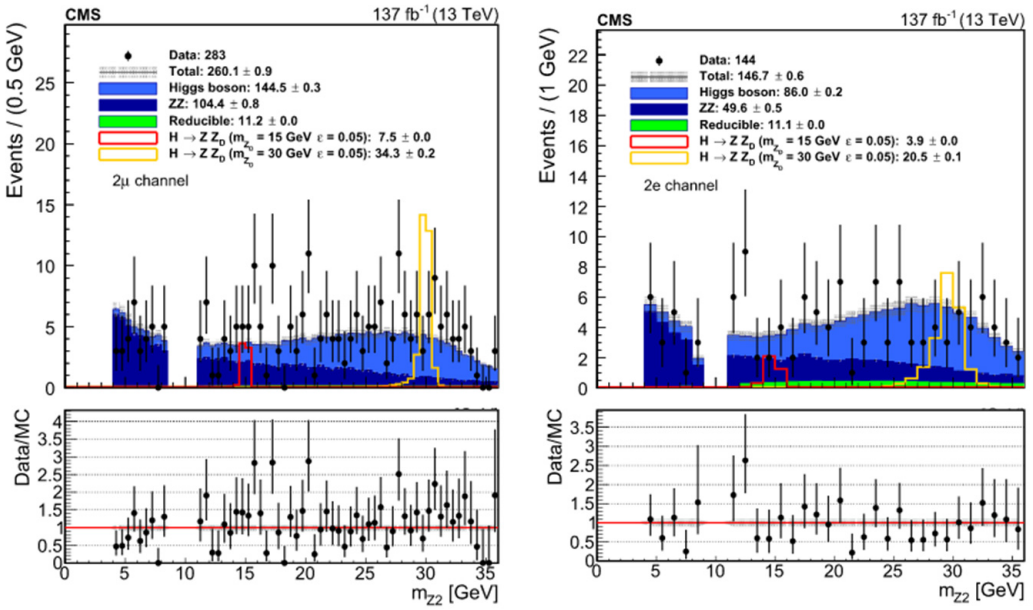

Figure 28. Event yields for the muon and electron channels against m_{Z2} using the ZX option. The overall event yields with the ZX selection corresponding to data, as well as the expected yields for each background and signal process, as well as the statistical uncertainty resulting from the amount of simulated data, are shown in the legend. Reprinted/adapted with permission from Ref. [1]. 2022, Physica Scripta, Th. Lagouri.

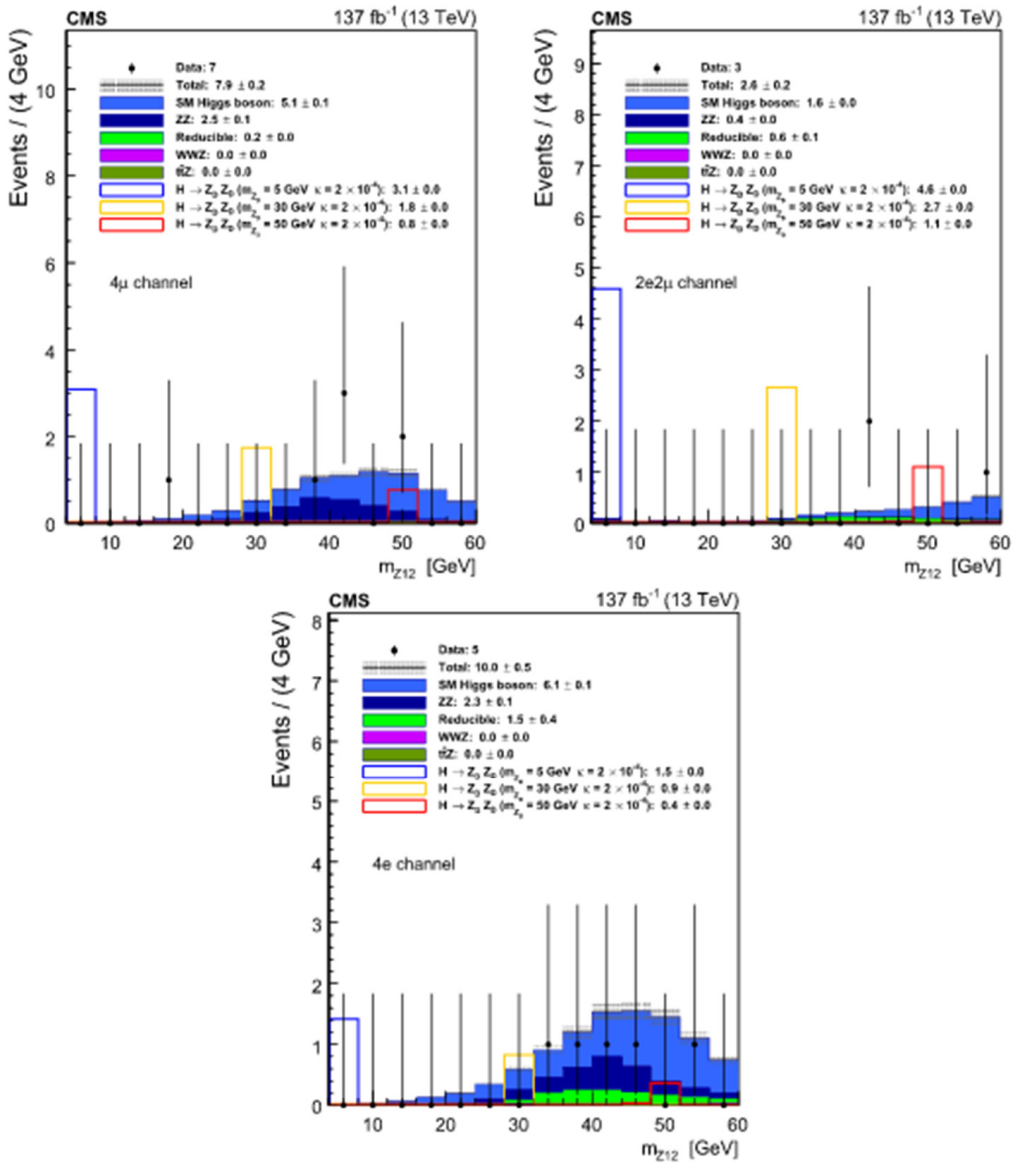

Figure 29. For the 4μ, $2e2\mu$, and $4e$ final states, event yields on $(m_{Z1} + m_{Z2})/2$ with the XX selection. The total event yields are shown in the legend, with the XX selection corresponding to data, as well as the expected yields for each background and signal process, as well as the statistical uncertainty resulting from the amount of simulated data. Reprinted/adapted with permission from Ref. [1]. 2022, Physica Scripta, Th. Lagouri.

These findings are then used to set upper limits on model-independent branching fractions and dark photon model parameters (and ALP models).

- Model-Independent Limit

Upper limits of 95% CL are calculated using "model-independent" branching fractions with the ZX and XX selections, assuming three decay scenarios: flavor "democratic" decay of X to a muon or an electron pair, exclusive X decays to a muon pair, and exclusive X decays to an electron pair. After event selections, acceptance effects deriving from various signal models are added as systematic uncertainty on the signal yields. Because the event selection is not optimized using angular correlations between the leptons, there should be little model dependency. With the ZX and XX choices, the exclusion limits on the model-independent branching fractions are shown in Figures 30 and 31.

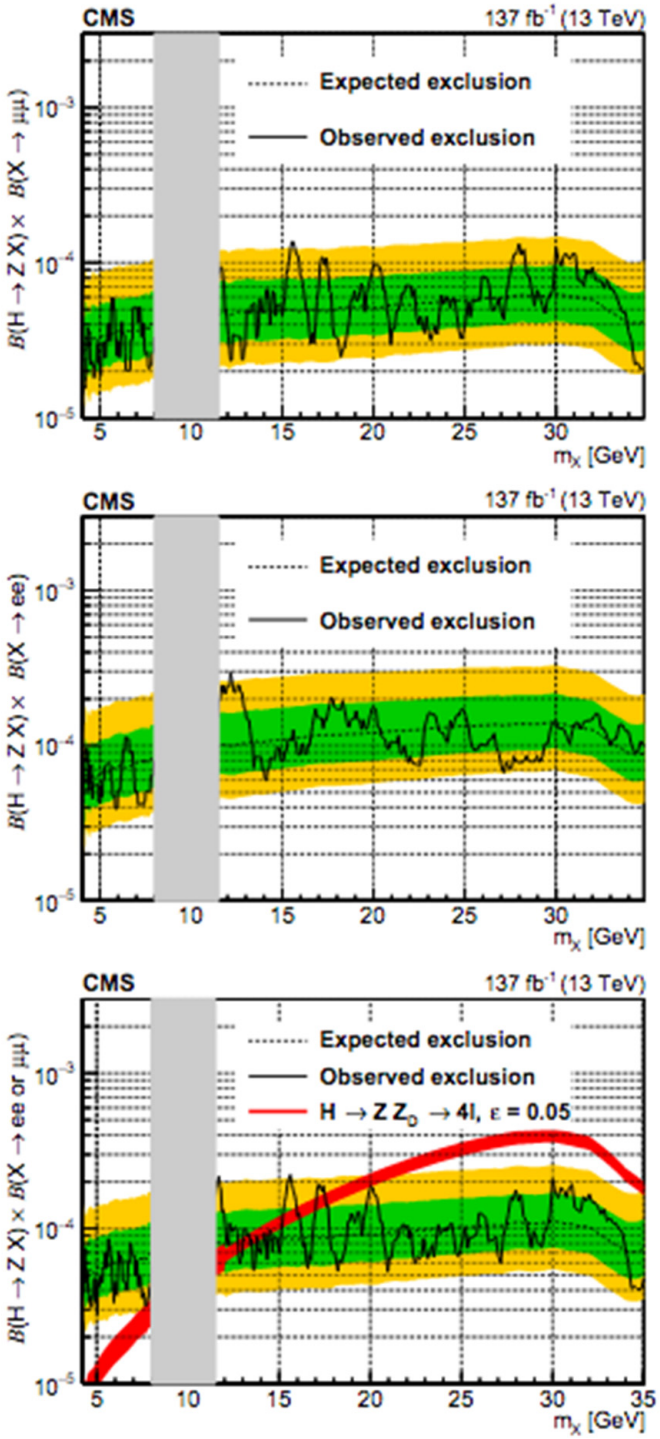

Figure 30. Expected and observed 95% CL limits on $B(H \to ZX)B(X \to \mu\mu)$ if X decays to dimuons only, $B(H \to ZX)B(X \to ee)$ if X decays to dielectrons exclusively, and $B(H \to ZX)B(X \to ee \text{ or } \mu\mu)$ if X decays to dielectrons and dimuons equally. The expected upper limit is displayed in dashed black, with one and two standard-deviation bands in green and yellow, respectively. The observed upper limit is represented by the solid black curve. The theoretical cross section for the signal process $H \to ZX \to 4l$ is represented by the red curve. The switch from experimental to theoretical uncertainty estimates of $B(Zd \to ee \text{ or } \mu\mu)$ causes a discontinuity in the uncertainty at 12 GeV (as described in [42]). The kinetic-mixing parameter is denoted by the symbol ε. The grey band represents the excluded region of Y around the $b\bar{b}$ bound states. Reprinted/adapted with permission from Ref. [1]. 2022, Physica Scripta, Th. Lagouri.

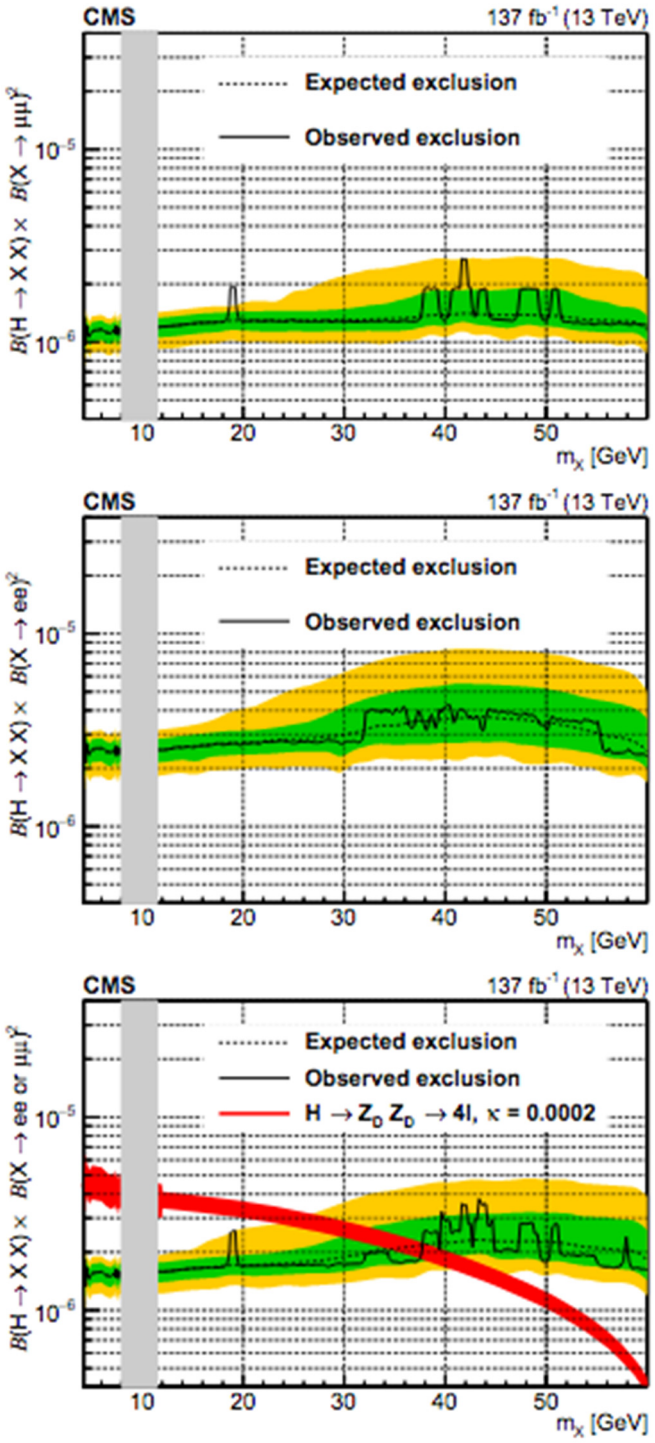

Figure 31. Expected and observed 95% CL limits for $B(H\to XX)$x$B(X\to ee$ or $\mu\mu)^2$ assuming a democratic decay of X to dielectron and dimuons, B $(H\to XX)B(X\to\mu\mu)^2$ assuming X decays to dimuons exclusively, and $B(H\to XX)$x$B(X\to ee)^2$ assuming X decays to di-electrons alone. The expected upper limit is displayed in dashed black, with one and two standard-deviation bands in green and yellow, respectively. The observed upper limit is represented by the solid black curve. The theoretical cross section for the signal process $H\to XX\to 4l$ is represented by the red curve. The switch from experimental to theoretical uncertainty estimates of $B(Zd\to ee$ or $\mu\mu)$ causes a discontinuity in the uncertainty at 12 GeV (as described in [42]). The Higgs-mixing parameter is represented by the symbol κ. The grey band represents the excluded region around the $b\bar{b}$ bound states of Υ. Reprinted/adapted with permission from Ref. [1]. 2022, Physica Scripta, Th. Lagouri.

- Limit on Dark Photon Model Parameters

As shown in Figure 32, upper limits at a 95% confidence level are determined using the "Higgs mixing parameter", κ, and $B(H \rightarrow ZdZd)$ with the XX selection, assuming $\kappa >> \varepsilon$. The postulated branching fractions $B(Zd \rightarrow$ ee or $\mu\mu)$ are determined in [29]. Experimental data of $R_{\mu\mu}/R_{had}$ up to m_{Zd} = 12 GeV and a "next-to-leading order" theory calculation for m_{Zd} > 12 GeV are used in the calculations. To account for these impacts, this estimate for m_{Zd} < 12 GeV (m_{Zd} >12 GeV) has been provided a cautious 20% (10%) uncertainty. Due to the presence of the Higgs boson, the LHC has a particular sensitivity to the parameter. Furthermore, our analysis provides some sensitivity to the "kinematic mixing parameter", ε, although the upper bounds are nearly an order of magnitude smaller than those obtained from the Drell–Yan search and the LHCb Collaboration.

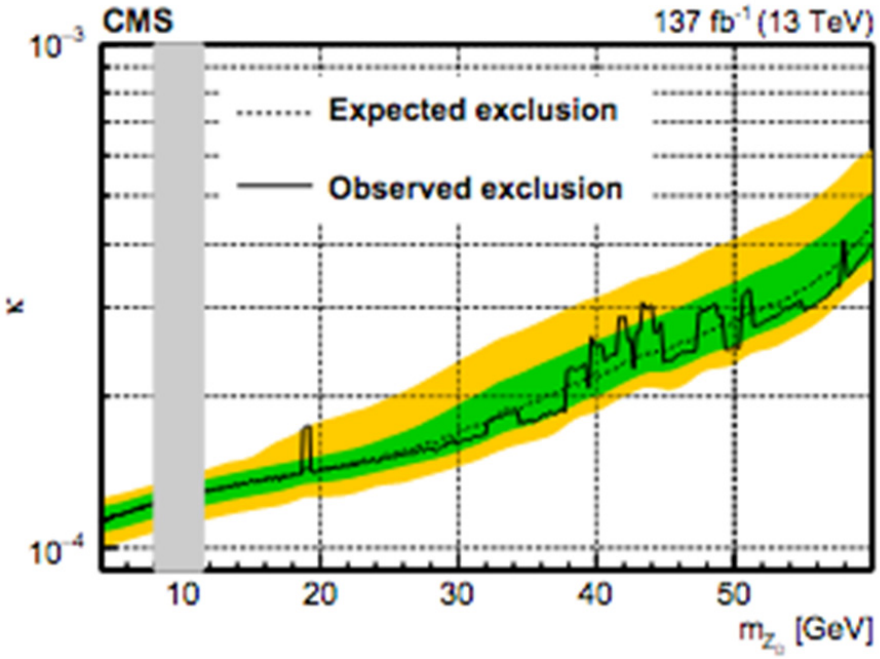

Figure 32. Expected and observed 95% CL limits on κ as a function of m_{ZD}, based on the XX selection. The expected upper limit is displayed in dashed black, with one and two standard-deviation bands in green and yellow, respectively. The observed upper limit is represented by the solid black curve. Reprinted/adapted with permission from Ref. [1]. 2022, Physica Scripta, Th. Lagouri.

Upper limits at a 95% confidence level are calculated on the "Higgs mixing parameter" κ and B($H \rightarrow ZdZd$) with the XX selection, as shown in Figure 32, assuming $\kappa >> \varepsilon$. Branching fractions $B(Zd \rightarrow ee$ or $\mu\mu)$ assumed are calculated in [29]. The calculations are based on experimental measurements of $R_{\mu\mu}/R_{had}$ up to m_{Zd} = 12 GeV and a "next-to-leading order" theory calculation for m_{Zd} > 12 GeV. To account for these effects, a conservative 20% (10%) uncertainty is assigned to this estimate for m_{Zd} < 12 GeV (m_{Zd} > 12 GeV). LHC provides unique sensitivity to the parameter κ due to the presence of the Higgs boson. In addition, this analysis provides some sensitivity to the "kinematic mixing parameter" ε, but the upper limits are almost an order of magnitude weaker than those from the Drell–Yan search and from the LHCb Collaboration and hence are not reported.

Strong upper limits are set on two relevant "Wilson coefficients", $C^{eff}{}_{ZH}/\Lambda$ and $C^{eff}{}_{aH}/\Lambda^2$, for the axion-like particle model, encompassing the parameter space in which the axion-like particle can explain the "muon anomalous magnetic moment (see Figure 33).

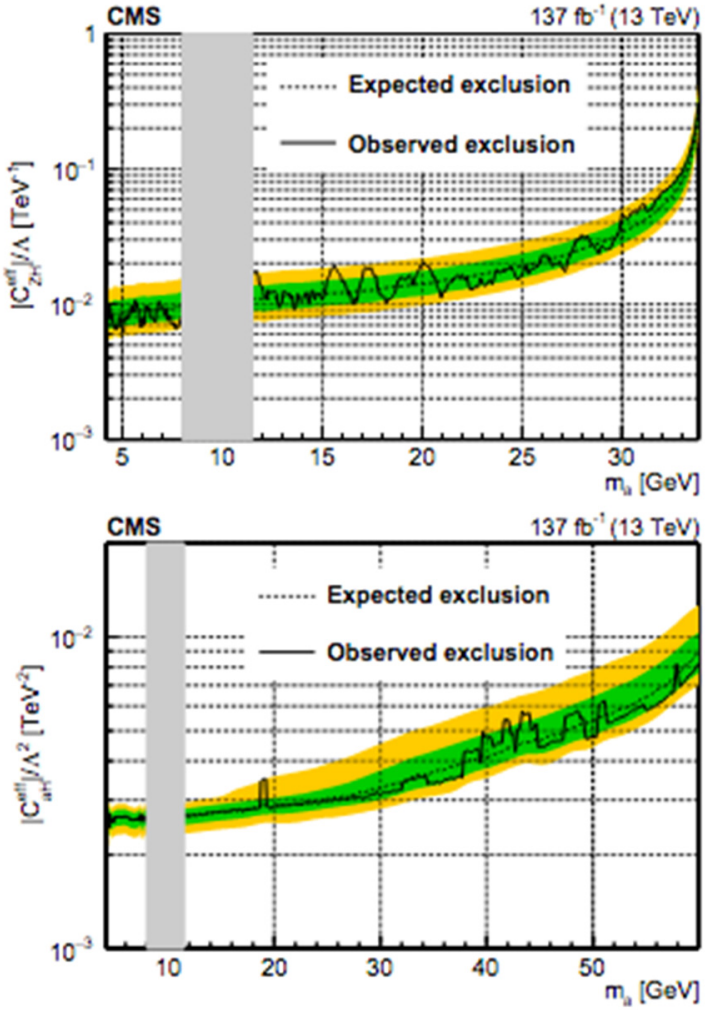

Figure 33. Exclusion limits on $C^{eff}{}_{ZH}/\Lambda$ (**top**) and $C^{eff}{}_{aH}/\Lambda^2$ (**bottom**) in the case of democratic decays of the ALP to dimuons and dielectrons as a function of m_a at 95% CL. As a function of m_a, the expected and observed 95% CL limit on $C^{eff}{}_{aH}/\Lambda$ and $C^{eff}{}_{aH}/\Lambda^2$. The expected upper limit is displayed in dashed black, with one and two standard-deviation bands in green and yellow, respectively. The observed upper limit is represented by the solid black curve. Reprinted/adapted with permission from Ref. [1]. 2022, Physica Scripta, Th. Lagouri.

4.2. Higgs Dacays Dark (Massless) Photon (ATLAS, CMS)

4.2.1. Dark ("Massless") Photon in ZH Events with CMS at $\sqrt{s}$ = 13 TeV

The CMS Collaboration proposed a search in [44] for a Higgs boson that is produced in association with a Z boson and decays to an undiscovered particle along with an isolated photon. A data collection with an integrated luminosity of 137 fb^{-1} was used to conduct the search, which was recorded at a center-of-mass energy of 13 TeV. The findings were explained using a theoretical scenario in which the undetected particle is a "massless" dark photon. These are the first results on Higgs boson decays to final states that include a massless dark photon that was previously undetectable.

Several BSM models predict Higgs boson decay to particles and photons that are undetectable [28]. The intended final state in this search is $Z((\rightarrow ll)\ H(\rightarrow \gamma\gamma_D)$, where $l = e$, μ, and γ_D is a massless dark photon that couples to the Higgs boson through a charged dark sector and goes undetected in the CMS detector. B ($H\rightarrow$invisible + γ), the branching fraction to such an invisible particle and a photon, can be as high as 5% and be consistent with all model parameters and existing LHC constraints. Figure 34 depicts a Feynman diagram for such a process. While the main focus is on the case where the production

cross section (σ_{ZH}) is assumed to be the same as for the SM-like Higgs boson with a mass of 125 GeV, the same analysis is also used to search for heavy neutral Higgs bosons with masses ranging from 125 to 300 GeV, because similar decays are also possible for potential non-SM scalar bosons.

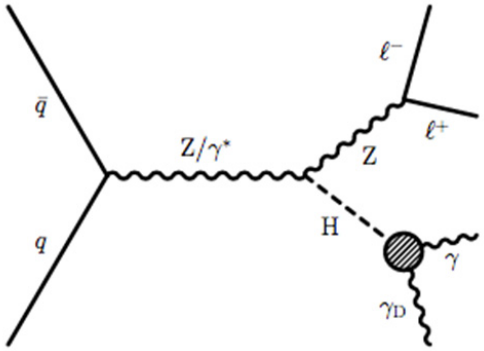

Figure 34. The production $Z(\rightarrow ll)H(\rightarrow \gamma\gamma_D)$ final state is depicted in a Feynman diagram. Reprinted/adapted with permission from Ref. [1]. 2022, Physica Scripta, Th. Lagouri.

The primary backgrounds in this analysis come from *WZ* and *ZZ* production, where an electron is misidentified as a photon, or extra leptons are not identified because they fail the lepton identification requirements or the kinematic selections. The invariant mass of the lepton pair falls within the *Z* boson mass window in the second set of backgrounds due to *WW* and top quark production. Other multi-boson production processes, such as $Z\gamma$, also make minor contributions. A binned maximum-likelihood fit to numerous signal and control regions is conducted to improve the discrimination between the prospective signal and the remaining background processes.

Analysis Event Selection

"Two same-flavor oppositely-charged" (SFOC) high p_T isolated leptons, electrons, or muons, consistent with a *Z* boson decay, large ${p_T}^{miss}$, an isolated high p_T photon, and negligible "jet activity" make up the signal topology. The signal cross section is several orders of magnitude lower than that of the principal "reducible" background processes; therefore, obtaining a sample of acceptable purity necessitates careful selection. A "leading" ("sub-leading") lepton with $p_T > 25$ (20) GeV and at least one photon with transverse momentum ${p^\gamma}_T > 25$ GeV are required to match the anticipated topology. The di-lepton mass must be compatible with that of a *Z* boson within 15 GeV of the pole mass m_Z to reduce background processes when the lepton pair is not from the decay of a *Z* boson.

A ${p_T}^{miss}$ greater than 110 GeV and transverse momentum of the dilepton system ${p^{ll}}_T$ greater than 60 GeV are required to reject the majority of the *Z* background as well as processes with little or moderate boost. In order to eliminate the background from *WZ* events with a third lepton from the *W* boson decay, events are excluded if there are any loosely identifiable leptons in addition to the two leptons that satisfy the entire selection criteria. Events are discarded if any jet passes the b-tagging selection or if there are more than two detected jets in the event in order to suppress the top quark background. Table 5 shows an overview of the selections for the analysis.

Table 5. The primary background processes and the selection criteria are summarized. Reprinted/adapted with permission from Ref. [1], 2022, Physica Scripta, Th. Lagouri.

Variable	Selection	Reject
Number of leptons	Exactly 2 leptons, p_T > 25/20 GeV	WZ, ZZ, VVV
Number of photons	≥1 photon, $p_T{}^{\gamma}$ > 25 GeV	All but Z_{γ}
$\mathbf{\mid m_{ll} - m_Z \mid}$	<15 GeV	WW, Top quark
$\mathbf{p_T{}^{miss}}$	>110 GeV	Z_{γ}
$\mathbf{p_T{}^{ll}}$	>60 GeV	Z_{γ}
b jet veto	Applied	Top quark, VVV
Jet counting	≤2	Top quark, VVV
$\mathbf{\Delta\Phi(ll,\ p_T{}^{miss} + p_T{}^{\gamma})}$	>2.5 rad	Z_{γ}
$\mathbf{\mid p_T(p_T{}^{miss} + p_T{}^{\gamma}) - p_T{}^{ll} \mid / p_T{}^{ll}}$	<0.4	Z_{γ}
$\mathbf{\Delta\Phi(jet,\ p_T{}^{miss})}$	>0.5 rad	Z_{γ}
$\mathbf{m_{ll\gamma}}$	>100 GeV	Z_{γ}
$\mathbf{m_T}$	< 350 GeV	WW, Top quark

Results

A binned maximum-likelihood fit to the m_T spectrum is used to distinguish between the potential signal and the remaining background processes. The signal spectrum has a Jacobian peak with an end-point at $m_T \sim m_H$, but the background processes either have a flat distribution or indicate an increase as m_T decreases. Because the contamination from electrons misidentified as photons is higher at large $|\eta^{\gamma}|$ values, better sensitivity is attained by evaluating events with the selected photon separately at low- and high-$|\eta^{\gamma}|$ levels. For the signal region and the $e\mu$, WZ, and ZZ control regions, each bin of the m_T distribution is divided into a low-$|\eta^{\gamma}|$ ($|\eta^{\gamma}| < 1$) and a high-$|\eta^{\gamma}|$ ($|\eta^{\gamma}| > 1$) bin in the maximum-likelihood fit.

Figure 35 shows the m_T distributions for events with $|\eta^{\gamma}| < 1$ and $|\eta^{\gamma}| > 1$ following event selection. There is a good match between the data and the background-only prediction. Upper limits for the product of σ_{ZH} and $B(H \to invisible + \gamma)$ as a function of m_H are calculated. This result can be interpreted as an upper limit on $B(H \to invisible + \gamma)$ for m_H = 125 GeV, assuming an SM Higgs boson generation rate]. The upper limits for the test statistic are derived using a modified frequentist method using the CLs criterion and an asymptotic method. On $B(Hinvisible + \gamma)$, the observed (predicted) 95% CL upper limit at m_H = 125 GeV is 4.6 $(3.6^{+2.0}{}_{-1.2})$%.

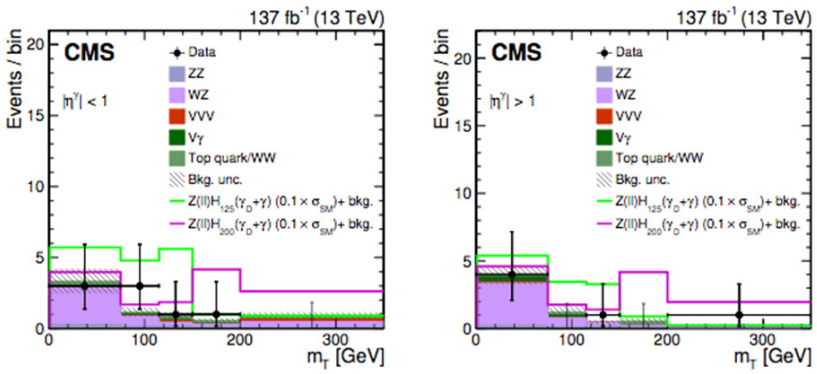

Figure 35. After fitting to data, the m_T distributions in the signal region for two m_H values for events with $|\eta^{\gamma}| < 1$ (**left**) and $|\eta^{\gamma}| > 1$ (**right**). For both m_H values presented, the signal size corresponds to 0.1 σ_{ZH}. All background processes are piled on top of the signal processes. The hatching band represents

statistical and systematic uncertainties in expected background yields. The horizontal bars reflect the bin widths, whereas the vertical bars represent the data statistical uncertainty. Reprinted/adapted with permission from Ref. [1]. 2022, Physica Scripta, Th. Lagouri.

Figure 36 shows the expected and observed cross-section upper limits on the product of σ_{ZH} and B ($H_{invisible}$ +γ) as a function of m_H at 95% CL. As m_H increases from 125 to 300 GeV, exclusion limits on the product of σ_{ZH} and B($H_{invisible}$ +γ) range from ~40 to ~4 fb at 95% CL. These restrictions also apply to other models in which a scalar particle decays into a photon and light invisible particles.

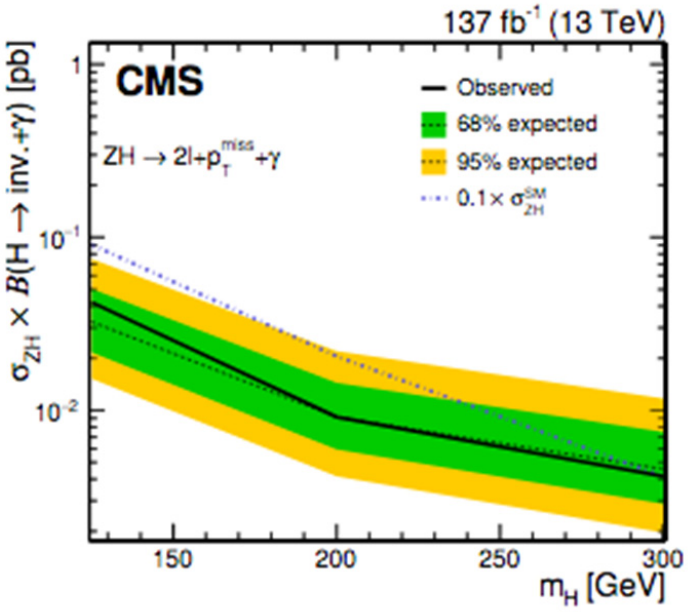

Figure 36. Expected and observed upper limits on the product of σ_{ZH} and $B(H \to invisible + \gamma)$ as a function of m_H at 95% CL. The "dot-dashed" line is the expected signal for 0.1 σ_{ZH}. Reprinted/adapted with permission from Ref. [1]. 2022, Physica Scripta, Th. Lagouri.

4.2.2. Dark (Massless) Photon in VBF Higgs Events with CMS at $\sqrt{s}$ = 13 TeV

The CMS Collaboration presents a search for a Higgs boson H produced by vector boson fusion (VBF) and decaying to an undiscovered particle and an isolated photon in [45]. The search is based on data from 2016 to 2018 that correspond to an integrated luminosity of 130 fb^{-1} and were collected at a center-of-mass energy of 13 TeV. The findings are explained using a theoretical scenario in which the undetected particle is a "massless" dark photon. This is the first time such decays have been looked for in the vector boson fusion channel.

Several BSM models predict such Higgs boson decays [28]. The target channel in this search is $qqH(\to\gamma\gamma_D)$, in which the final-state quarks (q) are produced by the VBF process, and γ_D is a massless dark photon that couples to the Higgs boson through a dark sector. The dark photon manages to go away undetected. Figure 37 depicts a Feynman diagram of this operation. $B(H \to inv.+\gamma)$, the branching fraction for a Higgs boson decaying to such an invisible particle and a photon, might be as high as 5% while yet remaining consistent with present experimental limits. While the search is primarily focused on VBF production, the additional contribution from gluon fusion production (ggH) is significant if initial-state gluon radiation matches the experimental signature of the VBF process. As a result, the ggH process is also taken into account for the SM Higgs boson. Additionally, for heavy neutral Higgs bosons with masses between 125 and 1000 GeV, a model-independent search for VBF production is carried out because analogous decays are also feasible for probable non-SM scalar bosons.

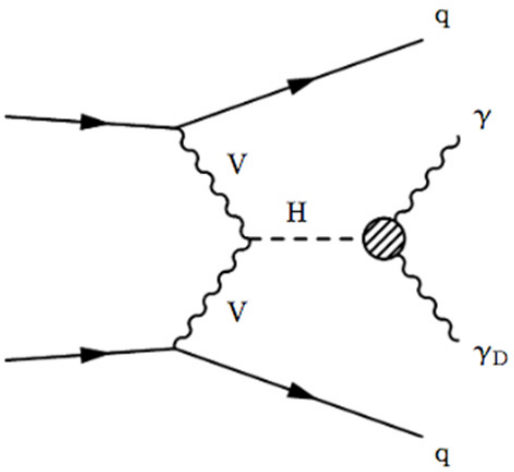

Figure 37. The VBF production of the $qqH((\rightarrow\gamma\gamma_D)$ final state is depicted in a Feynman diagram. Reprinted/adapted with permission from Ref. [1]. 2022, Physica Scripta, Th. Lagouri.

Analysis Event Selection

A Higgs boson is accompanied by two jets with a large pseudorapidity separation ($|\Delta\eta_{jj}|$) and a large dijet mass in the VBF production mode (m_{jj}). Because of its distinctive signal, SM backgrounds are suppressed, making the VBF channel an extremely sensitive mode in the search for exotic Higgs boson decays. The invisible particle can recoil with high transverse momentum (p_T) against the VBF dijet system, resulting in an event with a large missing transverse momentum ($p_T{}^{miss}$), which can be utilized to pick signal-enriched samples. Two "forward" high-p_T jets, consistent with VBF production, large $p_T{}^{miss}$, and an isolated high-p_T photon make up the signal topology. The two "leading" jets must be in opposite hemispheres, with $|\Delta\eta_{jj}| > 3$ and $m_{jj} > 500$ GeV, and the so-called "Zeppenfeld" ($z_\gamma{}^*$) variable] must be 0.6 to pick the VBF topology.

Table 6 shows a summary of the signal region (SR) selection for the analysis.

Table 6. The following is a list of the selection criteria in the SR, organized by trigger path and data-taking year. Rows with a single item indicate that all data-taking years and trigger paths are subject to the same condition. Reprinted/adapted with permission from Ref. [1], 2022, Physica Scripta, Th. Lagouri.

Data-taking year	2016	2017/2018	
Trigger	VBF + γ	Single-photon	$p_T{}^{miss}$
Number of photons		≥1 photon	
$\mathbf{p_T{}^{\gamma}}$	>80 GeV	>230 GeV	>80 GeV
Number of leptons		0	
$\mathbf{p_T{}^{j1}/p_T{}^{j2}}$		>50 GeV	
$\mathbf{p_T{}^{miss}}$	>100 GeV	>140 GeV	>140 GeV
Jet counting		2–5	
$\mathbf{m_{jj}}$		>500 GeV	
$\mathbf{|\Delta\eta_{jj}|}$		>3.0	
$\mathbf{\eta_{j1}\,\eta_{j2}}$		<0	
$\mathbf{\Delta\Phi(jet,\ p_T{}^{miss})}$		>1.0 radians	
$z_\gamma{}^*$		<0.6	
$\mathbf{p_T{}^{tot}}$		<150 GeV	

The most substantial background comes from the production of $W(e\nu)$ +jets, where the photon candidate is an electron that has been misidentified. The production of a photon with a Z boson, where the Z boson decays into a neutrino-antineutrino pair ($Z(\nu\nu)+\gamma$), and the production of a photon with a W boson, where the W boson decays into a lepton–neutrino pair ($W(l\nu)+\gamma$) are the most important processes for larger values of ${p_T}^{miss}$. Initial-state QCD radiation can produce a VBF-like two-jet signature for these processes. If the charged lepton is outside the detector's acceptance, the $W(l\nu)+\gamma$ process becomes an irreducible background. Another important background process is the creation of γ+jets with a ${p_T}^{miss}$ that has been mismeasured. $Z(\nu\nu)$+jets and QCD multi-jet creation are less important background processes that can contribute to the SR when a jet is misidentified as a photon.

Results

To distinguish between the signal and the remaining background processes, a binned maximum-likelihood fit to the transverse mass of the ${p_T}^{miss}$ and photon system, m_T, is conducted after the selection. Furthermore, events in the SR and all CRs are divided into two m_{jj} regions: below 1500 GeV and above 1500 GeV. This value was chosen to guarantee that each zone receives nearly half of the VBF signal events.

Figure 38 depicts the m_T distributions in the SRs. The signal spectrum has a Jacobian peak with an end-point at $m_T \sim m_H$, but the background processes either have a flat distribution or indicate an increase as m_T decreases.

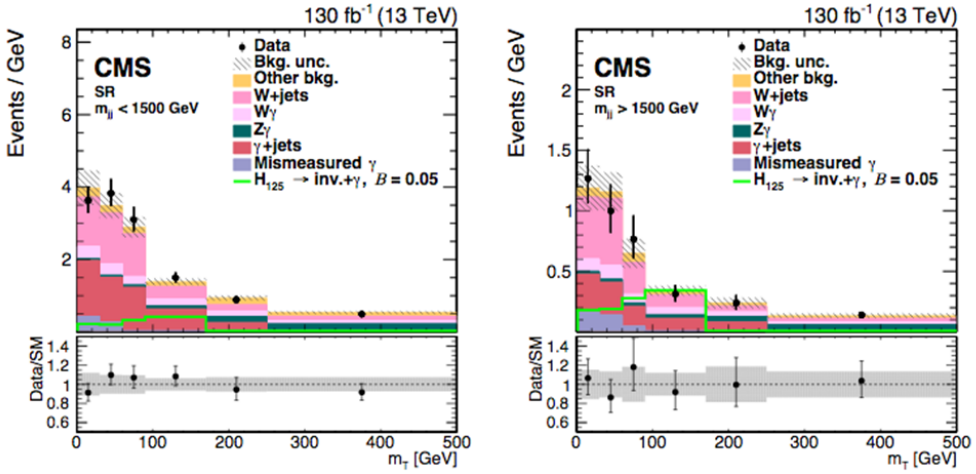

Figure 38. The simultaneous fit m_T distributions for events with m_{jj} < 1500 GeV in the SRs (**left**) and for events with m_{jj} > 1500 GeV in the SRs (**right**). Contributions from Z+jets, non-prompt, top quark, VV, and VVV processes are included in the category other background. The final bin contains overflow events. The shaded bands in the expected yields represent a combination of statistical and systematic uncertainties. The light green line depicts the potential contribution from inclusive SM Higgs boson production, assuming a branching fraction of 5% for $H \rightarrow inv.+\gamma$ decays. A per-bin ratio of the data yield and the background expectation is shown in the lower panel of the figures. The shaded band represents the background expectation's combined systematic and statistical uncertainty. Reprinted/adapted with permission from Ref. [1]. 2022, Physica Scripta, Th. Lagouri.

There is no notable excess of events over the SM background expectation. As m_H increases from 125 to 1000 GeV, the expected and observed cross-section upper limits on the product of the signal cross section σ_{VBF} for VBF production and $B(H \rightarrow inv.+\gamma)$ as a function of m_H are illustrated in Figure 39 and range from ~160 to ~2 fb.

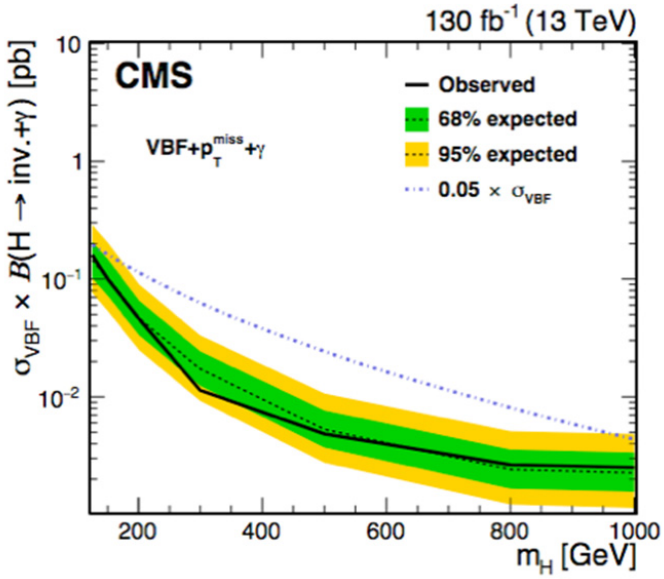

Figure 39. Expected and observed upper limits on the product of σ_{VBF} and $B(H \to inv.+\gamma)$ as a function of m_H at 95% CL. The "dot-dashed" line depicts the expected signal for 0.05 σ_{VBF} when SM couplings are assumed. Between the values obtained for the probed m_H values, a linear interpolation is conducted. Reprinted/adapted with permission from Ref. [1]. 2022, Physica Scripta, Th. Lagouri.

These limits also apply to other models in which a scalar particle decays into a photon and light invisible particles. The finding is taken as an upper limit on $B(H \to inv.+\gamma)$ for m_H = 125 GeV, assuming an SM Higgs boson production rate. In this example, the additional contribution from *ggH* production in the VBF category is taken into account, accounting for a 60% increase in signal yields and mostly contributing to the $m_{jj} < 1500$ GeV region. At m_H = 125 GeV, the measured (expected) 95% CL upper limit on $B(H \to inv.+\gamma)$ is 3.4 ($2.7^{+1.2}_{-0.8}$) %.

The results of the study [45] are paired with the results of a separate search for the same Higgs boson decay in which the Higgs boson is created in association with a *Z* boson (*ZH*) [44]. The combination is carried out using production rates for a 125 GeV SM-like Higgs boson. All experimental uncertainties are handled as correlated between the two analyses in the combination, while the rest are treated as uncorrelated. Table 7 shows the observed and expected 95% CL limits for the VBF category, ZH category, and their combination at m_H = 125 GeV on $B(H \to inv.+\gamma)$. On $B(H \to inv.+\gamma)$, the combined observed (expected) upper limit at 95% CL at m_H = 125 GeV is 2.9 (2.1%).

Table 7. Observed and expected 95% CL limits for the VBF category, *ZH* category, and their combination at m_H = 125 GeV on B(H→inv.+γ). Reprinted/adapted with permission from Ref. [1], 2022, Physica Scripta, Th. Lagouri.

VBF		ZH		VBF+ZH	
Obs. (%)	**Exp. (%)**	**Obs. (%)**	**Exp. (%)**	**Obs. (%)**	**Exp. (%)**
3.4	$2.7^{+1.2}_{-0.8}$	4.6	$3.6^{+2.0}_{-1.2}$	2.9	$2.1^{+0.9}_{-0.6}$

4.2.3. Dark Photon Search with CMS at $\sqrt{s}$ = 13 TeV: Displaced Vertex

The CMS Collaboration [46] uses a data sample corresponding to an integrated luminosity of 35.9 fb^{-1} of *pp* collisions at a center-of-mass energy of $\sqrt{s}$ = 13 TeV to look for novel light bosons decaying into muon pairs. The search requires simply the pair production of a new light boson and its subsequent decay to a pair of muons. The NMSSM model and a dark supersymmetry model with non-negligible light boson lifetimes are then used to interpret it. In both situations, the results are far better than those previously published.

The Standard Model (SM) is recognized to provide an inadequate description of particle physics, and some extensions anticipate the creation of additional light bosons. This paper presents a model-independent search for the pair production of a light boson that decays into a pair of muons. $pp \to h \to 2a + X \to 4\mu + X$, where h is a Higgs boson (SM or non-SM), a is the new light neutral boson, and X are spectator particles anticipated in numerous models, is a simple example of pair creation in pp collisions.

While production via the h boson is possible, it is not necessary for this search: all that is required is the creation of a pair of identical light bosons at a common vertex, with each light boson decaying to a pair of muons. The dimuon and new light boson production vertices are allowed to be displaced; these muon pairings are referred to as "dimuons." Because of the signature's general character, any limit placed on the product of the cross section, branching fraction to dimuons squared, or acceptance is model agnostic, allowing it to be reinterpreted in the context of specific models.

The NMSSM and SUSY models with hidden sectors (dark SUSY) are two different classes of benchmark models used to construct the study and ensure that the results are truly model independent. Two of the three charge parity (CP) even neutral Higgs bosons, h_1 or h_2, can decay to one of the two CP odd neutral Higgs bosons via $h_{1,2} \to 2a_1$ in the NMSSM benchmark models. Following that, the light boson a_1 decays to a pair of oppositely charged muons, which is comparable to $B(a_1 \to 2\mu)$.

The breakdown of a new $U(1)_D$ symmetry in the dark SUSY benchmark models results in a massive dark photon γ_D. A tiny kinetic mixing parameter, ε, with SM photons allows this dark photon to connect to SM particles. The dark photon's lifetime, and consequently its displacement, is determined by the dark photon's mass $m_{\gamma D}$. An SM-like Higgs boson h decays via $h \to 2n_1$, where n_1 is the lightest non-dark neutralino in the signal topologies examined. Both n_1 decay via $n_1 \to n_D + \gamma_D$, with n_D being a dark neutralino that is undetectable. The dark photon γ_D decays into a pair of muons with opposite charges.

This is a search for a_1 with a mass between 0.25 and 3.55 GeV for the NMSSM benchmark models. This is a search for γ_D with a mass between 0.25 and 8.5 GeV and a lifetime up to $c\tau_{\gamma D} = 100$ mm for the benchmark dark SUSY models.

Analysis Event Selection

The data were obtained using a trigger that employs muon reconstruction techniques with an efficiency of more than 80% up to the max vertex displacement (98 mm) investigated in this study [46].

Dimuons are made up of two oppositely charged muons connected by a "common vertex" and must have an "invariant mass" $m_{(\mu\mu)}$ less than 9 GeV. Each event must include exactly two dimuons. The dimuons must be derived from the same primary vertex. Each dimuon must also be properly isolated. The dimuon masses should be consistent to within five times the detector resolution because they are predicted to come from the same type of light bosons. The signal region (SR) in the two-dimensional plane of the dimuon invariant masses $m_{(\mu\mu)1}$ and $m_{(\mu\mu)2}$ is carved out by this criterion. In Figure 40, the signal region is depicted.

Most SM backgrounds with topologies similar to our signal are effectively reduced and eliminated using the signal selection criteria. As a result, the SR contribution from this analysis is likely to be quite minor. Bottom quark pair production ($b\bar{b}$), prompt double J/ψ meson decays, and electroweak production of four muons are found to have non-negligible SM backgrounds. Υ meson contributions are also studied, but they are shown to be negligible below the 8.5 GeV upper bound on the new light boson's mass. Backgrounds from cosmic rays are insignificant. In the SR, the overall background contribution is calculated to be 7.95 ± 1.12 (stat) $\pm$ 1.45 (syst) events.

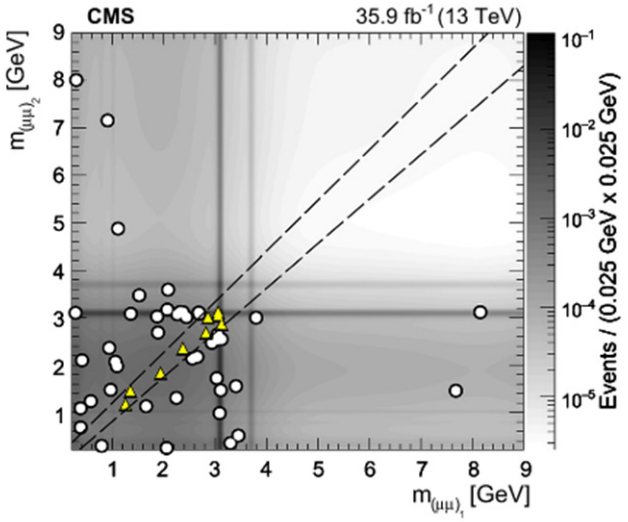

Figure 40. Distribution of the isolated dimuon systems' invariant masses $m_{(\mu\mu)1}$ vs. $m_{(\mu\mu)2}$; triangles represent data events that meet all of the selection criteria and fall within the SR $m_{(\mu\mu)1} \approx m_{(\mu\mu)2}$ (outlined by dashed lines); white bullets represent data events that meet all of the selection criteria but do not fall within the SR. In the $b\bar{b}$ background template, the grayscale heatmap depicts the normalized distribution of predicted events. Reprinted/adapted with permission from Ref. [1]. 2022, Physica Scripta, Th. Lagouri.

Results

The SR contains nine events after applying all selection criteria to the data sample. Figure 40 depicts their distribution in $m_{(\mu\mu)1}$ and $m_{(\mu\mu)2}$. The total of all background estimations agrees with this conclusion.

On the product of the production cross section times branching fraction to dimuons squared times acceptance, a model-independent upper limit of 95% confidence level (CL) is determined. The CLs approach is used to set limits. The logarithm of the likelihood ratio is utilized as the test statistic. In Figure 41, the limit is plotted as a function of m_a spanning the range $0.25 < m_a < 8.5$ GeV, with the limit varying between 0.15 and 0.39 fb. The maximum upper limit, ignoring the enormous peak in the upper limit at the J/ψ meson mass, is 0.25 fb. In the context of specific models, this result can be interpreted.

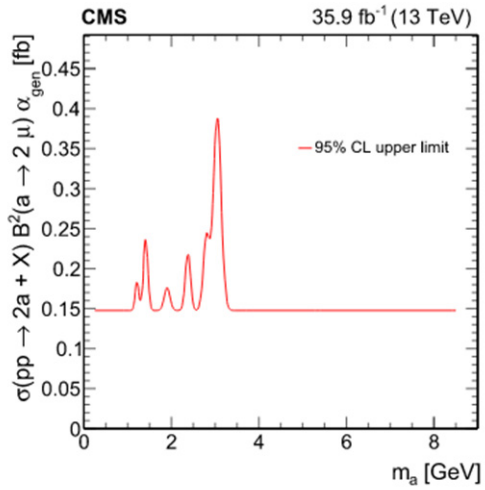

Figure 41. Over the range $0.25 < m_a < 8.5$ GeV, the 95% CL upper limit set on $\sigma(pp \to 2a+X)B^2(a \to 2\mu)_{agen}$. Reprinted/adapted with permission from Ref. [1]. 2022, Physica Scripta, Th. Lagouri.

The product of the Higgs boson production cross section and the branching fractions of the Higgs boson (cascade) decay to a pair of dark photons is set to a 90% CL upper limit in the dark SUSY scenario. The experimental search limit is depicted in Figure 42 as areas excluded in a two-dimensional plane of ε and $m_{\gamma D}$. Limits from other experimental searches are also included in Figure 42. Limits are presented for values of B ($h \to 2\gamma_D + X$) in the range of 0.1–40 percent for both this and the ATLAS searches.

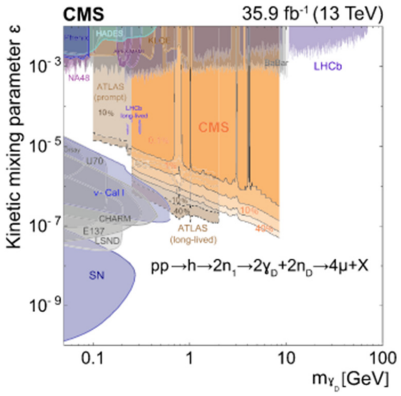

Figure 42. The 90% CL upper bounds (black solid curves) from this search are interpreted in the dark SUSY scenario, where the process is $pp \to h \to 2n_1 \to 2\gamma_D + 2n_D \to 4\mu + X$, with m_{n1} = 10 GeV and m_{nD} =1 GeV. In the plane of the parameters (ε and $m_{\gamma D}$), the limits are shown. Other experiments' constraints are also shown, along with their 90% CL exclusion contours. Different values of $B(h \to 2\gamma_D + X)$ ranging from 0.1 to 40% are represented by the colored contours for the CMS and ATLAS limits. Reprinted/adapted with permission from Ref. [1]. 2022, Physica Scripta, Th. Lagouri.

The 40% value is ruled out by the most recent findings on the branching fraction of Higgs boson decay to invisible particles. Its sole purpose is to compare limits found in a prior iteration of this search. The kinetic mixing parameter, ε, the mass of the dark photon $m_{\gamma D}$, and the lifetime of the dark photon $\tau_{\gamma D}$ are all connected by an analytic function f($m_{\gamma D}$) that is completely dependent on the dark photon mass, namely, $\tau_{\gamma D}$ (ε, $m_{\gamma D}$) = $\varepsilon^{-2} f(m_{\gamma D})$. The dark photon's lifetime can range from 0 to 100 mm, and $m_{\gamma D}$ can be anywhere between 0.25 and 8.5 GeV.

This search constrains a wide and previously unexplored area in the ε and $m_{\gamma D}$ parameter space due to the extensions in the ranges of these parameters. The constraints on ε reported in this study [46] are about 2.5 times better than those in [47], and the upper bound of $m_{\gamma D}$ has been extended from 2 to 8.5 GeV.

4.3. Long Lived Particles (LLPs) Search with Leptons-Jets (Prompt and Displaced) (ATLAS)

4.3.1. Displaced Leptons-Jets ATLAS Search at $\sqrt{s}$ = 13 TeV

A search for long-lived dark photons produced by the decay of a Higgs boson or a heavy scalar boson into displaced collimated SM fermions is presented in this ATLAS study [48]. The data used in the search correspond to an integrated luminosity of 36.1 fb^{-1} recorded in pp collisions at $\sqrt{s}$ = 13 TeV with the ATLAS detector at the LHC in 2015–2016.

The existence of a dark sector weakly connected to the SM is predicted by several extensions of the SM. Some unstable dark states may be produced at colliders, depending on the structure of the dark sector and its interaction with the SM, and could decay into SM particles with large branching fractions. In such scenarios, a dark Higgs boson is inserted to provide mass to the dark gauge bosons in order to avoid a new long-range force. Through mixing between the two Higgs sectors, the dark Higgs boson may potentially lead to an exotic decay mode of the Higgs boson, which is one of the preferred production mechanisms that may be investigated at the LHC. This is the mode that this search looked into. For Higgs-boson decays into exotic final states, branching fractions of up to 10% are currently not ruled out.

The case when the two sectors connect via a vector portal is investigated in this study [48], in which a dark photon (γ_d) interacts kinetically with the SM photon and decays into SM leptons and light quarks. The lifetime of the dark photon is determined by the kinetic mixing term (ε), which has a wide range of values, $\varepsilon \sim 10^{-11}$–$10^{-2}$. The γ_d has a long lifetime for a small kinetic mixing value; hence, it decays at a macroscopic distance from its production point. Small values of the kinetic mixing term, $\varepsilon < 10^{-5}$, and a dark photon mass range between twice the muon mass and twice the tau mass are the focus of this study. Dark photons are expected to be produced with enormous boosts because of their tiny mass, resulting in collimated groups of leptons and light hadrons in a jet-like structure, referred to as dark-photon jets hereafter (DPJs).

For the suppression of the primary multi-jet background, the study [48] uses multivariate approaches that are optimized for the different DPJ channels. For the first time in ATLAS DPJ searches, this technique allows for the use of the fully hadronic signature, resulting in higher sensitivity compared to prior ATLAS results utilizing data collected in 2011 and 2012 at 7 and 8 TeV, respectively [49]. The findings are similar to those of ATLAS searches for prompt DPJs using 7 and 8 TeV data [49], which probed higher values of ε, and for displaced dimuon vertices using 13 TeV data, which probed higher dark photon mass values.

The CDF and D0 collaborations at the Tevatron and the CMS and LHCb collaborations at the LHC conducted related searches for dark photons. Additional constraints on dark photon scenarios come from experiments such as beam-dump and fixed-target, e^+e^- colliders, electron and muon anomalous magnetic moment measurements, and astrophysical observations. For γ_d masses greater than 100 MeV, a displaced dark photon with a kinetic mixing term of $\varepsilon < 10^{-5}$ is allowed due to the different constraints.

Benchmark Models

Among the many models that anticipate dark photons, one class, in particular, is intriguing for the LHC because it includes a hidden sector that communicates with the SM via the Higgs portal for production and the vector portal for decay. The benchmark model employed in this analysis is the Falkowski–Ruderman–Volansky–Zupan (FRVZ) model in which a Higgs boson (H) decay produces a pair of dark fermions f_{d2}. This concept is examined in two separate scenarios, each including the emission of two or four dark photons. Each dark fermion decays into a γ_d and a lighter dark fermion, which is considered to be the hidden lightest stable particle, as seen in Figure 43 (left) (HLSP). Each dark fermion in the second scenario, depicted in Figure 43 (right), decays into an HLSP and a dark scalar s_d, which decays into a pair of dark photons.

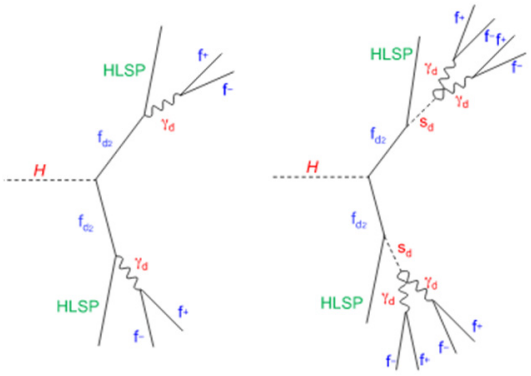

Figure 43. The FRVZ model's two processes were utilized as benchmarks in the study. The dark fermion f_{d2} decays into a γ_d and an HLSP in the first process (**left**). The dark fermion f_{d2} decays into an HLSP and a dark scalar s_d, which decays into a pair of dark photons in the second step (**right**). The γ_d decays into SM fermions, which are indicated by the letters f^+ and f^-. Reprinted/adapted with permission from Ref. [1]. 2022, Physica Scripta, Th. Lagouri.

A dark photon with a mass $m_{\gamma d}$ of a few GeV that kinetically interacts with the SM photon decays into leptons or light mesons, with branching fractions that depend on its mass. The kinetic mixing parameter is related to the mean lifetime τ of the γ_d, expressed in seconds, by the formula "$\tau \propto (10^{-4}/\varepsilon)^2(100\ \text{MeV}/m_{\gamma d})$".

Analysis Event Selection

DPJs that have been displaced are reconstructed using criteria that are dependent on the γ_d decay channel. A γ_d decaying into a muon pair is looked for in the MS by looking for two closely spaced muon tracks, whereas a γ_d decaying into an electron or pion pair is searched for as an energy deposit in the calorimeters detected as a single narrow jet, provided the large boost of the γ_d. DPJs comprising two dark photons that each decay into an electron or pion pair are reconstructed as a single jet using MC simulations.

The number of muons and jets found within a particular cone of angular size R surrounding a muon or jet candidate with the highest transverse momentum is used to classify DPJs. The cone size is set to R = 0.4 since MC simulations show that with m_H = 125 GeV, this selection retains up to 90% of the dark-photon decay products in the $H\rightarrow 4\gamma_d$ +X decay channel. The following is a summary of the DPJ classification:

muonic-DPJ (DPJ): at least two muons are required, and no jets are allowed in the cone to select DPJs with all constituent dark photons decaying into muons.

hadronic-DPJ (hDPJ): one jet is required to choose DPJs in which all constituent dark photons decay into electron or pion pairs in the HCAL, and no muons are allowed in the cone. The electromagnetic fraction of the jet energy must be less than 0.4, calculated as the ratio of energy deposited in the ECAL to total jet energy (E_{ECAL}/E_{total}). Because of the multi-jet production, this serves to reduce the overwhelming background.

Results

When H is the Higgs boson and the DPJ–DPJ channel is used, the results for $H\rightarrow 2\gamma_d$ $+X$ are interpreted in terms of the "kinetic mixing parameter" ε and γ_d mass, which are displayed as exclusion contours in Figure 44. These limits are based on the NNLO gluon–gluon fusion Higgs boson production cross section and four hypothetical Higgs boson decay branching fractions into γ_d, ranging from 1 to 20%. For the mass interval 0.25–2 GeV, the γ_d detection efficiency for a γ_d mass of 0.4 GeV is chosen because the detection efficiency is consistent across this range. Variations in decay branching fraction as a function of γ_d mass are estimated and accounted for in the 90% CL exclusion region analyses.

The hDPJ–hDPJ channel's low sensitivity prevents the exclusion of mass areas where the γ_d decays into hadronic resonances: γ_d mass regions at 0.8 and 1.0 GeV, where the γ_d decays into the ρ, ω, and φ resonances. Exclusions for a Higgs boson decay branching fraction into γ_d of 10% in a search for displaced dark-photon jets [49] and prompt dark-photon jets [49] at ATLAS are also shown in Figure 44 In the region of high γ_d mass and low ε, the search of [49], which searched the same region as our research, is slightly more sensitive. This is because dark-photon jets with both muon and hadron constituents are included, which are not employed in the current investigation. The search of [49] excluded high values (shorter lifetimes), a region that is relevant to our study.

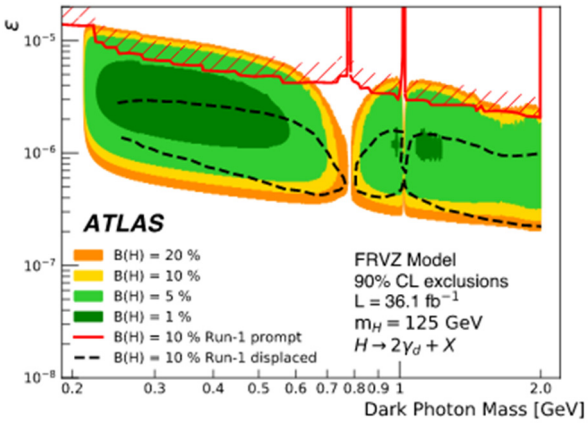

Figure 44. As a function of the γ_d mass and the kinetic mixing parameter ε, the 90% CL exclusion areas for the Higgs boson decay $H \rightarrow 2\gamma_d + X$. These limits are calculated using the FRVZ model, with Higgs boson decay branching fractions into γ_d ranging from 1 to 20%, and the NNLO Higgs boson production cross sections via gluon–gluon fusion. The picture also displays excluded regions from the run-1 ATLAS displaced [49] (black line) and prompt [49] (red line) dark-photon jets searches, with a decay branching percentage of the Higgs boson into γ_d of 10%. Reprinted/adapted with permission from Ref. [1]. 2022, Physica Scripta, Th. Lagouri.

4.3.2. Prompt Lepton Jets Search with ATLAS at $\sqrt{s}$ = 8 TeV

In Ref. [49], an ATLAS search for a novel light boson with a mass of around 1 GeV and decaying to a collimated electron and/or muon jets is provided (lepton jets). The analysis is based on data obtained by the ATLAS detector at the LHC in pp collisions with a center-of-mass energy of 8 TeV, of a total of 20.3 fb^{-1}. There must be at least two lepton jets in each event.

The so-called "dark matter" is charged under a "non-Abelian" dark-sector gauge symmetry that is broken at an energy scale O(1 GeV) in numerous models of physics beyond the SM. The dark-sector ground state can transition to and from excited states by emitting a dark gauge boson, known as the "dark photon" (γ_d), which links very weakly to the SM particles via kinetic mixing. The LHC might produce excited dark-sector states in these models by interacting with particles found in "supersymmetry" (SUSY) or Higgs scalar bosons (here referred to as "SUSY-portal" and "Higgs-portal" models, respectively), which would subsequently decay via the emission of dark photons.

If dark photons have masses of O(1 GeV), the dark photon produced by the decay chain of heavier particles such as the SM Higgs boson or "SUSY" particles will be greatly enhanced. The dark photon decays predominantly into a collimated pair of leptons or light hadrons, depending on its mass. The experimentally more accessible leptonic final state has a specific signal that stands out against huge hadronic backgrounds. A lepton jet is a collimated cluster of energetic leptons (LJ).

This ATLAS search [47] is for final states, including two prompt lepton jets. Several new physics models predict at least two lepton jets in the final stages. The focus of the analysis is on the presence of lepton jets, with little regard for the rest of the event topology. The kinetic mixing parameter, ε, and the dark-photon decay width, $\Gamma_{\gamma d}$, are connected by a relation in where a is the "fine structure constant" and $m_{\gamma d}$ and m_l are the masses of dark photons and charged leptons, respectively. The study focuses on dark photons with prompt decays or decay lengths that are consistent with zero within the experimental resolution.

With ATLAS data at $\sqrt{s}$ = 7 TeV, previous searches for prompt lepton jets yielded upper limits on the production of two lepton jets in a SUSY-portal model and a Higgs-portal model. The CMS and D0 collaborations also established upper limits on prompt lepton-jet production [49]. ATLAS has conducted related searches for non-prompt lepton jets [37] and has imposed limits on smaller values of the kinetic mixing parameter, $\varepsilon < 10^{-5}$. Additional constraints on the kinetic mixing parameter and dark-photon mass have been obtained,

for example, from beam-dump and fixed target experiments, e^+e^- collider experiments, electron and "muon magnetic moment" measurements, and astrophysical observations.

Benchmark Models

The data are interpreted using two benchmark models. A pair of squarks is formed in the SUSY-portal paradigm, and the squarks' cascade decays comprise dark sector particles and one or more dark photons. The SM Higgs boson decays into a pair of dark fermions, each of which decays into one or more dark photons in cascades in the Higgs-portal scenario. Depending on the branching fractions, dark photons decay into lepton pairs, which can be reconstructed as a lepton jet or light hadrons. The dark photons must decay quickly with a mean lifetime ($c\tau$) close to zero in all signal models employed to understand the data. Long-lived dark photon samples with $c\tau$ = 47 mm are utilized in the Higgs-portal model to extrapolate the signal efficiency of zero $c\tau$ dark photons to non-zero $c\tau$ dark photons.

As depicted in Figure 45, a hypothetical decay of the Higgs boson to a pair of dark fermions f_{d2} is considered. Dark fermions f_{d2} decay to a dark photon (γ_d) and a lighter dark fermion (f_{d1}), which is also known as the Hidden Lightest Stable Particle (HLSP) (Figure 45, left). A dark fermion f_{d2} decays to a lighter dark fermion f_{d1} (referred to as HLSP) and a dark scalar s_{d1} in another process. The s_{d1} decays into two dark photons (Figure 45, right). The gluon-fusion production process produces the Higgs boson (m_H = 125 GeV) with an estimated production cross section of SM = 19.2 pb for pp collisions at $\sqrt{s}$ = 8 TeV. The mass of f_{d2} is set to 5 GeV, the masses of f_{d1} and sd_1 are set to 2 GeV, and the mass of the dark photon (γ_d) is set to 0.4 GeV.

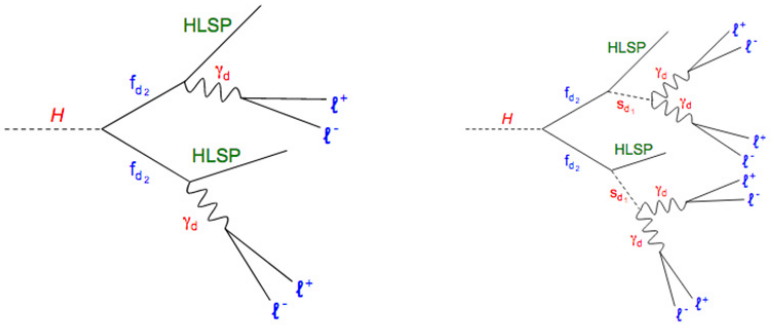

Figure 45. The Higgs boson decays to two dark fermions, f_{d2}, each of which decays to a Hidden Lightest Stable Particle (HLSP) and a dark photon (**left**) or an HLSP and a dark scalar s_{d1} (**right**) which decays to a pair of dark photons γ_d. Reprinted/adapted with permission from Ref. [1]. 2022, Physica Scripta, Th. Lagouri.

Analysis Event Selection

A primary collision vertex with at least three tracks with transverse momentum $p_{\mathrm{T}} > 400$ MeV is required for pre-selected events. The trigger must be satisfied by all events, and offline reconstructed objects (electrons or muons) must match the leptons that fired the trigger.

Signal MC events are combined with background MC events and "background-dominated" data from a "jet-triggered" sample to produce optimum criteria that are applied to preselected events to retain "Lepton-Jet" (LJ) events while rejecting background events. The background content in the final sample of LJ candidate events is determined using a data-driven technique.

Bundles of finely collimated high-p_{T} leptons make up lepton jets. Only prompt γ_d leptonic decays (e^+e^- or $\mu^+\mu^-$) are chosen in this research. A multijet background cannot be separated from hadronic γ_d decays. The following is a list of lepton jet candidates:

- Electron jet (eLJ): A lepton jet candidate is called an electron jet if at least one reconstructed electron with $E_T > 10$ GeV is discovered within $\Delta R = 0.5$ of the lepton jet but no muons (eLJ)

- Muon jet (muLJ): A muon jet candidate is one that has at least two muons with $p_{\mathrm{T}} > 10$ GeV but no electrons within $\Delta R = 0.5$ of the lepton jet (muLJ).
- Mixed jet (emuLJ): A lepton jet candidate is called a mixed jet if at least one reconstructed electron with $E_T > 10$ GeV and at least one muon with $p_{\mathrm{T}} > 10$ GeV is discovered inside $\Delta R = 0.5$ of the lepton jet cone (emuLJ).

There are six different types of events: eLJ–eLJ, muLJ–muLJ, eLJ–emuLJ, muLJ–emuLJ, emuLJ–emuLJ, emuLJ–emuLJ, emuLJ–emuLJ, emuLJ–emuLJ, emuLJ–emuLJ, p_{T}- and η-depend on the efficiency of lepton jet reconstruction.

SM backgrounds, predominantly hadronic jets that are misidentified as lepton jets, are included in the reconstructed sample of lepton jets. The variables used to distinguish between signal and background processes are based on the properties of reconstructed lepton jets and are listed below:

- eLJ variables: track isolation, percentage of high-threshold TRT hits, f_{HT}, the energy of the strip with the greatest energy deposit, ${E_{s1}}^{\mathrm{max}}$, fraction of energy deposited in the EM calorimeter's third sampling layer, f_{s3}, electromagnetic energy fraction, f_{EM}
- muLJ variables: calorimeter isolation, track isolation
- emuLJ variables: track isolation, the energy of the strip with the highest energy deposit, ${E_{s1}}^{\mathrm{max}}$, fraction of energy deposited in the EM calorimeter's third sampling layer, f_{s3}, Hadronic leakage, ${E_T}^{\mathrm{had}}$

In order to suppress SM backgrounds, cuts on the variables above are applied. Cuts are examined in a multi-dimensional space.

Except for the diboson top-quark pair ($t\bar{t}$), which is obtained using MC simulations, all background contributions are calculated using the data-driven ABCD-likelihood technique. Hadronic multijet events, γ+jets events, $W(\rightarrow lv)$+jets, $Z(\rightarrow l^+l^-)$+jets, $t\bar{t}$, and diboson (WW, WZ, ZZ,) events are among the MC samples considered. Only the hadronic multijet, +jets, and $Z(\rightarrow l^+l^-)$+multijet events contribute considerably among the backgrounds investigated. MC simulations are used to investigate the contribution of low-mass Drell–Yan events $\gamma^* (\rightarrow l^+l^-)$+jets in the $2 < m_{ll} < 8$ GeV and $10 < m_{ll} < 60$ GeV ranges (Sherpa). Because tracks have soft p_{T} spectra, this contribution is negligible, as the analysis requires tracks in a lepton jet to have $p_{\mathrm{T}} > 10$ GeV.

The lepton jet backgrounds from SM processes are determined using an ABCD-likelihood technique.

Results

There is no notable deviation from SM predictions, and the influence of new phenomena beyond the SM on the number of events involving lepton jets is provided with 95% confidence-level upper limits. In the electron, muon, and mixed channels, limits are set for squark+squark$\rightarrow 2(s_d \rightarrow \gamma_d \gamma_d)+X$, $H \rightarrow 2\gamma_d+X$, and $H \rightarrow 2(s_d \rightarrow \gamma_d \gamma_d)+X$ processes.

In order to allow a comparison with the displaced lepton jets analysis [49], 90% confidence-level exclusion limits for $H \rightarrow 2\gamma_d+X$ production for various branching fractions (5%, 10%, 20%, 40%) are derived by combining the results from the eLJ–eLJ, muLJ–muLJ, and eLJ–muLJ channels after accounting for all systematic uncertainties.

The 90% confidence-level exclusion contour for 5%, 10%, 20%, and 40% branching fractions of the Higgs boson decay to $2\gamma_d+X$ is shown in Figure 46, interpreted in the ε and γ_d mass planes in the ε region 10^{-2}–10^{-6} and in the mass region [0.1–2] GeV. Only the data from the eLJ–eLJ channel contribute in the low-mass area, below the $\mu^+\mu^-$ threshold. The results in the figure are dependent on the dark photon's connection to the SM photon as well as the dark photon's mass. Other excluded regions from ATLAS's search for non-prompt lepton jets [49] and other experiments are shown in Figure 46

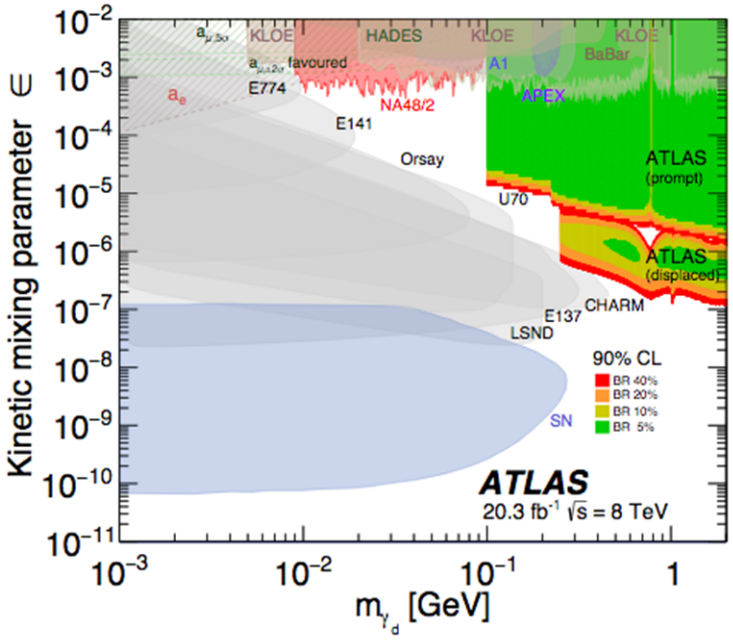

Figure 46. Two-dimensional exclusion plot in the dark-photon mass $m_{\gamma d}$ and the kinetic mixing ε parameter space. For $H \to 2\gamma_d + X$ decays, the branching ratios are provided. Based on the current combined results from the eLJ–eLJ, muLJ–muLJ, and eLJ–muLJ channels utilizing 8 TeV data at ATLAS, the 90% confidence-level exclusion region for prompt $H \to 2\gamma_d + X$ production with 5%, 10%, 20%, and 40% branching fractions into $2\gamma_d + X$ decay is extracted. The excluded regions are determined by comparing the overall signal expectation for the $H \to 2\gamma_d + X$ production model with the signal expectation's upper 90% confidence level. The ATLAS exclusions by both the prompt [47] and displaced lepton jet analyses [37] are represented in the legend. Reprinted/adapted with permission from Ref. [1]. 2022, Physica Scripta, Th. Lagouri.

Existing 90% confidence-level exclusion regions are shown from "beam-dump" experiments E137, E141, and E774, Orsay, U70, CHARM, LSND, A1, the "electron and muon anomalous magnetic moment", HADES, KLOE, the test-run results reported by APEX. While the results of other experiments are independent of the topology of dark-photon production, the ATLAS results are reliant on the topology, i.e., the mass of the Higgs boson and the method by which it is produced as well as its decay into dark photons. CMS's findings have been published elsewhere [50].

The R-ratio of e^+e^- collider data, where the R-ratio is the ratio of the hadronic cross section to the muon cross section in electron–positron collisions, is used to evaluate the ε values.

4.4. Displaced Leptons and Long-Lived Particles (LLPs) (ATLAS, CMS)

4.4.1. Higgs Decay: Displaced Muons with ATLAS at $\sqrt{s}$ = 13 TeV

ATLAS search [51] uses *pp* collision data obtained by the ATLAS detector at the LHC at $\sqrt{s}$ = 13 TeV, corresponding to an integrated luminosity of 32.9 fb^{-1}, to search for a long-lived particle decaying into a final state that includes a pair of opposite-sign electric charge muons.

The lightest neutralino is the next-to-lightest supersymmetric particle in the supersymmetric model, with a relatively long lifetime due to its weak coupling to the gravitino, which is the lightest supersymmetric particle. The lifetime constraints for very light gravitino masses and various neutralino masses in the region of 300–1000 GeV are determined. For various assumptions for the $H \to ZdZd$ branching fraction, the lifetime limits are interpreted as exclusion contours in the plane of the coupling between the Zd and the SM Z boson

vs. the *Zd* mass (in the range 20–60 GeV) in the dark photon model. Long-lived particles (LLPs) appear naturally in a variety of BSM models [28].

Small couplings, mass scales associated with BSM physics, and split supersymmetry are examples of high-mass (greater than a few hundred GeV) LLPs, as are supersymmetry (SUSY) with R-parity violation, general gauge-mediated (GGM) supersymmetry breaking, and split super-symmetry. Hidden-valley models, stealth supersymmetry, and dark-sector gauge bosons [28] are examples of scenarios with low-mass LLPs.

The vertices of events with long-lived particles may be substantially displaced from the *pp* interaction point (IP). The findings of a search for displaced vertices (DVs) created by a pair of opposite-sign electric charge muons, termed "OS" muons, are presented in this paper [51]. The search is targeted at LLP decays with masses ranging from 20 to 1100 GeV and DVs at distances ranging from a few centimeters to a few meters from the IP. LLP lifetimes of $c\tau$ = 0.1–100 cm were previously excluded from ATLAS Collaboration searches for high-mass LLPs that decay within the inner detector to provide displaced dilepton vertices [52]. ATLAS has also looked for LLPs with very low masses (less than 10 GeV) using pairs of highly collimated leptons, with sensitivity to LLP lifetimes of c = 0.1–20 cm. The ATLAS, CMS, LHCb, CDF, D0, BABAR, Belle, and ALEPH collaborations have performed several other LLP searches targeting a wide range of lifetimes and signatures.

Benchmark Models

To adjust selection criteria and evaluate signal efficiency for use in converting signal yields into cross sections, Monte Carlo simulated samples from two separate BSM physics models are employed. The two models considered a general gauge-mediated supersymmetry and a dark-sector gauge boson model, which represent a wide range of BSM physics possibilities as well as final-state topologies and kinematics to which the analysis may be sensitive. In Figure 47, the two procedures are depicted.

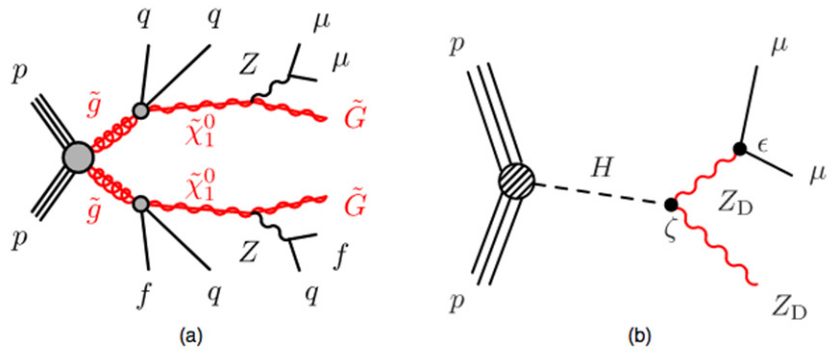

Figure 47. Two diagrams for signal processes considered: (**a**) long-lived neutralino $\overline{\chi}^{01}$ decay in a GGM scenario, and (**b**) long-lived dark photons *Zd* produced by Higgs boson decay. The quarks, *q*, can have a variety of flavors (excluding the top quark). The symbol *f* denotes fermions with a mass less than half that of the *Z* boson. Reprinted/adapted with permission from Ref. [1]. 2022, Physica Scripta, Th. Lagouri.

A "hidden" or "dark" sector of matter is featured in a number of BSM theories, which do not interact directly with SM particles but may interact weakly with SM matter via coupling to the Higgs field. The dark-matter problem and electroweak baryogenesis are addressed in these "Higgs portal" models. The dark vector gauge boson *Zd*, in the dark sector $U(1)_D$ symmetry, often known as a "dark" photon, is provided mass via a singlet scalar field H_D that breaks the symmetry and is equivalent to the Higgs field *H* in the visible SM sector in the model studied for this study [28].

Both a hypercharge portal and a Higgs portal are included in the BSM terms in the Lagrangian density, allowing for kinetic *Z*-*Zd* mixing [i.e., mixing between $U(1)_\gamma$ and

$U(1)_D$] and H-H_D mixing, which are controlled by the tiny coupling parameters ε and ζ, respectively. There are two scalar mass eigenstates, one that is primarily H_D and the other that is mostly H, as well as two vector-boson mass eigenstates, one that is mostly Zd and the other that is mostly SM Z. The physical (mass) states are indicated by H, H_D, Z, and Z_D for clarity.

In the case when the singlet scalar H_D is heavier than the SM H boson, kinematically prohibiting the process $H \to H_D H_D$, and Zd is lighter than half the H mass, events with a displaced dimuon vertex signature might be detectable in LHC experiments. Due to their induced couplings to the electroweak current, Zd bosons are produced on-shell in Higgs boson decays and decay to SM fermions. A small value of ε ($\lesssim 10^{-5}$), on the other hand, results in a long-lived Zd state: $c\tau_{Zd} \propto 1 = \varepsilon^2$. The value of and the masses of the scalar singlets determine the branching fraction for $H \to ZdZd$, with values as high as 25% not yet ruled out by limitations from Higgs coupling fits.

For $\varepsilon \ll 1$, $B(Zd \to \mu^+\mu^-)$, the Zd branching fraction to muons is independent of ε but varies with m_{Zd}, ranging from 0.1475 for m_{Zd} = 20 GeV to 0.1066 for m_{Zd} = 60 GeV. The Higgs boson is created by gluon-gluon fusion, with a cross section of 44.1 pb computed at "next-to-next-to-leading order" in the "strong coupling constant", and the "summation of soft gluon emission" determined with "next-to-next-to-leading-logarithmic precision".

Analysis Event Selection

Candidate signal events are chosen by looking for $\mu^+\mu^-$ pairings that are compatible with being produced in a vertex that is at least a few centimeters away from the IP. The criteria are meant to effectively inhibit background from SM processes that produce muons near the IP while accepting signal events with a wide range of LLP masses, lifetimes, and velocities. The pp collision interaction vertices are reconstructed from at least two tracks with p_T greater than 400 MeV that are compatible with originating from the x-y plane beam-collision zone. At least one reconstructed interaction vertex is required for some events. By demanding that the dimuon invariant mass, $m_{\mu\mu}$, be more than 15 GeV, the background from muons with low momentum in multi-jet events, as well as Υ decays to dimuons, is decreased.

Table 8 summarizes the preselected dimuon vertices, which are separated into two zones to be used in searches for low- and high-mass signal models.

Table 8. In addition to the preselection requirements, there are selection criteria for low- and high-mass locations. Further, also included are definitions for the low- and high-mass signal areas. Reprinted/adapted with permission from Ref. [1], 2022, Physica Scripta, Th. Lagouri.

Selection	Low Mass	High Mass
$\mathbf{p_T}^{\mu}$ **[GeV]**	> 10	>20
$\mathbf{m_{\mu\mu}}$ **[GeV]**	15–60	>60
Dimuon transverse boost	...	>20
	SR_{low}	SR_{high}
Muon candidates	Both MSonly	Both MSonly
Muon candidate charge	Opposite charge	Opposite charge

The transverse boost of the dimuon pair, defined as the ratio of the dimuon system's transverse momentum to its invariant mass, must be greater than 2 to further suppress the DY background in the high-mass region, where Z+jets production predominates and increases search sensitivity. The decay of a heavy BSM particle produces the dimuon state (a Z boson in the GGM model) with a rather significant boost, which reduces the DY background by a factor of 20 with a slight reduction in signal efficiency.

Muons that are not expected to have a corresponding ID track are known as "non-prompt" muons. "Cosmic-ray" muons, "Beam Induced Background" (BIB) muons, fake

MS tracks formed from random hit combinations, and those emerging from pion or kaon decay are all examples of background non-prompt muons.

Results

Due to the lack of a significant excess of vertices over the SM background expectation, 95% confidence-level (C.L.) upper limits on signal event yields and production cross sections are calculated for various values of the long-lived particle's proper decay distance $c\tau$ in each of the two BSM scenarios considered. The test statistic is a Poisson likelihood, and the limits are computed following the CLs prescription.

The $c\tau_{Zd}$ values are excluded in the ranges 0.3–2000 cm, 0.9–2400 cm, and 2.1–1100 cm, respectively, in the dark-sector model with a dark-Higgs-boson mass of 300 GeV, $B(H\rightarrow ZdZd)$ = 10% and Zd masses of 20, 40, and 60 GeV. These limits are represented in Figure 48 as 95% exclusion contours in the plane of the Zd-Z kinetic mixing parameter, ε, and the Zd mass. For $20 < m_{Zd} < 60$ GeV, ε values of the order 10^{-8} are excluded.

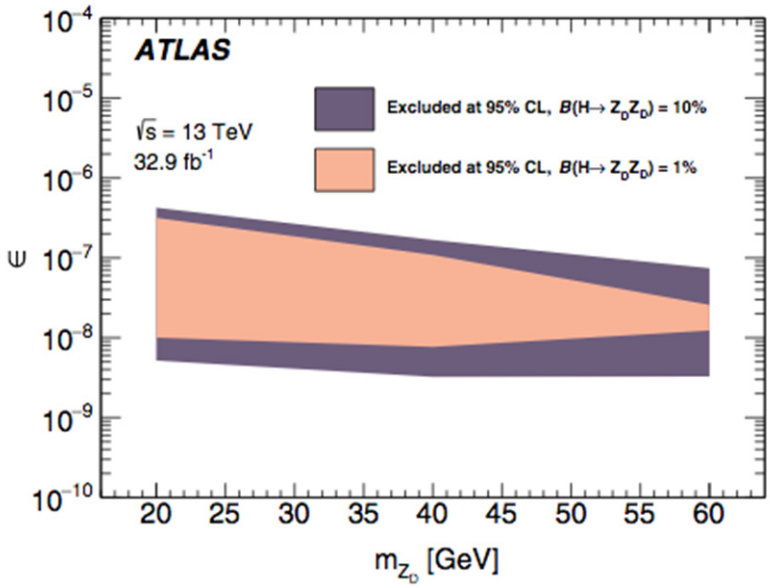

Figure 48. For values of $B(H\rightarrow ZdZd)$ = 1% or 10%, and m_{HD} = 300 GeV, the observed 95% C.L. excluded regions in the plane of Zd-Z kinetic mixing parameter, ε, versus Zd mass. For the range m_{Zd} = 20–60 GeV the value of $B(Zd\rightarrow\mu^+\mu^-)$ fluctuates between 0.1475 and 0.1066. Reprinted/adapted with permission from Ref. [1]. 2022, Physica Scripta, Th. Lagouri.

4.4.2. Higgs Decay: Displaced Leptons with CMS at $\sqrt{s}$ = 8 TeV

Long-lived particles that decay into final states containing a pair of electrons or a pair of muons are studied using the CMS search [47]. A distinctive topology comprised of a pair of charged leptons emerging from a displaced secondary vertex is the experimental signature. In proton–proton collisions at $\sqrt{s}$ = 8 TeV, events with an integrated luminosity of 19.6–20.5 fb^{-1} in the electron (muon) channel were collected with the CMS detector at the CERN LHC.

Many extensions of the Standard Model predict long-lived particles, which could present themselves as delayed decays to leptons. Such particles could, for example, be found in "supersymmetric" (SUSY) situations such as "split SUSY" or "SUSY" with extremely "weak R-parity violation", "hidden valley" models, and the "minimum B-L extension" of the SM.

A comprehensive search for massive, long-lived exotic particles that decay to final states containing a pair of charged leptons is provided in this paper [47]. It is a look for events with a pair of electrons or muons (dileptons) originating from a common secondary vertex within the CMS tracker's volume and a large transverse displacement from the

event source vertex. This topological signature has the potential to provide strong evidence for physics beyond the Standard Model. It is also almost clear of background from SM processes.

The search findings are acquired nominally in the context of two specific models, but they are accomplished in a model-independent approach, allowing them to be extended to a wide range of models in which long-lived particles decay to final states that include dileptons. The long-lived particle in the first model is a spinless boson X with a non-zero branching percentage to dileptons. The X is produced as a pair in the decay of a non-SM Higgs boson, $H \rightarrow XX$, $X \rightarrow l^+l^-$, where the Higgs boson is produced via gluon-gluon fusion and l is either an electron or a muon. The long-lived particle in the second scenario is a neutralino $\widetilde{\chi}^0$ that can decay into a neutrino and two charged leptons via R-parity violating couplings.

The neutralino is produced in squark-pair events, where a squark can decay via the process $\widetilde{q} \rightarrow q\widetilde{\chi}^0$, $\widetilde{\chi}^0 \rightarrow l^+l^-v$. In the CMS tracker volume, both models anticipate up to two displaced dilepton vertices per event, of which only one must be identified. The term "LL particle" is used in this work to refer to any long-lived particle, such as the X or $\widetilde{\chi}^0$ particle utilized in signal models.

Different combinations of the mass of the H boson (m_H = 125, 200, 400, 1000 GeV/c^2) and the mass of the X boson (m_X = 20, 50, 150, 350 GeV/c^2) are used to generate several samples. For simulation purposes, the Higgs boson resonance is considered to be narrow; however, this assumption has no bearing on the analysis. Furthermore, each sample is made with three different X boson lifetimes in the laboratory frame, corresponding to mean transverse decay lengths of roughly 2, 20, and 200 cm.

Analysis Event Selection

To be considered for pp collisions, events must have a primary vertex with at least four associated tracks and a position that is no more than 2 cm in the direction transverse to the beam and no more than 24 cm in the direction along the beam from the nominal interaction point.

Lepton identification algorithms that are less rigorous than the typical CMS algorithms are utilized to maximize the efficiency of reconstructing leptons from highly displaced vertices, which are not needed to suppress the very low backgrounds in this analysis.

In order to reject particles produced promptly, the tracks must have a transverse impact parameter significance of $|d_0|/\sigma_d > 12$ with respect to the primary vertex, where σ_d is the $d_0$uncertainty. For most of the LL particle lifetimes evaluated in this work, this value is chosen to offer an expected background much below one event, which provides the best signal sensitivity. In order to reject background from jets, both lepton candidates must be isolated. The two tracks are connected by a common vertex that must have a value of $\chi^2/\text{dof} < 10$ (5) in the electron (muon) channel.

Back-to-back tracks of cosmic ray muons can be reconstructed. The three-dimensional opening angle between the two muons must be less than 2.48 radians in order to reject them. By requiring that the two lepton candidates are not both matched to the same trigger item or offline photon, the background from misidentified leptons is reduced. Finally, $|\Delta\Phi| < \pi/2$ must be satisfied by the signed difference in azimuthal angles, $\Delta\Phi$, between the dilepton momentum vector, $\overline{p}_{ll}$, and the vector from the primary vertex to the dilepton vertex, $\overline{v}_{ll}$, where $\Delta\Phi$ is measured in the range $0 < \Delta\Phi < \pi$.

Results

Background events are equally likely to populate the signal and control zones, but LL particle events are almost entirely populated in the signal region. As a result, the presence of a signal in the data would manifest as a statistically significant excess of events in the signal region over the control region. No events are identified in the signal or control sections of the electron or muon channels after all selection criteria have been met. As a result, there is

no statistically significant difference. Figure 49 depicts the $|d_0|/\sigma_d$ distributions of events in the signal and control zones.

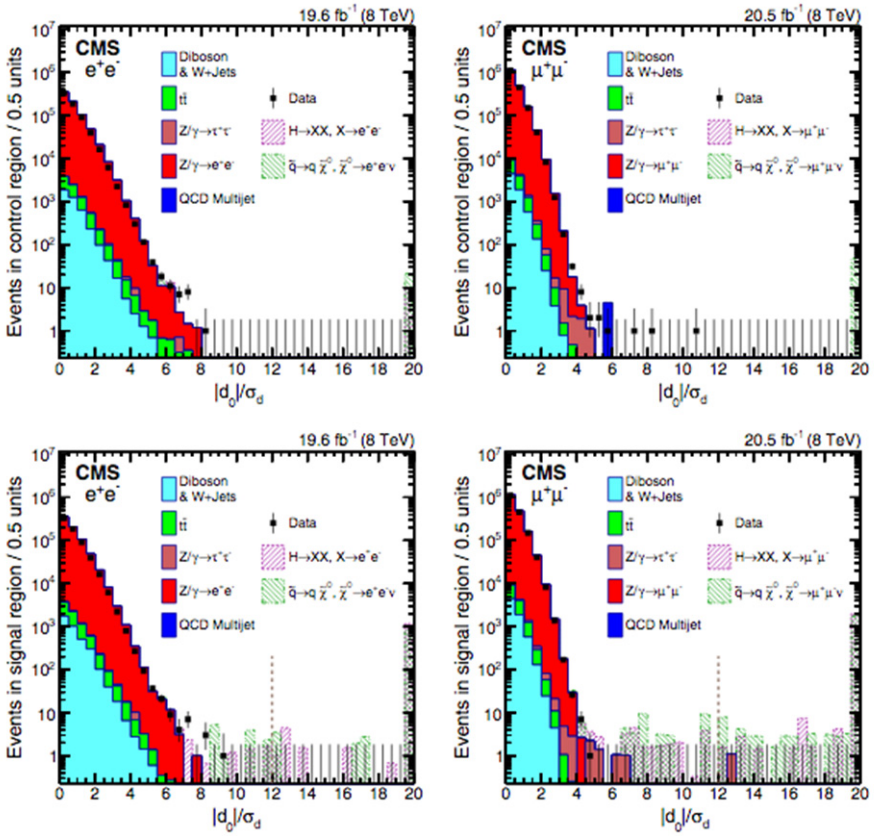

Figure 49. The $|d_0|/\sigma_d$ distribution for the electron (**left**) and muon (**right**) channels, with events in the control region ($|\Delta\Phi| > \pi/2$) shown in the top row and events in the signal region ($|\Delta\Phi| < \pi/2$) shown in the bottom row. The distribution of the lepton with the smallest $|d_0|/\sigma_d$ is depicted out of the two that make up a candidate. The data are represented by solid points, the simulated background is represented by shaded histograms, and the simulated signal is represented by hashed histograms. For m_H = 1000 GeV/c^2 and m_X = 350 GeV/c^2, the histogram corresponding to the $H \rightarrow XX$ model is provided. For $m\tilde{q}$ = 350 GeV/c^2 and $m\tilde{\chi}^0$ = 140 GeV/c^2, the histogram corresponding to the $\tilde{\chi}^0 \rightarrow l^+l^-v$ model is provided. Each simulated signal sample is individually layered on top of the overall simulated background, and the background histograms are stacked. The d_0 residual tracker misalignment corrections indicated in the text have been applied. The selection requirement of 12 is shown by the vertical dashed line $|d_0|/\sigma_d$. Any entries beyond the right-hand side of a histogram are displayed in the histogram's background last visible bin. Reprinted/adapted with permission from Ref. [1]. 2022, Physica Scripta, Th. Lagouri.

The signal processes' upper 95% confidence level (C.L.) limits were determined using the Bayesian technique outlined in]. The limits are calculated by comparing the number of events seen in the signal region to the expected number in the signal plus the background hypothesis.

The 95% C.L. upper bounds on $\sigma(H \rightarrow XX)B(X \rightarrow l^+l^-)$ are determined for each combination of the H and X boson masses that is modeled, as well as a range of mean appropriate decay lengths $c\tau$ of the X boson. Figures 50 and 51 illustrate the observed limits for the electron and muon channels, respectively. Low trigger efficiency for neighboring muons and the resulting ΔR requirement results in less stringent muon channel constraints in the m_H = 1000 GeV/c^2 and m_X = 20 GeV/c^2 situation.

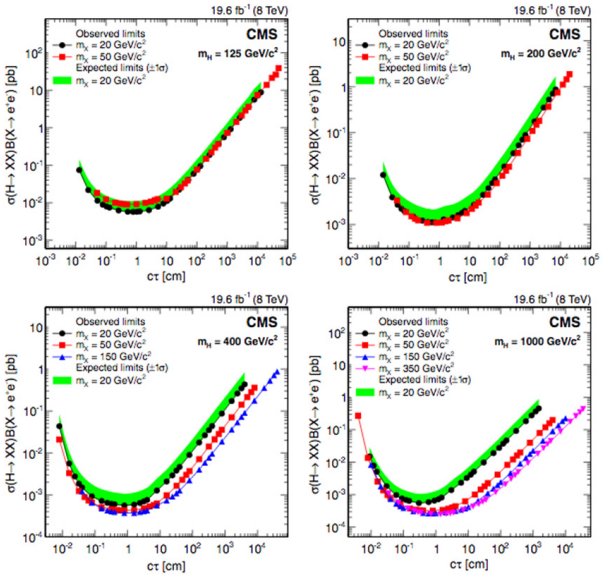

Figure 50. For Higgs boson masses of 125 (**top left**), 200 (**top right**), 400 (**bottom left**), and 1000 GeV/c^2, the 95% C.L. upper limits on $\sigma(H{\to}XX)\ B(X{\to}e^+e^-)$ are plotted as a function of the mean proper decay length of the X boson (**bottom right**). The results of numerous X boson mass hypotheses are displayed in each plot. For a 20 GeV/c^2 X boson mass, the shaded band depicts the 1σ range of variation in the projected 95% C.L. limits. The corresponding bands for the remaining X boson masses, which have been excluded for clarity, show similar agreement with the known limits. Reprinted/adapted with permission from Ref. [1]. 2022, Physica Scripta, Th. Lagouri.

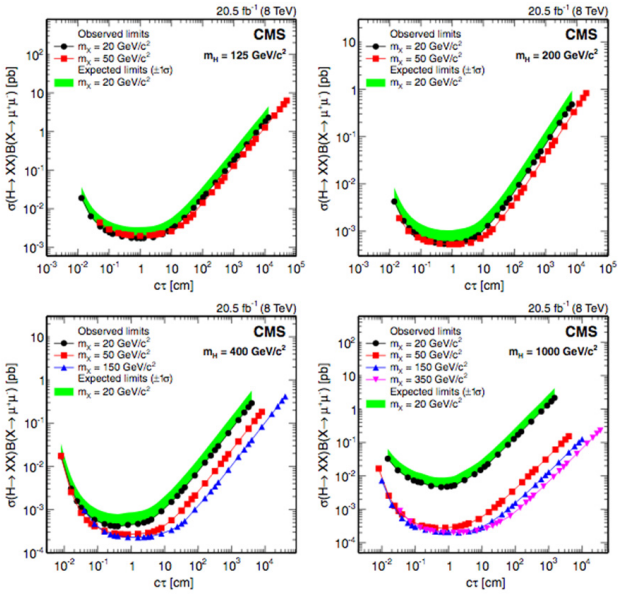

Figure 51. For Higgs boson masses of 125 (**top left**), 200 (**top right**), 400 (**bottom left**), and 1000 GeV/c^2, the 95% C.L. upper limits on $\sigma(H{\to}XX)\ B(X{\to}\mu^+\mu^-)$ are plotted as a function of the mean proper decay length of the X boson (**bottom right**). The results of numerous X boson mass hypotheses are displayed in each plot. For a 20 GeV/c^2 X boson mass, the shaded band depicts the 1σ range of variation in the projected 95% C.L. limits. The corresponding bands for the remaining X boson masses, which have been excluded for clarity, show similar agreement with the known limits. Reprinted/adapted with permission from Ref. [1]. 2022, Physica Scripta, Th. Lagouri.

Within the acceptance A, upper bounds on the cross-section times branching fraction were also calculated. Figures 52 and 53 demonstrate the limits for the electron and muon channels, respectively, on $\sigma(H{\to}XX)B(X{\to}l^+l^-)A(X{\to}l^+l^-)$.

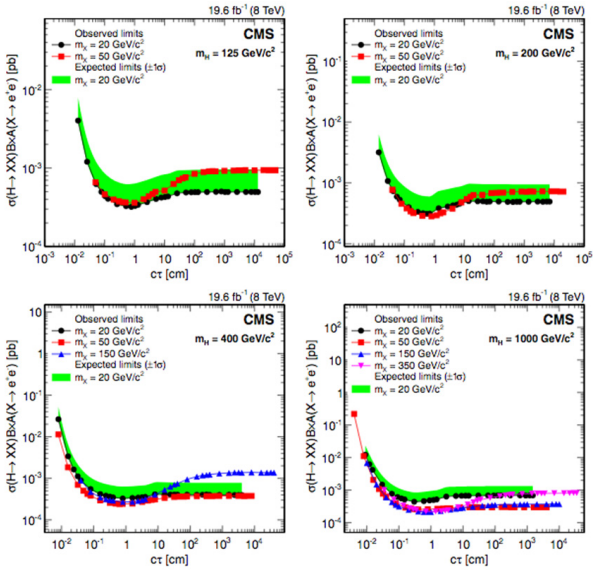

Figure 52. For Higgs boson masses of 125 (**top left**), 200 (**top right**), 400 (**bottom left**), and 1000 GeV/c^2, the 95% C.L. upper limits on $\sigma(H{\to}XX)\ B(X{\to}e^+e^-)\ A(X{\to}e^+e^-)$ are plotted as a function of the mean proper decay length of the X boson (**bottom right**). The results of numerous X boson mass hypotheses are displayed in each plot. For a 20 GeV/c^2 X boson mass, the shaded band depicts the 1σ range of variation in the projected 95% C.L. limits. The corresponding bands for the remaining X boson masses, which have been excluded for clarity, show similar agreement with the known limits. Reprinted/adapted with permission from Ref. [1]. 2022, Physica Scripta, Th. Lagouri.

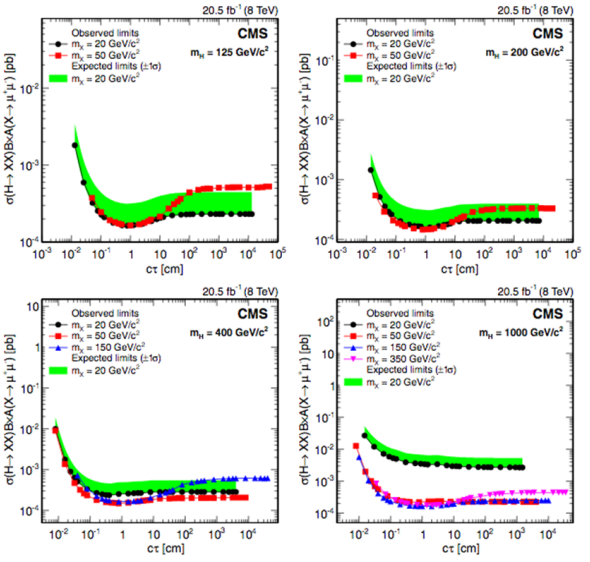

Figure 53. For Higgs boson masses of 125 (**top left**), 200 (**top right**), 400 (**bottom left**), and 1000 GeV/c^2, the 95% C.L. upper limits on $\sigma(H{\to}XX)\ B(X{\to}\mu^+\mu^-)A(X{\to}\mu^+\mu^-)$ are plotted as a function of the mean proper decay length of the X boson (**bottom right**). The results of numerous X boson mass hypotheses are displayed in each plot. For a 20 GeV/c^2 X boson mass, the shaded band depicts the 1σ range of variation in the projected 95% C.L. limits. The corresponding bands for the remaining X boson masses, which have been excluded for clarity, show similar agreement with the known limits. Reprinted/adapted with permission from Ref. [1]. 2022, Physica Scripta, Th. Lagouri.

Although the aforementioned limits were obtained in the context of two specific models, the analysis is applicable to any process that produces an LL particle and then decays to a final state containing dileptons. Because of their lower model reliance, the limitations inside the acceptability region (i.e., on σBA) should be used to establish approximate limits

on this more broad class of models. The restrictions on σBA illustrated in Figures 52 and 53 should be roughly realistic in most signal models in which each event involves two identical LL particles that decay in this way.

The predicted number of selected signal events for provided σB will be up to a factor of two lower in models where each event contains only one LL particle that can decay inclusively to dileptons, and hence the limits on σBA will be up to a factor of two worse than those shown in Figures 52 and 53. A generator-level simulation can be used to establish the acceptance A for any provided model, allowing limits on σBA to be converted to limits on σB. This is demonstrated in the following example. The above-mentioned restrictions on $\sigma(H \to XX)B(X \to l^+l^-)$ are for H bosons produced by gluon-gluon fusion. The momentum spectra of the H bosons would be slightly harder if they were produced by the total of all SM production methods. For $m_H = 125$ GeV/c^2, the acceptance would be increased by a factor of 1.18 (1.12) for $m_X = 20$ (50) GeV/c^2, resulting in an improvement in the limits on σB. For higher H boson masses, the change is smaller.

4.5. Low Mass Di-Muon Resonance Searches (CMS, LHCb)

4.5.1. Dimuon Resonances Search with CMS at $\sqrt{s} = 13$ TeV

Using $\sqrt{s} = 13$ TeV pp collision data recorded at the LHC, a CMS search [53] for a narrow resonance decaying to a pair of oppositely charged muons is reported. The search is based on traditional triggering and event reconstruction approaches in the 45–75 and 110–200 GeV resonance mass ranges. The search uses data collected using dimuon triggers with low transverse momentum thresholds, recorded at a high rate by retaining a reduced amount of trigger-level information in the 11.5–45 GeV mass range. For traditional and high-rate triggering, the values equate to integrated luminosities of 137 and 96.6 fb^{-1}, respectively.

The existence of DM is supported by a considerable body of cosmological data. One of the outstanding issues in particle physics and cosmology is figuring out where it came from. DM particles are expected to interact with SM particles only very weakly, if at all. This suggests that there could be a hidden, dark sector of particles interacting with SM particles via a hypothetical dark photon (Zd).

Ref. [53] presents a search for a narrow resonance decaying to a pair of oppositely charged muons in the 11.5–200 GeV mass range, excluding the 75–110 GeV mass range where Z boson production dominates. The findings are discussed in the context of a Zd that interacts with SM particles via "kinetic mixing" of its $U(1)_D$ gauge field with the SM's $U(1)_Y$ "hypercharge field". The "kinetic mixing coefficient" ε determines the degree of mixing and the strength of the connection of Zd to SM particles. The authors of [29] discuss the theory of kinetic mixing and its implications for electroweak symmetry breaking and electroweak precision variables. In direct searches, beam dump, fixed-target, rare meson decay, and collider experiments have set constraints on visible Zd decays.

Analysis Event Selection

The p_T thresholds in typical dimuon triggers greatly restrict signal acceptance for dimuon resonance masses below ∼40 GeV, negatively decreasing search sensitivity. Therefore, a dedicated set of triggers with significantly lower muon p_T thresholds were implemented.

The information regarding muons recovered at the HLT is quite limited in events picked with these triggers. As a result, when compared to normal triggers, these triggers can operate at significantly higher rates. This method is known as "data scouting," and the high-rate triggers are referred to as "scouting triggers". For 2017, the "scouting dimuon triggers" were completely operational, recording events at a rate of 2 kHz at a peak instantaneous luminosity of 2×10^{34} cm^{-2} s^{-1}. These triggers collected data corresponding to an integrated luminosity of 96.6 fb^{-1} in 2017 and 2018.

Within a cone of $\Delta R = 0.1$, events must have at least one well-reconstructed Primary Vertex (PV) and two oppositely charged muons that are geometrically matched to the HLT muon candidates in the standard trigger search. The muons with the highest and second highest p_T must have $p_T > 20$ and 10 GeV, respectively, and $|\eta| < 1.9$. For data obtained

in 2016, the muon p_T threshold is set to 26 (29) GeV in events selected with single-muon triggers (2017, 2018).

Events must have two muons of opposite charge, with $p_T > 4$ GeV and $|\eta| < 1.9$, that are compatible with coming from the same vertex, in order to be found using the "scouting triggers". The muons must meet certain criteria based on the "track quality" information provided at the event. The muon isolation must be less than 15% of the muon p_T. The (second) highest p_T muon must have $p_T > m_{\mu\mu}/(4)$ 3, where $m_{\mu\mu}$ is the dimuon invariant mass, in order to suppress background involving muons from heavy flavor decays, which normally have low p_T.

The $|\eta|$ of the two muons has a big impact on the $m_{\mu\mu}$ resolution. The p_T resolution of muons with a $p_T < 50$ GeV is ∼1% in the detector's central barrel region ($|\eta| < 0.9$), and 3% in the muon system's end caps ($|\eta| > 1.2$). As a result, events are classified into two groups. The barrel category includes events in which both muons have a value of $|\eta| < 0.9$, while the forward category includes events in which at least one of the two muons has a value of $0.9 < |\eta| < 1.9$.

Results

A simultaneous binned maximum likelihood fit to the $m_{\mu\mu}$ distributions in the barrel and forward event categories is undertaken to extract the signal from the data. The shape of the background, which is dominated by DY events, is modeled using a parametric function.

The $m_{\mu\mu}$ distribution of barrel category events in the 23.9–26.1 GeV window, which is employed to hunt for a 25 GeV resonance, is shown in Figure 54 (inset). The estimated signal contribution for a 25 GeV Zd with $\varepsilon^2 = 2 \times 10^{-5}$ is also presented, along with a fit to these data assuming no signal.

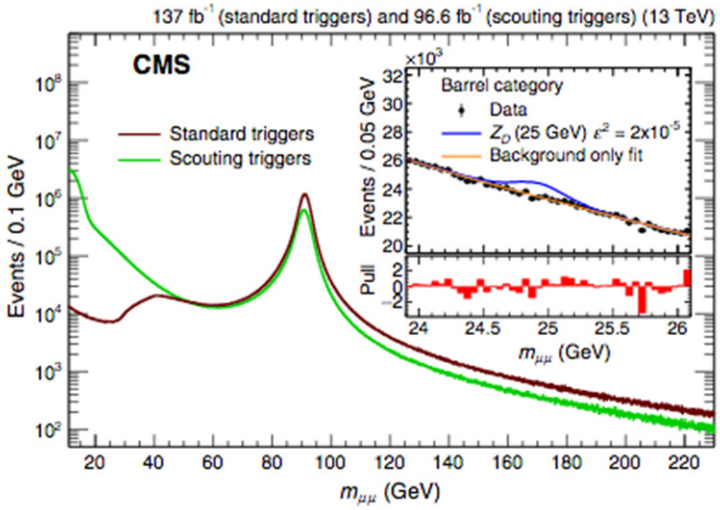

Figure 54. The $m_{\mu\mu}$ distributions of events picked using normal muon triggers (maroon, darker), as well as scouting dimuon triggers (green, lighter). All selection criteria must be met for an event to be considered. The inset is only for events in the barrel category with masses between 23.9 and 26.1 GeV. These data are fitted with a function characterizing the background, and a 25 GeV Zd signal corresponding to $\varepsilon^2 = 2 \times 10^{-5}$ is added. The statistical uncertainty is divided by the bin-by-bin difference between the number of events in the data and the prediction from the background fit in the bottom panel of the inset. Reprinted/adapted with permission from Ref. [1]. 2022, Physica Scripta, Th. Lagouri.

The data are determined to be in accordance with the expected background. Using an asymptotic CLs criterion, Figure 55 shows the upper limits for the product of the signal cross section, branching fraction to a pair of muons, and kinematic and geometrical acceptance for a narrow resonance at a 95% confidence level (C.L.).

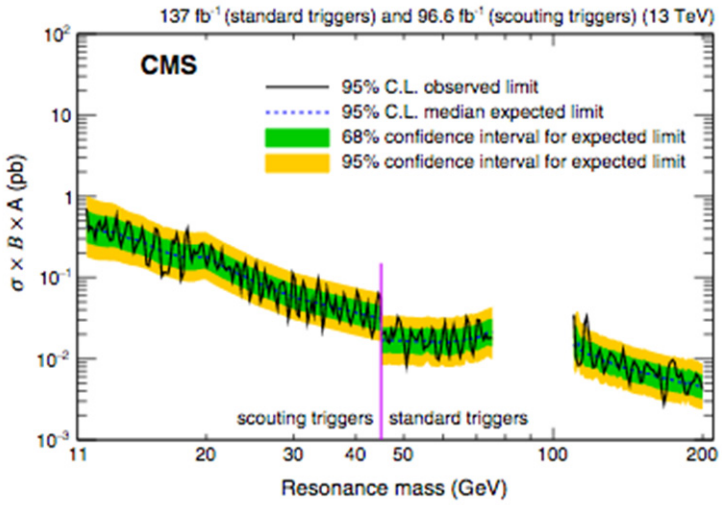

Figure 55. Expected and observed upper limits as a function of the mass of a narrow resonance on the product of the signal cross section (σ), branching fraction to a pair of muons (B), and acceptance (A) as a function of the mass of a narrow resonance at 95% C.L. The scouting (standard) triggers yielded results to the left (right) of the vertical purple line. Reprinted/adapted with permission from Ref. [1]. 2022, Physica Scripta, Th. Lagouri.

The findings of this investigation are discussed in the context of a dark photon model. As illustrated in Figure 56, we set upper limits at 90% C.L. on ε^2 as a function of Zd mass. These are compared to recent LHCb Collaboration results [54] and indirect constraints at 95% C.L. derived from electroweak observable measurements [29].

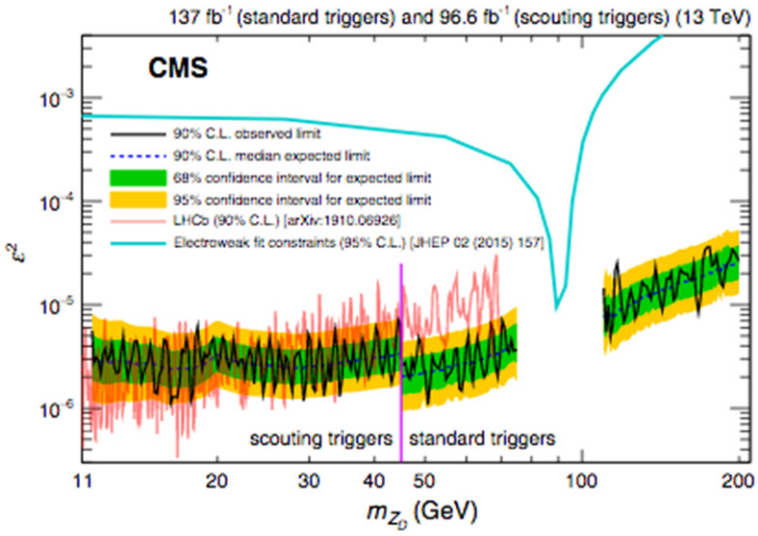

Figure 56. Expected and observed upper limits as a function of Zd mass at 90% C.L. on ε^2, the square of the kinetic mixing coefficient. The scouting (standard) triggers yielded results on the left (right) of the vertical purple line. Limits at 90% C.L. from the LHCb Collaboration's search are displayed in red, and limits at 95% C.L. from electroweak observable measurements are shown in light blue. Reprinted/adapted with permission from Ref. [1]. 2022, Physica Scripta, Th. Lagouri.

In the mass ranges of 30–75 and 110–200 GeV, this search establishes the most restrictive constraints to date. Furthermore, the limits achieved from this search are comparable to those reported previously at lower masses.

4.5.2. Dimuon Resonances Search with LHCb at $\sqrt{s}$ = 13 TeV

Both prompt-like and long-lived dark photons, A', produced in pp collisions at a center-of-mass energy of 13 TeV, are searched for in the LHCb [54]. These searches use a data sample equivalent to an integrated luminosity of 5.5 fb^{-1} recorded with the LHCb detector to look for $A' \to \mu^+\mu^-$ decays.

The "dark photon" (A'), a "hypothetical massive vector boson" that could mediate the interactions of dark matter particles, analogous to how the ordinary photon (γ) mediates the electro-magnetic (EM) interactions of charged SM particles, has recently received a lot of attention. The dark photon does not couple directly to SM particles, but due to kinetic mixing between the SM hypercharge and A' field strength tensors, it can obtain a modest coupling to the EM current.

This coupling, which is reduced by a factor labeled ε, relative to that of the photon, would offer a portal through which dark photons may be produced in the lab and decay into visible SM final states. If the kinetic mixing is caused by processes described by one- or two-loop diagrams involving high-mass particles, then $10^{-12} \lesssim \varepsilon^2 \lesssim 10^{-4}$ is expected [48]. One of the most important near-term goals of dark-sector physics is to investigate this few-loop ε region. If invisible dark-sector decays are kinematically prohibited, dark photons will decay into visible SM particles. Previous beam-dump, fixed-target, collider, and rare-meson-decay experiments have imposed constraints on observable A' decays. For dark-photon masses $m(A') \lesssim 10$ MeV, these experiments ruled out the few-loop region; nonetheless, the majority of the few-loop region at higher masses remains undiscovered. Only the visible situation is studied here.

Many concepts have been offered to further investigate the [$m(A')$; ε^2] parameter space. The LHCb Collaboration previously conducted a search using data corresponding to 1.6 fb^{-1} collected in 2016 [43]. For $10.6 < m(A') < 70$ GeV, the constraints put on prompt-like dark photons, where the dark-photon lifetime is modest compared to the detector resolution, were the most rigorous to date and similar to the best available limits for $m(A') < 0.5$ GeV. Although only limited parts of [$m(A')$; ε^2] parameter space were excluded, the search for long-lived dark photons was the first to attain sensitivity using a displaced-vertex signature.

This paper [54] reports on searches for both prompt-like and long-lived dark photons produced in proton–proton, pp, collisions at a center-of-mass energy of 13 TeV, looking for $A' \to \mu^+\mu^-$ decays with a data sample corresponding to an integrated luminosity of 5.5 fb^{-1} collected with the LHCb detector between 2016 and 2018. The methodologies used in these searches are the same as in [43], but the three-fold increase in integrated luminosity, enhanced trigger efficiency during data collection in 2017–2018, and improvements in the analysis result in much higher sensitivity to dark photons. From around the dimuon threshold to 70 GeV, the prompt-like A' search is used, achieving a factor of 5 (2) higher sensitivity to ε^2 at low (high) masses than [43]. The "long-lived" A' search is limited to the mass range $214 < m(A') < 350$ MeV, where the data have sensitivity and can access significantly wider regions of "[$m(A')$; ε^2] parameter space".

Analysis Event Selection

The $A' \to \mu^+\mu^-$ candidates are made up of two oppositely charged tracks that form a good-quality vertex and meet "stringent" muon-identification criteria, albeit these criteria were relaxed significantly in the low-mass area during data collection in 2017–2018. p_T (A') > 1 GeV and $2 < \eta(\mu) < 4.5$ are required for both searches. The prompt-like A' search uses muons with $p_T(\mu) > 1.0$ GeV and momentum p(μ) > 20 GeV in 2016, and $p_T(\mu) > 0.5$ GeV, $p(\mu) > 10$ GeV, and $p_T(\mu^+)p_T(\mu^-) > (1.0\ \text{GeV})^2$ in 2017–2018, which are compatible with originating from the PV. The long-lived A' search requires $2 < \eta(A') < 4.5$ and a decay topology consistent with a dark photon originating from a PV and uses muons that are inconsistent with originating from any PV with p_T (μ) > 0.5 GeV and $p(\mu) > 10$ GeV.

"Prompt" $\gamma^* \to \mu^+\mu^-$ production, numerous resonant decays to $\mu^+\mu^-$, whose mass-peak regions are not studied in this search, and the following sorts of "mis-reconstruction" contaminate the prompt-like A' sample: (hh) two muons produced in Q-hadron decays,

($h\mu Q$) a misidentified prompt hadron mixed with a muon produced in the decay of a heavy-flavor quark Q that is misidentified as prompt, and ($\mu_Q\mu_Q$) two muons produced in Q-hadron decays that are both misidentified as prompt. There is no contamination from a prompt muon or a misidentified prompt hadron.

When determining $m(\mu^+\mu^-)$, the influence of the $\gamma^* \to \mu^+\mu^-$ background is decreased ([54]) by restricting the muons to originate from the PV. For small $m(A')$, this enhances the resolution $\sigma[m(\mu^+\mu^-)]$ by nearly a factor of two.

Results

After accounting for the trials factor, there is no noticeable excess in the prompt-like $m(A')$ spectrum due to the number of signal hypotheses. When the upper limit on $n^{A'}{}_{ob}[m(A')]$ is less than $n^{A'}{}_{ex}$ $[m(A'); \varepsilon^2]$, dark photons are excluded at 90% C.L. The limits applied on prompt-like dark photons are the most stringent for $214 < m(A') \lesssim 740$ MeV and $10.6 < m(A') \lesssim 30$ GeV, as shown in Figure 57. A prompt-like A' search at any $m(A')$ places the strongest low-mass constraints.

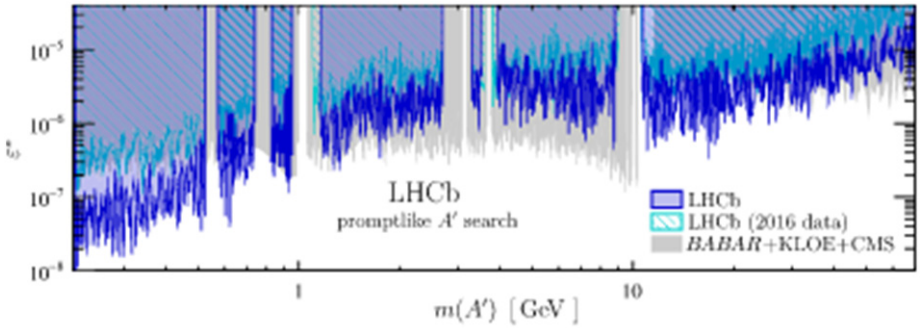

Figure 57. Regions of the $[m(A'); \varepsilon^2]$ parameter space excluded at 90% C.L. by the prompt-like A' search compared to the best published [54] and preliminary [43] limits. Reprinted/adapted with permission from Ref. [1]. 2022, Physica Scripta, Th. Lagouri.

Due to a stringent requirement imposed in the trigger, contamination from prompt particles is low for the long-lived A' search. Muons must be inconsistent with originating from any PV. As a result, photons that convert to $\mu^+\mu^-$ in the silicon-strip vertex detector that surrounds the pp interaction region known as the VELO, b-hadron decay chains that produce two muons, and the low-mass tail from $K^0{}_S \to \pi^+\pi^-$ decays, where both pions are misidentified as muons, are the dominant background contributions (all other strange decays are negligible).

In Figure 58, the predicted prompt-like $A' \to \mu^+\mu^-$ yields are displayed alongside the $n^{A'}{}_{ex}[m(A'); \varepsilon^2]$ values derived utilizing these data-driven $\varepsilon^{A'}{}_{\gamma^*}[m(A'); \tau(A')]$ values.

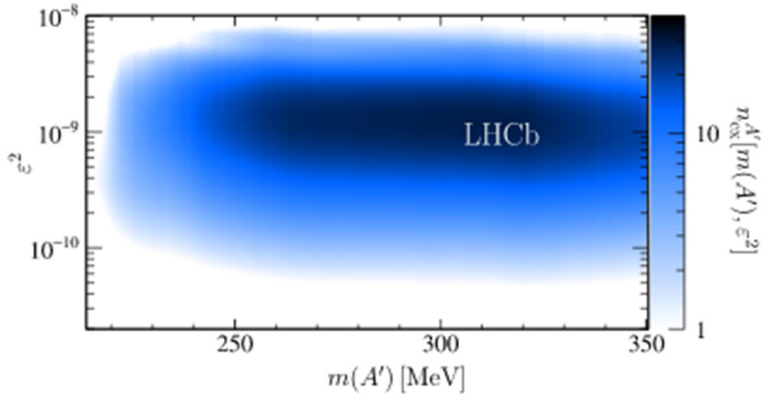

Figure 58. Expected reconstructed and selected long-lived $A' \to \mu^+\mu^-$ yield. Reprinted/adapted with permission from Ref. [1]. 2022, Physica Scripta, Th. Lagouri.

The upper limits on $n^{A'}{}_{ob}[m(A'); \tau(A')]$ are easily translated into constraints on $n^{A'}{}_{ob}[m(A'); \varepsilon^2]$ because the relationship between $\tau(A')$ and ε^2 is known at each mass. At 90% C.L., regions of the $[m(A'); \varepsilon^2]$ parameter space where $n^{A'}{}_{ob}[m(A'); \varepsilon^2]$ is less than $n^{A'}{}_{ex}[m(A'); \varepsilon^2]$ are excluded. Large portions of $[m(A'); \varepsilon^2]$ parameter space are excluded in Figure 59, which are considerably larger than the regions removed in [43].

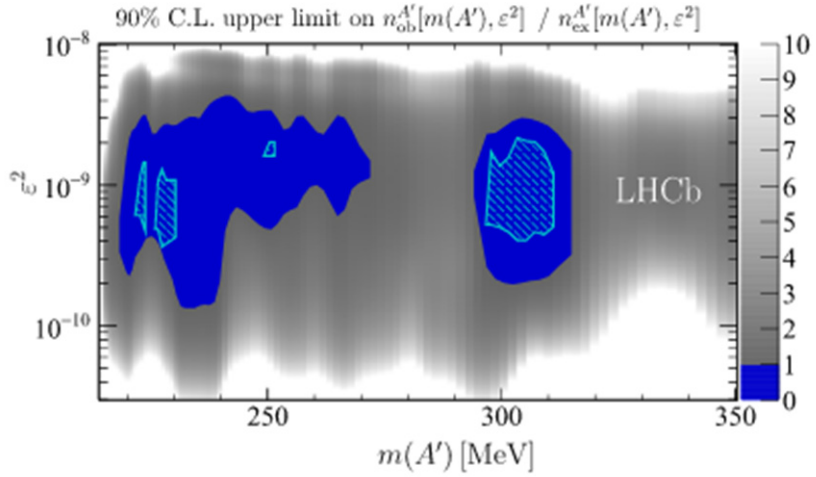

Figure 59. At 90% C.L., ratio of the observed upper limit on $n^{A'}{}_{ob}[m(A'); \varepsilon^2]$ to the expected dark-photon yield $n^{A'}{}_{ex}[\mathrm{m}(A'); \varepsilon^2]$, with regions less than unity excluded. The only constraints in this region come from the earlier LHCb search (hashed). Reprinted/adapted with permission from Ref. [1]. 2022, Physica Scripta, Th. Lagouri.

5. Summary of Dark Photon Studies at LHC

This study reviews the ATLAS and CMS searches for dark massive (Zd) or massless photons produced by Higgs decays that are prompt or displaced. ATLAS searches for dark photons decaying into displaced (or prompt) lepton jets have been reported in particular. Furthermore, ATLAS and CMS search for long-lived particles decaying to displaced dileptons were investigated. Finally, searches for low mass dimuon resonances with the CMS and LHCb are presented.

An ATLAS search for exotic decays of the SM Higgs boson into two new spin 1 particles $H \to ZZ$, two new spin 0 particles $H \to aa$, or a Z boson together with a single Z or a was recently published [34]. During the complete Run-2 period of 2015–2018, the ATLAS experiment recorded 139 fb^{-1} of proton–proton collision data at $\sqrt{s}$ = 13 TeV. The first search is for the process $H \to XX \to 4l$, where X is either Zd or a and the energy range is 15 GeV < m_X < 60 GeV. The second search is for the $H \to XX \to 4\mu$ process, where 1 GeV < m_X < 15 GeV. The process $H \to ZX \to 4l$, where 15 GeV < m_X < 55 GeV, is the subject of the third search. Limits on fiducial and total cross sections are determined after the results are verified to be compatible with the predicted backgrounds in the three searches described.

Under the assumptions of gluon-gluon fusion SM Higgs production and prompt decay of the Zd/a bosons, upper limits on the branching ratio of the Higgs boson to $ZdZd$ and aa as a function of intermediate boson mass are set. Furthermore, constraints are provided on the mixing parameters κ', ε, and δ, assuming the HAHM is introduced at the Higgs portal level with very weak kinetic mixing. Due to enhanced statistics, improved lepton reconstruction and identification, and more optimized event selection, the limits provided in this study outperform those in the prior publication [36] by a factor of 2–4. This work provides constraints on total cross sections and dark Higgs boson mixing parameters in addition to the results from the prior paper.

Also, CMS generic search was performed [42] for a dilepton resonance in Higgs boson decays to the four-lepton end state. The two decay topologies, $pp \to H \to ZX$ and $pp \to H \to XX$, were explored in the search. The search set substantial limitations on "model-independent"

branching fractions and model parameters of two well-motivated models BSM without finding any major deviation from SM expectations. Experiments were carried out on products of model-independent branching fractions of $B(H \to ZX)$, B($H \to XX$), and $B(X \to ee$ or $\mu\mu)$, assuming flavor-democratic decays of X to di-muons and di-electrons, exclusive decays of X to dimuons, and exclusive decays of X to di-electrons. In Higgs-mixing-dominated scenarios, the search also yielded unique limitations on the "Higgs-mixing parameter" $\kappa < 0.004$ in a dark photon model with the XX selection but also searches for Zd in Drell–Yan processes produced better exclusion limits on ε in "kinematic-mixing"-dominated scenarios.

The CMS collaboration proposed a search in [44] for a Higgs boson that is created in conjunction with a Z boson and decays to an undetected particle along with an isolated photon. A data set with an integrated luminosity of 137 fb^{-1} was used in the search, which was recorded at a center-of-mass energy of 13 TeV at the LHC. There was no substantial excess of events compared to the SM background. The findings were explained using a theoretical scenario in which the undetected particle is a massless dark photon. As a function of Higgs boson mass, an upper limit was placed on the product of the cross section for associated Higgs and Z boson production and the branching fraction for such a Higgs boson decay. This translates to an observed (expected) upper limit on the branching fraction of 4.6 (3.6) % at a 95% confidence level for a mass of 125 GeV, assuming the SM production cross section. These were the first constraints on Higgs boson decays to final states containing a massless dark photon that had not been found.

The CMS Collaboration [46] used a data sample corresponding to an integrated luminosity of 35.9 fb^{-1} of proton–proton collisions at a center-of-mass energy of $\sqrt{s} = 13$ TeV obtained with the CMS detector at the LHC to look for new light bosons decaying into muon pairs. The search simply required the pair production of a new light boson and its subsequent decay to a pair of muons, which was "model agnostic". There was no significant deviation from the expected background. As a function of new light boson mass, a "model-independent" limit was established on the product of the production cross section times branching fraction to dimuons squared times acceptance as a function of new light boson mass. Over a range of new light boson masses from 0.25 to 8.5 GeV, this limit varied between 0.15 and 0.39 fb. It was then interpreted in terms of the "NMSSM" model and a dark "SUSY" model with non-negligible light boson lifetimes. There was a significant improvement over previously announced limits in both cases.

The ATLAS detector at the LHC is being employed in a search [48] for the production of displaced dark-photon jets in a sample of pp collisions at $\sqrt{s} = 13$ TeV, which corresponds to a 36.1 fb^{-1} integrated luminosity. According to the FRVZ model, no significant excess of events is seen as compared to the background expectation, and 95% confidence-level upper bounds are established on the production cross section times branching fraction of scalar bosons that decay into dark photons. The upper limits are calculated as a function of the dark photon's γ_d proper decay length $c\tau$. In comparison to ATLAS search using 8 TeV pp data, improved background suppression and the use of hadronic γ_d decays result in greater sensitivity.

Dark photon decays were excluded at 95% CL for $c\tau \in [1.5, 307]$ mm and $c\tau \in [3.7, 178]$ mm for the production of two and four dark photons, respectively, in the pure muonic channel, assuming a branching ratio $B(H \to 2(4)\gamma_d + X) = 10\%$ for $m_H = 125$ GeV. The excluded regions for $m_H = 800$ GeV were $c\tau \in [5, 1420]$ mm and $c\tau \in [10.5, 312]$ mm, assuming $\sigma \times B(H \to 2(4)\gamma_d + X) = 5$ pb. The $m_H = 800$ GeV excluded regions become $c\tau \in [7.3, 1298]$ mm and $c\tau \in [13.6, 231]$ mm in the pure hadronic channel. When H is the Higgs boson, the results for $H \to 2\gamma_d + X$ were interpreted as 90% "confidence-level" restrictions on the "kinetic mixing parameter" as a function of dark-photon mass. These results outperformed prior LHC searches in terms of constraints.

An ATLAS search [49] for a novel light boson with a mass of around 1 GeV that decays to collimated electron and/or muon jets was conducted (lepton jets). The research used data obtained by the ATLAS detector at the LHC in pp collisions with a center-of-mass energy

of 8 TeV of 20.3 fb^{-1}. At least two lepton jets were required in each event. The ATLAS investigation showed no statistically significant deviation from the SM's predictions and set 95% confidence-level upper limits on the contribution of novel phenomena beyond the SM, such as the SUSY-portal and Higgs-portal models, to the number of lepton jet events. In the SUSY-portal and Higgs-portal models, the 95% confidence-level upper bounds were determined on the production cross section times branching ratio for two prompt lepton jets. Based on combined results from the H$\rightarrow 2\gamma_d + X$ topology, the results were also interpreted in terms of a 90% confidence-level exclusion region in kinetic mixing and dark-photon mass parameter space. These results offered exclusion in hitherto undiscovered parts of parameter space and extended the results of prior searches.

In a sample of *pp* collisions recorded by the ATLAS detector at the LHC with a center-of-mass energy of $\sqrt{s}$ = 13 TeV and an integrated luminosity of 32.9 fb^{-1}, the ATLAS Collaboration announced a search for BSM long-lived particles decaying into two muons of opposite-sign electric charge. Dimuon vertices with displacements from the *pp* interaction point in the range of 1–400 cm and invariant mass $m_{\mu\mu}$ inside one of two signal regions: 20–60 GeV or >60 GeV, were found during the search. There is no substantial excess in the number of vertices in either signal region as compared to the predicted background. As a result, upper limits on the product of cross section and branching fraction, as a function of lifetime, were calculated for the production of long-lived particles in either a dark-sector model with dark-photon masses in the range 20–60 GeV, produced from Higgs boson decays, or a general gauge-mediated supersymmetric model with a gluino mass of 1100 GeV and neutralino masses in the range 300–1000 GeV. The lowest and upper lifetime limits for the models evaluated were set at 1 to 2400 cm in $c\tau$, depending on the parameters of the selected model.

When using *pp* collision data gathered at $\sqrt{s}$ = 8 TeV, a CMS search [47] was conducted for "Long-Lived" (LL) particles that decay to a final state containing a pair of electrons or a pair of muons. No similar events have been observed. In the context of two specific models, quantitative constraints have been imposed on the product of the cross section and branching fraction of such a signal. A Higgs boson with a mass of 125–1000 GeV decays into a pair of "hypothetical" LL neutral bosons with a mass of 20–350 GeV, each of which can decay to dileptons in the first model. Upper bounds for LL particles with mean appropriate decay lengths of 0.01–100 cm are typically in the range of 0.2–10 fb, weakening to 250 fb for the lowest estimated Higgs mass of 125 GeV. A pair of squarks decays to a quark, and an LL neutralino $\widetilde{\chi}^0$ in the second model, which is based on R-parity violating supersymmetry; the neutralino can then decay to e^+e^-v or $\mu^+\mu^-v$. For $\widetilde{\chi}^0$ mean proper decay lengths in the range 0.1–100 cm and squark masses above 350 GeV, the upper limits were frequently in the range 0.2–5 fb. The limitations were typically 10 times weaker with a lower squark mass of 120 GeV. In the Higgs boson and supersymmetric models, these limits were sensitive to branching fractions as low as 10^{-4} and 10^{-6}, respectively. Limits that were restricted to the detector acceptance were also supplied, decreasing model dependence and allowing the results to be reinterpreted in the context of different models. These restrictions were the most rigorous to date throughout much of the parameter space studied.

Using *pp* collision data recorded by the CMS experiment at $\sqrt{s}$ = 13 TeV, a CMS search [53] for a narrow resonance decaying to a pair of muons has been presented. Fully reconstructed data containing a pair of muons with transverse momenta greater than 20 and 10 GeV, corresponding to an integrated luminosity of 137 fb^{-1}, was utilized to search for resonance mass ranges of 45–75 and 110–200 GeV. Data collected with high-rate dimuon triggers yielded an integrated luminosity of 96.6 fb^{-1}, which was used to search for resonances in the mass range of 11.5–45.0 GeV. This was the first search using data collected with dimuon triggers with transverse momentum thresholds of 3 GeV and data with reduced trigger-level muon information. The data were discovered to be in line with the background prediction. In the mass ranges of ∼30–75 and 110–200 GeV, the search yielded the lowest upper bounds on the kinetic mixing coefficient of a dark photon to date.

With center-of-mass energy of 13 TeV, LHCb searches [54] were conducted for prompt-like and long-lived dark photons created in pp collisions. Both searches use a data sample equivalent to an integrated luminosity of 5.5 fb^{-1} recorded with the LHCb detector during 2016–2018 to look for $A' \to \mu^+\mu^-$ decays. In both searches, no evidence for a signal was detected, and 90% C.L. exclusion regions were placed on the γ–A' kinetic mixing strength. With $214 < m(A') \lesssim 740$ MeV and $10.6 < m(A') \lesssim 30$ GeV, the prompt-like A' search produced the most rigorous restrictions on dark photons from near the dimuon threshold up to 70 GeV. The "long-lived" A' search was limited to the mass range $214 < m(A') < 350$ MeV, where the data had sensitivity and placed world-leading limitations on low-mass dark photons with $O(1)$ ps lifetimes. The searches presented in this paper provide substantially better sensitivity to dark photons than the previous LHCb results due to a threefold increase in integrated luminosity, improved trigger efficiency during data collection in 2017–2018, and advances in analysis. The prompt-like A' search had a factor of 5 (2) higher sensitivity to ε^2 than [43] at low (high) masses, while the long-lived A' search gave access to far broader areas of $[m(A'); \varepsilon^2]$ parameter space. Even with a data sample collected with a hardware-trigger stage inefficient for low-mass $A' \to \mu^+\mu^-$ decays, these results revealed the LHCb experiment's exceptional sensitivity to dark photons. When compared to the 2016–2018 data sample, the removal of this hardware-trigger stage in Run 3 combined with the expected increase in luminosity should boost the potential yield of $A' \to \mu^+\mu^-$ decays in the low-mass area by a factor $O(100)$. Provided that most of the parameter space would have been accessible if the data sample had been three times larger, these enhancements will significantly boost the LHCb experiment's dark-photon discovery potential.

6. Conclusions and Future Prospects

It has been assumed for the past 50 years that BSM physics interacted with SM physics via (at least) some of the same gauge interactions. In this paradigm, the MSSM and "weakly-interacting" massive DM are the two most dominant and important models. Because of the paucity of additional particle discoveries, this initiative is currently losing some of its initial vigor. The MSSM's many properties, for example, work against its usefulness as a foil for the SM in mapping possible experimental differences in the absence of new states. A broader scenario has been receiving growing interest in recent times, primarily as a result of the lack of any real BSM signal. BSM matter is part of a new sector that is dark since it does not interact through SM gauge interactions. There could be a plethora of physics in the dark sector, with many particles (some of which are DM) and interactions. We can see this dark sector through a portal from our side in the visible universe. This portal, if it exists, can take numerous forms depending on the mediator's spin.

This review paper looked at the vector scenario, in which the portal is created by kinetic mixing between the SM electric (or hyper) charge gauge group and the dark sector's U(1) gauge symmetry. The discovery of the dark photon associated with this new Abelian gauge symmetry is significantly more intriguing than simply discovering a new particle since, if discovered, this new gauge boson would indicate the existence of a new interaction and a new sector of elementary particles. Past and present experiments have already constrained a significant portion of the space of the vector portal's parameters, both for massless and massive dark photons. The parameters are fewer, and the signatures are easier to interpret as compared to other BSM model searches.

As a result, looking for numerous complementing signatures is required in order to investigate the Hidden–Dark Sector as a significant and increasing component of BSM physics. Experiments at High Energy Colliders, High-Intensity Colliders, and Fixed Target Experiments are all continuing and interesting. There are several complimentary searches from different experiments, such as ATLAS, CMS, and LHCb at the LHC for larger mass ranges and smaller couplings, and fixed target experiments and heavy ions experiments at the B-factories. Future LLP experiments are also in the works. At the HL-LHC, there are exciting possibilities for future dark photon searches. The ATLAS and CMS detectors are undergoing major improvements with the goal of reaching a combined luminosity of

3000 fb^{-1} by 2035. For better vertexing and at a lower p_T threshold, improved detectors and triggers are being built. Towards NP, all existing and prospective experiments at CERN and elsewhere aim for complementary phase spaces.

The dark photon, a novel gauge boson whose existence has been postulated in the Hidden–Dark Sector, is particularly dark since it emerges from a symmetry of a hypothetical dark sector containing particles that are entirely neutral under SM interactions. This new gauge boson, despite its 'darkness', can be identified due to its kinetic mixing with regularly visible photons. This paper examines its physics from both a theoretical and experimental standpoint. The distinction between the massive and massless cases is discussed, as well as how the dark photon enters the laboratory and how DM physics connects astrophysical and cosmological findings. The current and prospective experimental restrictions on the parameters of massless and massive dark photons have been addressed.

The results of dark photon searches at the LHC linked to Higgs decay, and other dark sector hypotheses are reported. Many dark sector searches are conducted in search of prompt decay, displaced decay, and missing momentum (invisible/very long-lived) particles. Distinct mass, mixing, production, and decay modes are used to create different search techniques. However, due to triggers and other limits, the LHC experiments have a limited ability to lower mass.

Much exploratory research is also underway, with the goal of maximizing the research potential of CERN's accelerator complex and scientific infrastructure through programs that are complementary to the LHC, HL-LHC, and other future colliders. These programs, which are part of the "Physics Beyond Collider" (PBC) for BSM Physics, also known as "New Physics" (NP), would focus on fundamental physics topics that are conceptually similar to those addressed by high-energy colliders but require new types of beams and experiments. There are approximately 15 PBC ideas aimed at utilizing CERN's accelerator facility and scientific facilities. These ideas will be sensitive to NP in masses and couplings not available to other existing or proposed global projects, such as the LHC or FCC experiments, DM direct detection experiments, and flavor physics initiatives.

Following the NP mass range to which they are sensitive, three primary groups of investigations have been identified: (1) investigations sensitive to NP with masses in the sub-eV range and weakly coupled to SM particles: these are mostly searches for axions and axion-like particles using a variety of techniques; (2) accelerator-based experiments sensitive to NP with masses in the MeV–GeV range and weakly coupled to SM particles: these are experiments searching for extremely rare or forbidden processes that could be produced via high-intensity high-energy beams currently available or proposed at CERN; (3) experiments sensitive to NP with masses in the multi-TeV range and strongly coupled to SM particles: these are experiments searching for extremely "rare" or "forbidden" processes that could be produced via high-intensity and high-energy beams.

Finally, a new wave of experiments is about to begin, with the goal of shutting the remaining windows in the interaction between ordinary matter and the dark photon. In the dark dipole interaction, the limitations in the massless scenario appear to transfer the probable detection of the dark photon to very large values of the effective scale Λ. Exploring physics at such a large energy scale necessitates high sensitivity, which can be found only in future lepton colliders (where the dark dipole operator's contribution will be amplified by its scaling with energy) or in searches for rare flavor-changing decays such as those of the Kaon and B-meson systems.

In the case of the massive dark photon, the constraints have left two significant regions in the parameter space open. The first is for visible dark photons with masses of at least 100 MeV and mixing parameters of between 10^{-6} and 10^{-4}. Many future experiments will focus on this area. If this window is also closed, the vector portal's already weak interaction will become even more weak. The second window, an unseen dark photon with a very light mass and a "mixing parameter" of order $O(10^{-8})$ or even lighter and with a smaller mixing parameter, remains undiscovered. These two locations are of tremendous interest to astronomers and cosmologists, and they are a very busy area of hypotheses.

To summarize, no one experiment or experimental approach is sufficient to cover the huge parameter space suggested by dark photon models in terms of masses and couplings. Synergy and complementarity across a wide range of experimental facilities are critical, necessitating cross-community collaboration between the so-called intensity and energy frontiers.

Funding: This research received no external funding.

Conflicts of Interest: The author declares no conflict of interest.

References

1. Lagouri, T. Review on Higgs Hidden-Dark Sector Physics. *Phys. Scr.* **2021**, *97*, 24001. [CrossRef]
2. ATLAS Collaboration. Observation of a new particle in the search for the Standard Model Higgs boson with the ATLAS detector at the LHC. *Phys. Lett. B* **2012**, *716*, 1–29. [CrossRef]
3. CMS Collaboration. Observation of a new boson at a mass of 125 GeV with the CMS experiment at the LHC. *Phys. Lett. B* **2012**, *716*, 30–61. [CrossRef]
4. Beacham, J.; Burrage, C.; Curtin, D.; De Roeck, A.; Evans, J.; Feng, J.L.; Gatto, C.; Gninenko, S.; Hartin, A.; Irastorza, I.; et al. Physics beyond colliders at CERN: Beyond the Standard Model working group report. *J. Phys. G Nucl. Part. Phys.* **2020**, *47*, 010501. [CrossRef]
5. Odintsov, S.D.; Oikonomou, V.K. Aspects of Axion F(R) Gravity. *Europhys. Lett.* **2020**, *129*, 40001. [CrossRef]
6. Oikonomou, V. Unifying inflation with early and late dark energy epochs in axion gravity. *Phys. Rev. D* **2021**, *103*, 44036. [CrossRef]
7. Odintsov, S.D.; Oikonomou, V.K. Unification of inflation with dark energy in F(R) gravity and axion dark matter. *Phys. Rev. D* **2019**, *99*, 104070. [CrossRef]
8. Doglioni, C.; Tovey, D. ATLAS Communication 2019. Available online: https://atlas.cern/updates/feature/dark-matter (accessed on 5 March 2019).
9. Boveia, A.; Doglioni, C. Dark Matter Searches at Colliders. *Annu. Rev. Nucl. Part. Sci.* **2018**, *68*, 429–459. [CrossRef]
10. Available online: https://lpcc.web.cern.ch/index.php/content/lhc-dm-wg (accessed on 1 January 2022).
11. Available online: http://www.xenon1t.org (accessed on 1 January 2022).
12. Available online: http://luxdarkmatter.org (accessed on 1 January 2022).
13. Available online: https://pandax.sjtu.edu.cn (accessed on 1 January 2022).
14. Available online: https://glast.sites.stanford.edu (accessed on 1 January 2022).
15. Available online: https://www.mpi-hd.mpg.de/hfm/HESS/HESS.shtml (accessed on 1 January 2022).
16. Available online: https://magic.mpp.mpg.de (accessed on 1 January 2022).
17. Available online: https://veritas.sao.arizona.edu (accessed on 1 January 2022).
18. Available online: https://icecube.wisc.edu (accessed on 1 January 2022).
19. Available online: http://www.ams02.org (accessed on 1 January 2022).
20. ATLAS Collaboration. Search for new phenomena in events with an energetic jet and missing transverse momentum in pp collisions at $\sqrt{s} = 13$ TeV with the ATLAS detector. *Phys. Rev. D* **2021**, *103*, 112006. [CrossRef]
21. CMS Collaboration. Search for new particles in events with energetic jets and large missing transverse momentum in proton-proton collisions at $\sqrt{s} = 13$ TeV. *arXiv* **2021**, arXiv:2107.13021.
22. ATLAS Collaboration. Search for new resonances in mass distributions of jet pairs using 139 fb−1 of pp collisions at $\sqrt{s} = 13$ TeV with the ATLAS detector. *J. High Energy Phys.* **2020**, *145*. [CrossRef]
23. CMS collaboration. Search for high mass dijet resonances with a new background prediction method in proton-proton collisions at $\sqrt{s} = 13$ TeV. *J. High Energy Phys.* **2020**, *33*. [CrossRef]
24. Copeland, E.; Sami, M.; Tsujikawa, S. Dynamics of Dark Energy. *Int. J. Mod. Phys. D* **2006**, *15*, 1753–1935. [CrossRef]
25. Marsh, D.J. Axion cosmology. *Phys. Rep.* **2016**, *643*, 1–79. [CrossRef]
26. Essig, R.; Jaros, J.A.; Wester, W.; Adrian, P.H.; Andreas, S.; Averett, T.; Baker, O.; Batell, B.; Battaglieri, M.; Beacham, J.; et al. Dark Sectors and New, Light, Weakly-Coupled Particles. *arXiv* **2013**, arXiv:1311.0029.
27. Alexander, J.; Battaglieri, M.; Echenard, B.; Essig, R.; Graham, M.; Izaguirre, E.; Jaros, J.; Krnjaic, G.; Mardon, J.; Morrissey, D.; et al. Dark Sectors 2016 Workshop: Community Report. *arXiv* **2016**, arXiv:1608.08632. [CrossRef]
28. Curtin, D.; Essig, R.; Gori, S.; Jaiswal, P.; Katz, A.; Liu, T.; Liu, Z.; McKeen, D.; Shelton, J.; Strassler, M.; et al. Exotic decays of the 125 GeV Higgs boson. *Phys. Rev. D* **2014**, *90*, 075004. [CrossRef]
29. Curtin, D.; Essig, R.; Gori, S.; Shelton, J. Illuminating dark photons with high-energy colliders. *J. High Energy Phys.* **2015**, *157*. [CrossRef]
30. Holdom, B. Two U(1)'s and ϵ charge shifts. *Phys. Lett. B* **1986**, *166*, 196–198. [CrossRef]
31. Fabbrichesi, M.; Gabrielli, E.; Lanfranchi, G. *The Physics of the Dark Photon*; SpringerBriefs in Physics; Springer: Cham, Switzerland, 2021. [CrossRef]

32. CMS Collaboration. Measurement of the properties of a Higgs boson in the four-lepton final state. *Phys. Rev. D* **2014**, *89*, 092007. [CrossRef]
33. ATLAS Collaboration. Measurements of Higgs boson production and couplings in the four-lepton channel in pp collisions at center-of-mass energies of 7 and 8 TeV with the ATLAS detector. *Phys. Rev. D* **2015**, *91*, 012006. [CrossRef]
34. ATLAS Collaboration. Search for Higgs bosons decaying into new spin-0 or spin-1 particles in four-lepton final states with the ATLAS detector with 139 fb−1 of pp collision data at $\sqrt{s} = 13$ TeV. *J. High Energy Phys.* **2022**, *3*, 041. [CrossRef]
35. ATLAS Collaboration. Search for new light gauge bosons in Higgs boson decays to four-lepton final states in pp collisions at $\sqrt{s} = 8$ TeV with the ATLAS detector at the LHC. *Phys. Rev. D* **2015**, *92*, 092001. [CrossRef]
36. ATLAS Collaboration; Aaboud, M. Search for Higgs boson decays to beyond-the-Standard-Model light bosons in four-lepton events with the ATLAS detector at $\sqrt{s} = 13$ TeV. *J. High Energy Phys.* **2018**, *6*, 166. [CrossRef]
37. ATLAS Collaboration. Search for long-lived neutral particles decaying into lepton jets in proton-proton collisions at $\sqrt{s} = 8$ TeV with the ATLAS detector. *J. High Energy Phys.* **2014**, *11*, 88. [CrossRef]
38. ATLAS Collaboration. Measurement of the Higgs boson coupling properties in the H→ZZ∗→4ℓ decay channel at $\sqrt{s} = 13$ TeV with the ATLAS detector. *J. High Energy Phys.* **2018**, *3*, 95.
39. ATLAS Collaboration. Measurement of inclusive and differential cross sections in the H→ZZ∗→4ℓ decay channel in pp collisions at $\sqrt{s} ==$ 13 TeV with the ATLAS detector. *J. High Energy Phys.* **2017**, *10*, 132.
40. Read, A.L. Presentation of search results: The CLs technique. *J. Phys. G* **2002**, *28*, 2693. [CrossRef]
41. Cowan, G.; Cranmer, K.; Gross, E.; Vitells, O. Asymptotic formulae for likelihood-based tests of new physics. *Eur. Phys. J. C* **2011**, *71*, 1554. [CrossRef]
42. CMS Collaboration. Search for low-mass dilepton resonances in Higgs boson decays to four-lepton final states in proton–proton collisions at $\sqrt{s} = 13$ TeV. *Eur. Phys. J. C* **2022**, *82*, 290. [CrossRef]
43. LHCb Collaboration. Search for Dark Photons Produced in 13 TeV pp Collisions. *Phys. Rev. Lett.* **2018**, *120*, 061801. [CrossRef]
44. CMS Collaboration. Search for dark photons in decays of Higgs bosons produced in association with Z bosons in proton-proton collisions at $\sqrt{s} = 13$ TeV. *J. High Energy Phys.* **2019**, *10*, 139. [CrossRef]
45. CMS Collaboration. Search for dark photons in Higgs boson production via vector boson fusion in proton-proton collisions at $\sqrt{s} = 13$ TeV. *J. High Energy Phys.* **2021**, *3*, 11. [CrossRef]
46. CMS Collaboration. A search for pair production of new light bosons decaying into muons in proton-proton collisions at 13 TeV. *Phys. Lett. B* **2019**, *796*, 131. [CrossRef]
47. CMS Collaboration. Search for long-lived particles that decay into final states containing two electrons or two muons in proton-proton collisions at $\sqrt{s} = 8$ TeV. *Phys. Rev. D* **2015**, *91*, 052012. [CrossRef]
48. ATLAS Collaboration. Search for light long-lived neutral particles produced in pp collisions at $\sqrt{s} = 13$ TeV and decaying into collimated leptons or light hadrons with the ATLAS detector. *Eur. Phys. J. C* **2020**, *80*, 450. [CrossRef]
49. ATLAS Collaboration. A search for prompt lepton-jets in pp collisions at $\sqrt{s} = 8$ TeV with the ATLAS detector. *J. High Energy Phys.* **2016**, *2*, 62. [CrossRef]
50. CMS Collaboration. A search for pair production of new light bosons decaying into muons. *Phys. Lett. B* **2016**, *752*, 146. [CrossRef]
51. ATLAS Collaboration. Search for long-lived particles in final states with displaced dimuon vertices in pp collisions at $\sqrt{s} =$ 13 TeV with the ATLAS detector. *Phys. Rev. D* **2019**, *99*, 012001. [CrossRef]
52. ATLAS Collaboration. Search for massive, long-lived particles using multitrack displaced vertices or displaced lepton pairs in pp collisions at $\sqrt{s} = 8$ TeV with the ATLAS detector. *Phys. Rev. D* **2015**, *92*, 072004. [CrossRef]
53. CMS Collaboration. Search for a Narrow Resonance Lighter than 200 GeV Decaying to a Pair of Muons in Proton-Proton Collisions at $\sqrt{s} = 13$ TeV. *Phys. Rev. Lett.* **2020**, *124*, 131802. [CrossRef] [PubMed]
54. LHCb Collaboration. Search for A′→$\mu^+\mu^-$ Decays. *Phys. Rev. Lett.* **2020**, *124*, 041801. [CrossRef] [PubMed]